

UC Irvine

UC Irvine Electronic Theses and Dissertations

Title

The effects of airborne ultra-fine particulate exposure on cognition and neuropathology in an amyloid model of Alzheimer's disease

Permalink

<https://escholarship.org/uc/item/3dw5c3fz>

Author

Kilian, Jason

Publication Date

2020

Copyright Information

This work is made available under the terms of a Creative Commons Attribution License, available at <https://creativecommons.org/licenses/by/4.0/>

Peer reviewed|Thesis/dissertation

UNIVERSITY OF CALIFORNIA,
IRVINE

The effects of airborne ultra-fine particulate exposure on cognition and neuropathology in an amyloid model of Alzheimer's disease

DISSERTATION

submitted in partial satisfaction of the requirements for the degree of

DOCTOR OF PHILOSOPHY

in Environmental Health Sciences

by

Jason Kilian

Dissertation Committee:
Associate Professor Masashi Kitazawa, PhD (Chair)
Associate Professor Kim Green, PhD
Professor Stephen Bondy
Adjunct Professor Michael T. Kleinman, PhD

2020

Astrocyte transport of glutamate and neuronal activity reciprocally modulate tau pathology in *Drosophila*. *Neuroscience* 2017. © 2017 IBRO. Published by Elsevier Ltd. All rights reserved.

© 2020 Jason Kilian. All rights reserved.

Contents

List of Tables	v
List of Figures.....	vi
Acknowledgements.....	xiii
Vita.....	xiv
Chapter 1: Introduction.....	1
1.1 Dissertation Statement.....	1
1.2 Significance.....	1
1.3 Alzheimer’s Disease: Background and Pathology.....	2
1.4 Amyloid Precursor Protein and Amyloid- β	3
1.4.1 Tau Protein in AD Pathology.....	6
1.4.2 Inflammation.....	7
1.5 Alzheimer’s Disease and Particulate Matter.....	8
1.5.1 Particulate Matter: Sources and Composition.....	8
1.5.2 Epidemiological Studies of PM and General Air Pollution Neuronal Disease Risk	12
1.5.3 Animal Studies of the effects of PM in the CNS.....	17
1.5.4 Human Studies of PM Effects on the Central Nervous System.....	21
1.6 Hypothesis.....	23
1.7 Dissertation Contribution.....	23
1.8 Conclusion.....	24
Chapter 2: Exposure to ultra-fine particulate matter impairs memory function and exacerbates amyloid pathology in the <i>App</i> ^{NL-G-F} knock-in mouse model.....	25
2.1 Abstract:.....	25
2.2 Introduction:.....	25
2.3 Methods.....	27
2.3.1 Animals.....	27
2.3.2 Exposure Paradigm.....	28
2.3.3 Cognitive Assessments.....	29
2.3.4 Protein Extraction and Western Blot Analysis.....	29
2.3.5 Immunofluorescent Staining.....	31
2.3.6 Real-Time Polymerase Chain Reaction.....	32
2.3.6 A β Quantitation.....	33

2.3.7 Statistical Analysis	33
2.4 Results:	33
2.4.1 Concentration of ambient particulates	34
2.4.2 UF PM exposure impairs cognition in young <i>App</i> ^{NL-G-F/+} -KI mice	34
2.4.3 UF PM exposure does not affect Amyloid β burden or glial inflammation in young <i>App</i> ^{NL-G-F/+} -KI mice	37
2.4.4 UF PM exposure in aged <i>App</i> ^{NL-G-F/+} -KI and wild-type mice	40
2.4.5 Concentration of ambient particles in the 12 month old animal cohort	41
2.4.6 UF PM exposure impairs cognition in 12 month old wild- type and <i>App</i> ^{NL-G-F/+} -KI mice	41
2.4.6 UF PM exposure increases A β plaque load in <i>App</i> ^{NL-G-F/+} -KI mice with established pathology	46
2.4.7 UF PM exposure does not impact tight junction markers in the blood-brain barrier in 12 month <i>App</i> ^{NL-G-F/+} -KI or wild-type mice	51
2.4.8 UF PM exposure reduces total protein level of GLT-1 in both wild-type and <i>App</i> ^{NL-G-F/+} -KI mice	53
2.5 Discussion:	55
Chapter 3: <i>In Utero</i> exposure to ultra-fine particulate matter impairs cognition and increases neuroinflammation in aged mice and increases Amyloid β plaque load in AD model mice.....	60
3.1 Abstract:	60
3.2 Introduction:	60
3.3 Methods:.....	62
3.3.1 Animals.....	62
3.3.2 Exposure Paradigm.....	63
3.3.2 Cognitive Assessments	64
3.3.3 Protein Extraction and Western Blot Analysis	65
3.3.4 Immunofluorescent Staining.....	66
3.3.5 A β Quantitation	67
3.3.6 Statistical Analysis	67
3.4 Results:	67
3.4.1 UF PM exposure in utero impairs cognition in 12 month old wild-type and <i>App</i> ^{NL-G-F/+} -KI mice.....	67
3.4.2 In utero UF PM exposure decreases synaptic marker PSD95 and increases glia inflammation in combination with the <i>App</i> ^{NL-G-F/+} -KI genotype.....	68

3.4.3 UF PM exposure in utero increased amyloid β plaque load in adult <i>App^{NL-G-F/+}-KI</i> mice	74
3.5 Discussion:	76
Chapter 4: Astrocyte transport of glutamate and neuronal activity reciprocally modulate tau pathology in <i>Drosophila</i>	80
4.1 Preamble.....	80
4.2 Abstract	80
4.3 Introduction	81
4.4 Materials and Methods:.....	83
4.4.1 Fly Stocks:	83
4.4.2 Lifespan Analysis:	84
4.4.3 Negative Geotaxis Climbing Assay:.....	84
4.4.4 Immunohistochemistry:	84
4.4.5 Immunoblot:	85
4.4.6 Eye Morphology	86
4.4.7 Statistical Analysis:	86
4.5 Results	86
4.5.1 dEaat1 expression modulates lifespan and behavioral phenotypes <i>Drosophila</i> overexpressing human tau	86
4.5.2 Expression of hTau or loss of Eaat1 does not significantly alter overall synaptic or neuronal loss in <i>Drosophila</i> brain.....	88
4.5.3 Changes in dEaat1 glutamate transporter expression do not change the accumulation of insoluble tau.....	91
4.5.4 Repeated overstimulation of neurons in the <i>Drosophila</i> eye increases tau load	92
4.6 Discussion	93
Chapter 5: Discussion, future projects, and conclusion.....	97
5.1 Future research in the <i>App^{NL-G-F}-KI</i> model of AD	100
5.2 Tau models of AD and PM	101
5.3 Analysis of PM associated metals in the brain.....	102
5.4 Conclusion.....	103
References.....	104
Appendix A- Abbreviations.....	129

List of Tables

Chapter 1

Table 1. Particulate Matter Size Fractions.....10

List of Figures

Chapter 1

Figure 1. A depiction of primary deposition areas of particulate matter (PM) in the body and potential routes to affect the CNS. Larger particles (PM₁₀, orange) are trapped in the upper respiratory tract, while the fine (PM_{2.5}, green) and ultra-fine (PM_{0.1}, blue) fractions can penetrate deeply into the lung tissues. PM_{0.1} deposit in the alveoli and can cross into the interstitium and blood, where they may cause systemic effects. PM_{0.1} can also directly cross the olfactory epithelium into the CNS.....11

Figure 2. Proposed pathways by which PM exposure leads to neurotoxicity and cognitive deficits. Direct infiltration of PM into the brain can provide a pathway for metals and other neurotoxic chemicals to accumulate in neural tissues, and potentially provide a reactive surface. Systemic effects from PM infiltrating the blood via the alveoli include cardiovascular disease, which can lead to impaired cognition and promote AD pathology. Both pathways potentially contribute to the inflammatory, glial, and amyloid pathology responses observed in animal models and human studies. The cascade from these responses to neurotoxicity and cognitive loss is well documented, and consistent with results showing neuronal toxicity and behavioral effects observed with PM exposure.....23

Chapter 2

Figure 1: Exposure particle concentration. (A) Average particle count per cubic meter during the exposure period of *App*^{NL-G-F/+}-KI mice. (B) Average particle mass concentration during exposure for concentrated quasi-ultrafine PM (UF PM), total ambient air, and filtered air using the VACES system. Bars represent mean values, with error bars expressed as standard error of the mean.....34

Figure 2: UF PM exposure reduces memory task performance in young *App*^{NL-G-F/+}-KI mice. Object location memory (OLM) and object recognition memory (ORM) task results for *App*^{NL-G-F/+}-KI mice and synaptic marker quantification. Discrimination index is the difference between time spent exploring the novel object or object in novel place and the familiar as a percentage of the total time. (A) Discrimination index for OLM test. Quasi ultrafine particulate matter (UF PM) exposed mice showed significantly decreased ability to discriminate the novel object location compared to those exposed to filtered air. (B) Discrimination index for ORM. UF PM exposed mice showed decreased ability to discriminate the novel object compared to animals exposed to filtered air. Bars represent mean values, with error bars expressed as standard error of the mean (N =10 animals per group). * denotes p-value < 0.05.....35

Figure 3: UF PM exposure does not induce changes in synaptic markers in young *APP*^{NL-G-F/+}-KI mice. Quantification of synaptic markers PSD95 and synaptophysin by immunofluorescence and western blot. (A) Representative images of PSD95 (green) and synaptophysin (red) immunofluorescent staining and fluorescent intensity quantification for the CA1 region of the hippocampus. (B) Representative images of PSD95 (green) and synaptophysin (red) immunofluorescent staining taken from the parietal and somatosensory cortex and fluorescent

intensity quantification from the whole cortex. (C) Representative western blot of synaptophysin and PSD95 from hippocampal tissue samples with band intensity relative to tubulin. FA- Filtered Air, UF- UF PM, Tub- Tubulin. (D) Representative western blot of synaptophysin and PSD95 from cortical tissue with band intensity relative to tubulin. Bars represent mean values, with error bars expressed as standard error of the mean (N = 8 animals per group for immunostaining and N = 10 animals per group for immunoblot. Scale bars = 100 μ m). * denotes p value < 0.05.....36

Figure 4: A β deposition and protein load is unaffected by UF PM exposure in the 6 month old *App*^{NL-G-F/+}-KI mouse model Brain sections were stained with 82E1 antibody to detect A β plaques in *App*^{NL-G-F/+}-KI mice. (A) Representative images of cortical A β plaque burden from the parietal cortex in *App*^{NL-G-F/+}-KI mice exposed to filtered air or UF PM (left), and quantification of plaque burden expressed as percentage of the total area measured occupied by plaques (right). (B) Representative images of hippocampal A β plaque burden in *App*^{NL-G-F/+}-KI mice exposed to filtered air or UF PM from the hippocampal CA1 region (left), and quantification of plaque burden expressed as percentage of the total area measured occupied by plaques (right). In neither region was total plaque load increased. (C) Steady-state levels of full-length APP in tissue homogenates extracted from cortical and hippocampal tissues were not significantly affected by the PM exposure. FA- Filtered Air, UF- UF PM, Tub- Tubulin. (D) mRNA levels of *App* normalized to *Gapdh* mRNA. *App* mRNA levels from cortical tissue were also unaffected by the exposure. (E) No differences in soluble A β ₄₂ levels were found in the brain. Bars represent mean values, with error bars expressed as standard error of the mean (N = 8 animals per group for immunofluorescent staining and quantification, and N = 6 animals per group for immunoblot, V-PLEX, and qPCR. Scale bars = 100 μ m).....38

Figure 5: Glial markers GFAP and Iba1 do not increase with exposure to UF PM in 6 month old *App*^{NL-G-F/+}-KI mice (A) Representative images of microglial marker Iba1 (red) and A β (green) staining taken from the parietal cortex (top) and CA1 region of the hippocampus (bottom), as well as quantification of the mean fluorescent intensity of Iba1 staining for the cortex and hippocampus. Exposure to UF PM does not increase the levels of Iba1 in the brain. FA- Filtered Air, UF- UF PM. (B) Representative images of astrocytic marker GFAP (red) and A β (green) staining taken from the parietal cortex (top) and CA1 region of the hippocampus (bottom), as well as quantification of the mean fluorescent intensity of GFAP staining for the cortex and hippocampus. UF PM exposure does not change the levels of GFAP observed. (C) mRNA levels of cytokines *Il6* and *Il1 β* normalized to *Gapdh* mRNA. Neither *Il1 β* nor *Il6* mRNA levels from cortical tissue were significantly affected by the exposure status. (N = 8 animals per group for immunofluorescent staining and quantification, and N = 6 animals per group for immunoblot and qPCR. Scale bars = 100 μ m).....39

Figure 6: Aged exposure particle concentration. (A) Average particle count per cubic meter during the exposure period of *App*^{NL-G-F/+}-KI (APP) and wild-type (Wt) mice. (B) Average particle mass concentration during exposure for concentrated quasi-ultrafine PM (UF PM), total ambient air, and filtered air using the VACES system. Bars represent mean values, with error bars expressed as standard error of the mean.....41

Figure 7: UF PM exposure impairs memory in aged wild-type and *App^{NL-G-F/+}-KI* mice. Object location memory (OLM) and object recognition memory (ORM) task results for *App^{NL-G-F/+}-KI* (APP) and wild-type (Wt) mice. Discrimination index is the difference between time spent exploring the novel object or object in novel place and the familiar as a percentage of the total time. (A) Discrimination index for OLM test. Quasi ultrafine particulate matter (UF PM) exposed mice showed significantly decreased ability to discriminate the novel object location compared to those exposed to filtered air. (B) Discrimination index for ORM. UF PM exposed mice showed decreased ability to discriminate the novel object compared to animals exposed to filtered air. (N = 10-12 animals per group. Scale bars = 100 μ m). * denotes p value < 0.05, ** denotes p < 0.01, and *** denotes p < 0.001.....42

Figure 8: Synaptic markers do not change with UF PM exposure in aged *App^{NL-G-F/+}-KI* and wild-type mice. (A) Representative images of PSD95 (green) and synaptophysin (red) immunofluorescent staining and fluorescent intensity quantification from the parietal and somatosensory cortex in *App^{NL-G-F/+}-KI* (APP) and wild-type (Wt) mice. and fluorescent intensity quantification from the whole cortex. (B) Representative images of PSD95 (green) and synaptophysin (red) immunofluorescent staining taken from CA1 region of the hippocampus and quantification. (C) Representative western blot of synaptophysin and PSD95 from cortical tissue samples with band intensity relative to tubulin. (D) Representative western blot of synaptophysin and PSD95 from hippocampal tissue with band intensity relative to tubulin. Bars represent mean values, with error bars expressed as standard error of the mean (N = 4 animals per group for immunostaining and quantification and N = 4-6 animals per group for immunoblot. Scale bars = 100 μ m).....43

Figure 9: Entorhinal cortex reelin positive neurons are not reduced by UF PM. Representative images of reelin (red), NeuN (green), and merged staining in the entorhinal cortex and reelin positive neuron count in 12 month old wild-type (Wt) and *App^{NL-G-F/+}-KI* (APP) exposed to filtered air or quasi ultrafine PM. Bars represent mean values, with error bars expressed as standard error of the mean (N = 10 animals per group for behavior tests, N = 8 animals per group for immunostaining and quantification, and N = 10 animals per group for immunoblot. Scale bars = 100 μ m).....45

Figure 10: A β plaque burden is increased by UF PM exposure in the 12 month old *App^{NL-G-F/+}-KI* mouse model. Brain sections were stained with 82E1 antibody and ThioflavinS to detect diffuse and dense core A β plaques in 12 month old *App^{NL-G-F/+}-KI* (APP) mice. (A) Representative images of A β plaque burden detected by 82E1 from the parietal cortex (Cor) and CA1 region of the hippocampus (HC) in *App^{NL-G-F/+}-KI* mice exposed to filtered air or UF PM (top), and quantification of plaque burden expressed as percentage of the total area measured occupied by plaques (bottom). Area % covered by plaques increases with UF PM exposure in the cortex but not hippocampus. (B) Representative images of A β dense core plaque burden from the parietal cortex (Cor) and CA1 region of the hippocampus (HC) (top) and quantification of plaque burden (bottom). Dense core plaque burden in the cortex and hippocampus also increases with UF PM exposure. (C) Steady-state levels of full length APP in tissue homogenates extracted from cortical and hippocampal tissues were not significantly affected by the PM exposure. UF- UF PM. (D) mRNA levels of *App* normalized to *Gapdh* mRNA. *App* mRNA levels from cortical

tissue were also unaffected by the exposure. (E) No differences in insoluble A β ₄₀ or A β ₄₂ levels were found in the cortex or hippocampus by ELISA. Bars represent mean values, with error bars expressed as standard error of the mean (N = 6 animals per group for immunofluorescent staining and quantification, and N = 4 animals per group for immunoblot, V-PLEX, and qPCR. Scale bars = 100 μ m). * denotes p value < 0.05, ** denotes p < 0.01.....47

Figure 11: Glial markers GFAP and Iba1 do not increase with exposure to UF PM in 12 month old *App*^{NL-G-F/+}-KI mice. (A) Representative images of microglial marker Iba1 (red), CD68 (purple), and A β (green) staining from the parietal cortex (top) of wild-type (Wt) and *App*^{NL-G-F/+}-KI (APP) mice exposed to filtered air or ultra-fine PM and quantification of the mean fluorescent intensity of Iba1 staining for the cortex and hippocampus from all mice and total count of Iba1 and CD68 positive microglia in *App*^{NL-G-F/+}-KI mice (bottom). Exposure to UF PM does not increase the levels of Iba1 or Iba1+/CD68+ microglia in the brain in either group. (B) Representative images of astrocytic marker GFAP (red) and A β (green) staining from the parietal cortex (top) and quantification of the mean fluorescent intensity of GFAP staining for the cortex and hippocampus (bottom). UF PM exposure does not change the levels of GFAP observed in either group. (C) mRNA levels of cytokines *Il6* and *Il1 β* normalized to *Gapdh* mRNA. Neither *Il1 β* or *Il6* mRNA levels from cortical tissue were significantly affected by the exposure status or genotype. Bars represent mean values, with error bars as standard error of the mean (N = 6 animals per group for immunofluorescent staining and quantification, and N = 4 animals per group for immunoblot and qPCR. Scale bars = 100 μ m).....49

Figure 12: Tight junction markers do not decrease in wild-type or *App*^{NL-G-F/+}-KI mice exposure to UF PM (A) Representative images of ZO-1 staining of cerebral vasculature from the cortex in wild-type (Wt) and *App*^{NL-G-F/+}-KI (APP) mice exposed to filtered air or UF PM (left) and quantification of vascular width (right). No differences are seen across treatment or genotype. (B) Representative western blot of albumin in cortical protein extract. Differences between groups are not significant. (C) Representative western blot of tight junction marker Claudin-5 and (D) intercellular junction marker CD31 from vascular enriched protein samples. Neither genotype nor exposure status shows significant differences. Bars represent mean values, with error bars expressed as standard error of the mean (N = 4-5 animals per group for all assays. Scale bars = 100 μ m).....52

Figure 13: Levels of astrocytic glutamate transporter GLT-1 decrease in the hippocampus of mice exposed to UF PM (A) Representative western blots of GLT-1 protein levels relative to GFAP in the cortex (left) and hippocampus (right) from 6 month old *App*^{NL-G-F/+}-KI mice exposed to either filtered air or UF PM, with quantification of western blot band intensity (below). GLT-1 levels decrease in the hippocampus, but not cortex, of UF PM exposed animals. FA- Filtered air UF- UF PM. (B) Representative western blots of GLT-1 protein levels relative to GFAP in the cortex (left) and hippocampus (right) from 12 month old wild-type (Wt) or *App*^{NL-G-F/+}-KI (APP) mice exposed to either filtered air or UF PM with quantitation (below). GLT-1 is decreased in UF PM exposed animals compared to wild-type air exposed animals, but not within the *App*^{NL-G-F/+}-KI group. Bars represent mean values, with error bars expressed as standard error of the mean (N = 8 animals per group). * denotes p<0.05.....54

Chapter 3

Figure 1: UF PM exposure *in utero* impairs memory in aged wild-type and $App^{NL-G-F/+}$ -KI mice. Object location memory (OLM) and object recognition memory (ORM) task results for wild-type (Wt) and $App^{NL-G-F/+}$ -KI (APP) mice. Discrimination index is the difference between time spent exploring the novel object or object in novel place and the familiar as a percentage of the total time. (A) Discrimination index for the OLM task. UF PM exposed mice of either genotype mice showed significantly decreased ability to discriminate the novel object location compared to wild-type mice exposed to filtered air. (B) Discrimination index for ORM. $App^{NL-G-F/+}$ -KI UF PM exposed mice showed decreased ability to discriminate the novel object compared to wild-type animals exposed to filtered air. (N = 8-12 animals per group. Scale bars = 100 μ m). * denotes p value < 0.05 and ** denotes p < 0.01.....68

Figure 2: Synaptic marker PSD95 decreases in 12 month old mice with joint in utero UF PM exposure $App^{NL-G-F/+}$ -KI genotype. (A) Representative images of PSD95 (green) and synaptophysin (red) immunofluorescent staining taken from the parietal cortex with fluorescent intensity quantification from the whole cortex. PSD95 is decreased in the $App^{NL-G-F/+}$ -KI (APP) animals exposed to UF PM in utero as compared to wild-type (Wt) animals exposed to filtered air. (B) Representative images of PSD95 (green) and synaptophysin (red) immunofluorescent staining and fluorescent intensity quantification for the CA1 region of the hippocampus. As in the cortex, PSD95 is decreased in the $App^{NL-G-F/+}$ -KI animals exposed to UF PM (UF) in utero as compared to wild-type animals exposed to filtered air. (C) Representative western blot of synaptophysin and PSD95 from cortical tissue samples with band intensity relative to tubulin. (D) Representative western blot of synaptophysin and PSD95 from hippocampal tissue with band intensity relative to tubulin. Bars represent mean values, with error bars expressed as standard error of the mean (N = 4 animals per group. Scale bars = 100 μ m). * denotes p value < 0.05.....70

Figure 3: Glial marker GFAP increases with *in utero* exposure to UF PM in 12 month old $App^{NL-G-F/+}$ -KI mice. Iba1+/CD68+ microglia increase with *in utero* exposure to UF PM in 12 month old wild-type mice. (A) Representative images of microglial marker Iba1 (red), CD68 (purple), and A β (green) staining taken from the parietal cortex of wild-type (Wt) and $App^{NL-G-F/+}$ -KI (APP) mice exposed to filtered air or UF PM, as well as quantification of the mean fluorescent intensity of Iba1 staining and total count of Iba1 and CD68 positive microglia in $App^{NL-G-F/+}$ -KI mice from the cortex and hippocampus. Exposure to UF PM increases the number of Iba1+/CD68+ microglia in the cortex of wild-type animals, but not in $App^{NL-G-F/+}$ -KI animals. (B) Representative images of astrocytic marker GFAP (red) and A β (green) staining taken from the parietal cortex as well as quantification of the mean fluorescent intensity of GFAP staining for the cortex and hippocampus. UF PM exposure combined with $App^{NL-G-F/+}$ -KI genotype increases the levels of GFAP compared to wild-type animals exposed to filtered air. (C) Representative western blot of GLT-1 in the hippocampus and quantification. No changes are seen in GLT-1 levels. (N = 4-6 animals per group for immunofluorescent staining and quantification, and N = 6 animals per group for immunoblot. Scale bars = 100 μ m). * denotes p value < 0.05 and ** denotes p < 0.01.....72

Figure 4: A β plaque burden is increased in the cortex by *in utero* UF PM exposure in the 12 month old *App^{NL-G-F/+}-KI* mice.

Brain sections were stained with 82E1 antibody and Thioflavin-S to detect diffuse and dense core A β plaques in 12 month old *App^{NL-G-F/+}-KI* mice. (A) Representative images and quantification of total area of A β plaque burden detected by 82E1 from the parietal cortex (Cor, top) and CA1 region of the hippocampus (HC, bottom) in *App^{NL-G-F/+}-KI* (APP) mice exposed to filtered air or UF PM. Area % covered by plaques increases with UF PM exposure in the cortex, but not hippocampus. (B) Representative images of cortical and hippocampal A β dense core plaque burden from the parietal cortex (Cor, top) and CA1 region of the hippocampus (HC, bottom) and quantification of plaque burden for both. Dense core plaque burden does not increase with UF PM exposure. (C) Representative western blots and quantification. Steady-state levels of full length APP in tissue homogenates extracted from cortical and hippocampal tissues were not significantly affected by PM exposure in utero UF- UF PM. (D) Quantification of A β peptides. No differences in insoluble A β ₄₀ or A β ₄₂ levels in *App^{NL-G-F/+}-KI* mice were found in the brain by ELISA. Bars represent mean values, with error bars expressed as standard error of the mean (N = 6 animals per group for immunofluorescent staining and quantification, and N = 4 animals per group for immunoblot, V-PLEX, and qPCR. Scale bars = 100 μ m). * denotes p value < 0.05.....75

Chapter 4

Figure 1: RNAi decreased dEaat1 worsens and overexpressed dEaat1 partially rescues tau phenotypes.

(A) Survival curve of *nsyb>+(nSyb-LexA/+)*, *alrm>Eaat1.IR (UAS-Eaat1.dsRNA/Y;alrm-Gal4/+)*, *nsyb>tau (nSyb-LexA/+;LexAop-htau/+)*, *alrm>Eaat1.IR;nsyb>tau (UAS-Eaat1.dsRNA/Y;nSyb-LexA/alrm-Gal4;LexAop-htau/+)* flies, *alrm>Eaat1 (alrm-Gal4/+;UAS-Eaat1/+)*, and *alrm>Eaat1;nsyb;tau (nsyb-LexA/alrm-Gal4;LexAop-htau/UAS-Eaat1)* flies. By log rank test *alrm>Eaat1.IR* (p<0.001), *nsyb>tau* (p<0.001), *alrm>Eaat1.IR;nsyb>tau* (p<0.001), and *alrm>Eaat1;nsyb;tau* (p<0.001) show reduced lifespan compared to the control. *alrm>Eaat1.IR;nsyb>tau* flies have reduced lifespan as compared to both *alrm>Eaat1* (p<0.001) and *nsyb>tau* (p<0.001). *alrm>Eaat1;nsyb>tau* flies show increased lifespan compared to *nsyb>tau*, but reduced compared to *alrm>Eaat1*. n \geq 100 flies per genotype. (B) Climbing response, determined by the number of flies that climb \geq 8 cm in 10 seconds after mechanical impulse. Flies 3 days after eclosion were used to minimize age dependent performance decreases. *alrm>Eaat1.IR* (p<0.001), *nsyb>tau* (p<0.001), *alrm>Eaat1.IR;nsyb>tau* (p<0.001), and *alrm>Eaat1;nsyb;tau* (p<0.001) exhibited reduced response compared to *nsyb>+*, while *alrm>Eaat1* showed increased response (p<0.001). *alrm>Eaat1.IR;nsyb>tau* flies perform worse than *nsyb>tau* flies (p<0.01). n>= 5 independent biological replicates, with 10 flies per replicate. (C) Geotaxic response of control and test flies, expressed as a percentage of trials where 50% or more of the flies climbed \geq 8 cm by 180 seconds. n>=5. Each bar is the mean \pm standard error of the mean. ** p \leq 0.01, *** p \leq 0.001.....88

Figure 2: Human Tau expression shows no general neuronal loss but does induce reduction in a limited neuronal subset.

(A) Representative images of adult fly brains immunostained for the post-synaptic protein DLG1 for *nsyb*>+, *nsyb*>*tau*, *alrm*>*Eaat1.IR*;*nsyb*>*tau*, and *alrm*>*Eaat1.IR* flies. (B) Fluorescent quantification of total synaptic density in the central brain and protocerebrum structures by DLG1 staining of adult flies 12 days after eclosion. No differences were found between experimental genotypes. n = 5. (C) Representative western blot bands for DLG1 from whole brain homogenate with tubulin loading control. L- molecular weight ladder 1- *nsyb*>+ 2- *nsyb*>*tau* 3- *alrm*>*Eaat1.IR*;*nsyb*>*tau* 4- *alrm*>*Eaat1.IR*. (D) Densitometric quantification of DLG1 western blot band intensity normalized to tubulin loading control. n = 4. (E) PPL1 dopamine neuron cell bodies detected with anti-tyrosine hydroxylase (green) and anti-DLG1 (red). (F) Number of PPL1 cell bodies in adult flies 12 days after eclosion. n=4-9. Each bar is the mean \pm the standard error of the mean. ** $p \leq 0.01$, *** $p \leq 0.001$. Scale bars 100 μm90

Figure 3: Dysregulation of astrocytic dEaat1 does not affect human tau accumulation.

Protein samples taken from flies 10-12 days after eclosion, matching with the 50% survival point for the most severe phenotype (*alrm*>*Eaat1.IR*;*nsyb*>*tau*). (A) Representative western blot bands for soluble fraction human total (DAKO antibody) tau and phospho-tau (PHF1 antibody), with tubulin antibody for load control, of *nsyb*>+, *nsyb*>*tau*, *alrm*>*Eaat1.IR*;*nsyb*>*tau*, and *alrm*>*Eaat1*;*nsyb*>*tau* whole brain homogenate protein samples. Quantification of band intensity normalized to tubulin loading control. No difference between genotypes was found using two-way ANOVA. (B) Representative western blot bands for sarkosyl insoluble fraction total tau (DAKO antibody) and phospho-tau (PHF1 antibody) and quantification by band intensity. No difference between genotypes was found using two-way ANOVA. n=3-4. Each bar is the mean \pm the standard error of the mean.....91

Figure 4: Chronic activation of neurons in the eye increased tau accumulation.

(A) Brightfield images of the *Drosophila* eye of *GMR*>*TrpA1* (*GMR-Gal4/+;UAS-TrpA1/+*), *GMR*>*tau* (*GMR-Gal4/UAS-Tau^{wt}1.13*), and *GMR*>*TrpA1,tau* (*GMR-Gal4/UAS-Tau^{wt}1.13;UAS-TrpA1/+*) genotypes. *GMR*>*tau* and *GMR*>*TrpA1,tau* show roughness and reduced eye size. (B) Representative staining of *Drosophila* optic lobe neurons for human total tau of *GMR*>*TrpA1*, *GMR*>*tau*, and *GMR*>*TrpA1,tau* genotypes. (C) Representative staining of *Drosophila* optical lobe neurons for p-tau. (D) Fluorescence intensity quantification of tau immunofluorescence in the optic lobe in non-temperature treated *GMR*>*TrpA1*, *GMR*>*tau*, and *GMR*>*TrpA1,tau* flies. (E) Fluorescence intensity quantification of total human tau based immunofluorescence. (F) Fluorescence intensity quantification with p-tau antibody of optic lobes. N= 4-5. Each bar is the mean \pm the standard error of the mean. * $p \leq 0.05$, ** $p \leq 0.01$. Scale bars 50 μm93

Acknowledgements

I would like to acknowledge the support received from my colleagues, coworkers, and advisors at University of California, Merced (UCM) and University of California, Irvine (UCI) to successfully complete my dissertation project described here.

Foremost to my advisor, Professor Masashi Kitazawa, for providing the opportunity to work in his lab and his guidance, patience, and support in pursuing my degree.

I would like to thank the members of the Kitazawa lab both at UCM and UCI. To Dr. Carlos Rodriguez-Ortiz, Dr. Sharon Lim, and Dr. Heng Wei Hsu, thank you for guidance and assistance in learning, performing, and understanding experiments. To fellow students Joannee Zumkehr, Janielle Vidal, Barret Allen, Samantha Merwin, thank you for helping through my graduate work. Lastly, to my undergraduate workers Kenneth Mata (UCM) and Hansal Dalal (UCI), thank you for all of the work put into these projects.

I would like to thank Professor Fredrick Wolf, Dr. Greg Engel, Sarah Parkhurst, and Dr. Dan Landayan for their support of the work in Chapter 4 of this dissertation and guiding me in working with *Drosophila*.

I would like to thank Professor Michael Kleinman, Dr. David Herman, Rebecca Arechavala, Irene Hasen, and the rest of the members of the Kleinman lab at the UCI air pollution health effects lab. Your knowledge, assistance, and guidance in the realm of air pollution exposure was invaluable.

I would also like to thank Professor Frank LaFerla's lab at UCI for their help and access to equipment.

I would like to thank my other committee members Professor Stephen Bondy and Professor Kim Green for providing excellent feedback and direction in my research. Also, I thank Professor Virginia Kimonis and Professor Ulrike Luderer for agreeing to fill in for my advancement meeting and guidance provided there.

I would like to thank the following funding sources for this research: University of California, Merced Health Science Research Institute (HSRI) pilot seed grant (M.K. and F.W.W), the Alzheimer's Association grant (NIRG-12-242598, M.K.), and the National Institutes of Health (R01 ES024331, R21 ES028496).

I would like to thank Elsevier for granting permission to use copyrighted material in Chapter 4 of this dissertation.

Vita
JASON G. KILIAN

Education

PhD in Environmental Health Sciences toxicology emphasis UC Irvine School of Medicine	Spring 2020
PhD in Quantitative and Systems Biology UC Merced	Program Transfer 2016
BS in Genetics University of California, Davis	2010

Research Experience

1/2016-Present	Environmental Health Sciences Program, UC Irvine SoM. Graduate Researcher. Design experiments for testing Alzheimer's Disease model mice with exposure to air pollution. Support ongoing study of AD model mice exposure to environmental copper.
08/2013-12/2015	Quantitative and Systems Biology Program, UC Merced Graduate Researcher. Design and execute experiments in <i>Drosophila melanogaster</i> Alzheimer's Disease model. Support mouse model and cell culture AD research performed in the lab.

Teaching Experience

01/2017-03/2017	School of Biological Sciences, UC Irvine Teaching assistant for Evolution and Ecology lecture. Responsible for creating course material, leading discussion sections, and assigning discussion grade.
08/2014-05/2015	School of Natural Sciences, UC Merced Teaching Assistant for Microbiology laboratory course. Responsible for leading students in experiments in basic microbiology techniques and grading lab reports and tests.
01/2014-05/2014	School of Natural Sciences, UC Merced Teaching Assistant for Microbiology lecture. Responsible for leading discussion sections, creating activities, and all grading.
08/2013-12/2013	School of Natural Sciences, UC Merced Teaching Assistant for Introduction to Cell Biology. Aid professor with class load including grading and quiz creation and lead small

discussion and laboratory sections.

Publications

Hsu HW, Rodriguez-Ortiz CJ, Lim SL, Zumkehr J, Kilian JG, Vidal J, Kitazawa M. 2019. "Copper-Induced Upregulation of MicroRNAs Directs the Suppression of Endothelial LRP1 in Alzheimer's Disease Model." *Toxicological Sciences*. 170(1) 144-156.

Kilian, J, and Kitazawa, M. 2018. "The emerging risk of exposure to air pollution on cognitive decline and Alzheimer's disease – Evidence from epidemiological and animal studies." *Biomedical Journal*. 41(3) 141-162.

Kilian, J, Hsu HW, Mata K, Wolf FW, Kitazawa M. 2017. "Astrocyte transport of glutamate and neuronal activity reciprocally modulate tau pathology in *Drosophila*." *Neuroscience* 348 191-200. 10.1016/j.neuroscience.2017.02.011

Zumkehr J, Rodriguez-Ortiz CJ, Cheng D, Kieu Z, Wai T, Hawkins C, Kilian J, Lim SL, Medeiros R, Kitazawa M. 2015. "Ceftriaxone ameliorates tau pathology and cognitive decline via restoration of glial glutamate transporter in a mouse model of Alzheimer's disease." *Neurobiology of Aging*. 36(7) 2260-2271.

Conference Presentations

Kilian, J, Herman DA, Johnson R, Vidal J, Dalal H, Rodriguez-Ortiz CJ, Renusch SR, Kleinman MT, Kitazawa M. 2018. Exposure to Ultra-fine Particulate Matter Impairs Memory in APP Knock-in Mice without overt changes in Amyloid Pathology. Poster. Society of Toxicology annual meeting. Baltimore, Maryland.

Kilian, J, Herman DA, Johnson R, Hasen I, Ting A, Renusch SR, Kleinman MT, Kitazawa M. 2018. Chronic exposure to ultra-fine particulate matter exacerbates cognitive decline in the APP-KI mouse model of Alzheimer's disease. Poster. UCI ReMIND. Irvine, California.

Professional Memberships

- Society of Toxicology

Technical Skills

Protein, DNA, and RNA assays in animal tissue and cell culture including RT-PCR, immunoblot, ELISA, immunostaining, gel electrophoresis, and plasmid cloning
Process mouse and fly tissue samples for protein, RNA, DNA
Behavioral tests in *Drosophila melanogaster* and mice

Abstract

The effects of airborne ultra-fine particulate exposure on cognition and neuropathology in an amyloid model of Alzheimer's disease

Jason G. Kilian

Doctor of Philosophy in Environmental Health Sciences

University of California, Irvine

2020

Associate Professor Masashi Kitazawa, Chair

Alzheimer's disease (AD) is the leading cause of dementia among the elderly and sixth leading cause of death in the US. No effective therapeutic intervention is currently available to treat, cure or halt this devastating disease. The prevalence of AD is expected to rise rapidly in coming years and is predicted to overwhelm our socioeconomic reserves. Thus, unveiling critical pathogenic mechanisms of the disease and risk factors that modulate the disease progression and onset is an urgent matter to slow this upswell. While aging and genetics are unequivocal risk factors for AD, there is a growing evidence supporting the pivotal role of environmental or modifiable factors in contributing the onset of AD. Among them, air pollution has recently been highlighted as a prominent culprit accelerating cognitive decline and increasing a risk for AD. However, little work has been done to elucidate its underlying molecular mechanisms by which exposure to air pollution contributes to the pathological development of AD. The purpose of this dissertation is to investigate the neurotoxic effects of airborne particulates in a humanized amyloid mouse model of AD. Previous reports indicate that PM exposure in non-AD model mice increases inflammatory markers such as cytokines, glial activation, and oxidative stress in the CNS and may increase expression of native mouse amyloid or alter its processing. Thus, we **hypothesize that exposure to ultra-fine particulates exacerbates memory impairment by increasing neuroinflammation and amyloid β burden in a humanized amyloid mouse model**

of AD. To test this, we exposure wild-type and *App*^{NL-G-F/+}-KI mice to concentrated ultra-fine particulate matter both *in utero* and at adult ages. We show exposure dependent decreases in memory behavior tasks, as well as increases in A β plaque burden in the *App*^{NL-G-F/+}-KI model. However, memory impairment occurs independently of plaque burden increase, and only in the *in utero* exposure group were neuroinflammatory markers increased. In the adult exposure, we instead saw a decrease in the astrocytic glutamate transporter GLT-1. Previous work has shown a link between glutamate transporter loss and tau pathology, indicating a potential amyloid independent pathway linking particulate exposure and AD pathology. This research provides evidence of A β plaque burden increase dependent only on particulate exposure, as well as evidence that exposure during development impacts AD neuropathology in adult mice.

Chapter 1: Introduction

1.1 Dissertation Statement

Exposure to airborne ultra-fine particulate matter exacerbates memory impairment and neuropathology in an Alzheimer's disease mouse model, indicating potential mechanisms linking particulate matter exposure to Alzheimer's risk in humans.

1.2 Significance

Alzheimer's disease (AD) is the most common form of dementia among the elderly, with an estimated number of patients of over 5.8 million in the U.S. and 35 million worldwide (Alzheimer's Association, 2018, 2020). Death by AD and other dementias is about 1.6 million in 2015, which is doubled from 2000 and it is currently ranked at the sixth leading cause of death worldwide (WHO, 2017). These numbers will be doubled or even tripled as the aged population rapidly increases in next few decades (Alzheimer's Association, 2020), and such rapid increase in the number of AD cases will create major socioeconomic burdens among us unless effective therapeutic interventions to slow, halt, or cure this devastating disease are developed. In lieu of conquering the disease, the most expedient and actionable course to curb the predicted rise in AD cases is to identify and eliminate environmental factors that increase risk of the disease.

Advancing age is the single greatest risk factor for AD, and genetic predispositions have also contributed significant risks to the disease onset. Although these two risk factors have been extensively studied to better understand the pathogenesis of AD, they are intrinsic and not essentially modifiable in terms of delaying the onset and progression of the disease. In addition, aging and genetic risk factors do not fully explain the cause of every AD case, as large cohorts of

homozygote and heterozygote twin studies reveal key involvement of additional modifiable risk factors in AD etiology (Brusco et al., 1998; Gatz et al., 2006; McGeer et al., 1996; Sullivan et al., 2012). Those include, but are not limited to, lifestyle, disease history, educational background, dietary habits, and exposure to environmental and occupational hazards (Campdelacreu, 2014; Yegambaram et al., 2015). Environmental risk factors, such as metals and toxic contaminations in drinking water, exposure to agricultural chemicals, and air pollution, impact on large bodies of the population and influence the risk of AD. Chronic exposure to airborne environmental factors has been shown to increase the risk for developing AD through epidemiological studies and in animal models (Cacciottolo et al., 2017; Jung et al., 2015; Oudin et al., 2016). Further work is required to determine the extent of the association between air pollution and AD pathology, as well as the mechanisms by which it occurs.

1.3 Alzheimer's Disease: Background and Pathology

AD cases are broadly classified based on age of onset as either familial or sporadic. Sporadic AD represents the great majority of diagnosed cases, accounting for over 95% of AD cases (NIA, 2016). Sporadic AD is typically diagnosed at the age of 65 or older. While there is no single cause of sporadic AD, age is the largest risk factor, with risk doubling for every five years past age 65. Familial AD accounts for the remaining cases. As the name implies, familial AD is caused by genetic factors- namely mutations in amyloid precursor protein (APP) or proteins involved in processing it. Familial is also known as young onset AD, as symptoms commonly manifest in the patient's 40s or 50s. Clinical manifestations of the two forms are highly similar outside of age of onset.

Clinical diagnosis of AD in patients relies on neuropsychological assessments and cerebral imaging. The most common assessment tool is the Mini-Mental State Examination (MMSE),

which is a short 30-point questionnaire testing cognitive impairment (Folstein et al., 1975).

Lower scores indicating increasing cognitive impairment, measured as mild, moderate, or severe. Magnetic resonance imaging (MRI) and positron emission tomography (PET) scans are the most common imaging techniques used to detect pathology in living patients; MRIs detect atrophy and volume change while PET scans can detect activity alterations. Typically, brain abnormalities are first observed in the entorhinal cortex, with the amygdala, hippocampus, and parahippocampus following.

While work is ongoing to determine accurate biomarkers for definitive diagnosis of AD, currently full diagnosis is confirmed only with post-mortem histopathological study. The main pathological hallmarks of AD are the presence of senile plaques composed of amyloid β ($A\beta$), neurofibrillary tangles (NFTs) composed of the hyper-phosphorylated microtubule associate protein tau, and neuronal and synaptic loss. While all of these markers are considered hallmarks for AD pathology, synaptic loss best correlates with cognitive decline. However, familial AD occurs entirely due to mutations affecting APP processing that produces $A\beta$ or aggregation capacity of $A\beta$. Thus, abnormal production and buildup of $A\beta$ are typically considered the primary initiating factors in AD pathology. The exact molecular processes linking $A\beta$ to the downstream pathology of AD and cognitive decline are still under investigation.

1.4 Amyloid Precursor Protein and Amyloid- β

The *APP* gene is located on chromosome 21 and consists of 18 exons. Alternative splicing of *APP* creates many isoforms, but the three primary isoforms are 695, 751, or 770 amino acids in length (U. C. Müller & Deller, 2017; Walsh et al., 2007). All of these isoforms are type 1 transmembrane proteins, with the 695 amino acid isoform as the most prevalent in neurons and the brain (Nalivaeva & Turner, 2013). Secretase proteins cleave APP in either the

amyloidogenic or non-amyloidogenic pathways, depending on which secretases are involved. For the non-amyloidogenic pathway α -secretases cleave APP at the extracellular domain and γ -secretase complex cleaves in the cell membrane domain, producing sAPP α , the amyloid precursor intercellular domain (AICD), and the P3 fragment (Chow et al., 2010). The amyloidogenic pathway creates A β peptides, which in turn aggregate and eventually form the senile plaques found in AD patients (Glennner & Wong, 1984). APP is cleaved by β -secretase and γ -secretase, into sAPP β , the AICD, and the A β peptides (Chow et al., 2010; García-González et al., 2019). The A β peptides have a propensity to aggregate into oligomeric forms, which can be highly toxic (Haass & Selkoe, 2007). While the peptides can vary from 38-43 amino acids in length, the A β ₁₋₄₂ and A β ₁₋₄₀ species are the most associated with AD. A β ₁₋₄₀ is the more common peptide under normal physiological conditions, but A β ₁₋₄₂ has higher propensity to aggregate, having a disproportionate representation in senile plaques, and has been shown to be the more toxic peptide (Marina et al., 2003; Lennart Mucke & Selkoe, 2012; Murphy & Levine, 2010).

The normal physiological functions of APP and its derivatives are still not completely understood. Reviews of available evidence suggest that APP is involved in synapse formation, synaptic transport, CNS metal homeostasis, and hormone regulation (U. C. Müller & Deller, 2017; Nalivaeva & Turner, 2013; Tang, 2019). The sAPP α and sAPP β fragments contain binding domains for heparin, copper, and other factors (U. C. Müller & Deller, 2017). These fragments also exhibit neuroprotective effects and are important for long-term potentiation (LTP) as well as neurite outgrowth, respectively (Chasseigneaux et al., 2011; Xiong et al., 2017). AICD functions as a transcription regulator for genes related to proteins implicated in A β degradation and Ca²⁺ homeostasis (K. Chang & Suh, 2010; Leissring et al., 2002; T. Müller et

al., 2008). The A β peptide itself exhibits antimicrobial properties (Brothers et al., 2018), which may help protect the CNS. It also stimulates LTP and synaptic plasticity (Morley et al., 2010; Puzzo et al., 2011), and exhibits neuroprotective effects such as limiting excitotoxicity at normal physiological concentrations (Pearson & Peers, 2006; Soucek et al., 2003; Yu et al., 2006), indicating a varied and robust role in the brain under normal physiological function.

As mentioned previously, amyloidogenic APP processing sufficiently explains the pathogenesis of familial AD, which in turn strongly argues for A β as a key initiating factor in sporadic AD. The genetic factors that cause familial AD are either mutations in *APP* itself or in γ -secretase component genes *PSEN1* and *PSEN2* leading to increased A β production or higher ratios of the more pathogenic A β ₁₋₄₂ compared to other forms (Finckh et al., 2005; Johnston et al., 1994; Mann et al., 1996; Mullan et al., 1992; Murrell et al., 1991). Additionally, duplication of *APP* either directly or through an additional copy of chromosome 21 as seen in Down syndrome significantly increase risk of AD and speed the onset of the disease (Lautarescu et al., 2017; Sleegers et al., 2006; Wisniewski et al., 1985).

While A β plaques are considered a primary hallmark of AD pathology, they are found even in cognitively normal patients and plaque load does not correlate strongly with the strength of cognitive impairment (Dickson et al., 1992). On the other hand, in many animal models memory impairment is seen before plaque accumulation (Götz et al., 2018). However, various A β oligomers have been shown in animal models to disrupt cognition and memory, impair synaptic plasticity, and inhibit synaptic transmitter release, as well as exhibiting toxicity in cell culture (Cleary et al., 2005; He et al., 2019; Klein, 2013; Shankar et al., 2008). A β dimers have also induce hyperphosphorylation of tau, which leads to aggregation into the NFTs seen in AD (Jin et al., 2011). Clinically, in patients increasing A β oligomer levels in the CNS correlate with

advancing levels of cognitive decline, indicating a more direct role in impairing cognitive function than plaques (Jongbloed et al., 2015; Tomic et al., 2009). However, the exact role of A β peptides and plaques in AD pathogenesis remains unknown.

1.4.1 Tau Protein in AD Pathology

Along with the A β plaques, the other historical marker of AD is the presence of NFTs composed of hyperphosphorylated tau protein. There are six isoforms of tau in humans, described by the number of N-terminal inserts- from zero to two- and whether the protein has three or four microtubule binding domains (Y. Wang & Mandelkow, 2016). The primary function of the protein in the CNS is to stabilize axonal microtubules, though it is also implicated in protein translation and memory formation regulation (C. Li & Götz, 2017; Y. Wang & Mandelkow, 2016). However, the protein is vulnerable to hyperphosphorylation on threonine and serine residues by calcium-dependent kinases which causes dissociation from microtubules and aggregation into insoluble filaments (Cowan et al., 2010; Martin et al., 2013; Y. Wang & Mandelkow, 2016). These filaments further aggregate into the NFTs observed in AD and other diseases (Wolfe, 2012). In AD patients, tau pathology correlates more strongly with degenerated brain regions than A β , indicating that tau pathology may be more directly upstream of neurodegenerative outcomes (C. Li & Götz, 2017; Wolfe, 2012).

In animal models, tau has been shown to induce neurodegeneration and impair neurogenesis (Ballatore et al., 2007; Chatterjee et al., 2009; Komura et al., 2015; Wittmann et al., 2001). In AD models, A β species are known to induce tau hyperphosphorylation (Götz et al., 2000; Jin et al., 2011; Oddo et al., 2006), and in turn tau is a mediator of some aspects of A β induced toxicity, including hippocampal LTP impairment (Chapuis et al., 2013; L. M. Ittner et al., 2010;

Roberson et al., 2007; Shipton et al., 2011). Interestingly, tau pathology can itself induce further tau pathology in a positive feedback loop. This can occur either by inducing neuronal excitation, likely by impairing glutamate clearance (Dabir et al., 2006; Hunsberger et al., 2015; J. W. Wu et al., 2016), or through a prion like mechanism where hyperphosphorylated tau causes normal tau to dissociate from microtubules and convert to pathological tau (Alonso et al., 1996; J. W. Wu et al., 2013). These mechanisms also allow the propagation of tau pathology along linked neuronal pathways (De Calignon et al., 2012; J. W. Wu et al., 2016). Impairment of glutamate clearance also been shown to strongly contribute to neuronal loss and cognitive deficits in AD models itself (Dabir et al., 2006; Masliah et al., 1996; Mookherjee et al., 2011), and rescue of glutamate transport can ameliorate these effects (Takahashi et al., 2015; Zumkehr et al., 2015).

1.4.2 Inflammation

While A β oligomer accumulation is viewed as the major upstream event in AD pathogenesis, there is increasing evidence for a critical role of inflammation response in the progression of AD- particularly in the sporadic cases that constitute the majority of patients (Stephenson et al., 2018; Xu et al., 2016). Specifically, genome risk studies identify multiple risk genes for sporadic AD that are expressed highly by the brain's resident macrophage cells, microglia (Hansen et al., 2018; Hemonnot et al., 2019; Stephenson et al., 2018). Microglia are capable of recognizing and digesting A β to clear it from the CNS under normal conditions (Cho et al., 2014; Y. Liu et al., 2005; Paresce et al., 1996). However, similar to the rest of the body chronic immune activation can exhibit negative effects in the CNS (Hansen et al., 2018; Stephenson et al., 2018). Relevant to AD pathology progression, chronic inflammation has been shown to mediate pathology in AD models. Microglia impact synaptic loss in A β pathology, and are required for amyloid induced production of radical oxygen species (Coraci, 2002; Hong, 2016).

While they are critical for A β clearance under normal circumstances, in the disease state microglia contribute to seeding amyloid aggregation (Venegas, 2017). Inflammation induced by LPS increases tau hyperphosphorylation (Lee, 2010) and removal of microglia inhibits tau propagation, indicating the importance of microglia in tau pathology (Asai et al., 2015). Studies using colony-stimulating factor 1 receptor inhibitors, shown to remove the great majority of microglia in the adult mouse brain (Elmore et al., 2014), show rescue of memory function and neuronal loss without altering amyloid pathology (Dagher et al., 2015; Spangenberg et al., 2016). Overall, these studies argue for a complex and critical role of microglia and inflammation in AD pathogenesis. Thus, other insults leading to neuroinflammation are likely to exacerbate AD pathology and risk.

1.5 Alzheimer's Disease and Particulate Matter

1.5.1 Particulate Matter: Sources and Composition

Exposure to unhealthy levels of polluted air is a worldwide problem, particularly in heavily urbanized areas in developing or developed countries where the ambient levels of air pollution can be over 10 times more concentrated than recommended health guidelines suggest (WHO, 2016). Major constituents of air pollution are PM, nitrogen oxide species (NO_x), sulfur oxide species (SO_x), carbon monoxide, ozone, hydrocarbons, volatile organic compounds (VOCs), metals, and other inorganic chemicals. While pollutants from natural sources, such as volcanic activities, wildfires, dust, and coastal aerosols, are difficult to reduce, those released by human activities can be more reasonably curbed if found to adversely impact health to a sufficient degree. The major sources of human contribution are traffic- and industrial-related combustion of fossil fuels, mining, agricultural activities, and burning fossil and biomass fuels for cooking and heating (Craig et al., 2008; Karagulian et al., 2015; Mazzei et al., 2008; Simoneit et al.,

2004). PM found in the atmosphere is either generated directly from these sources as primary PM or a result of complex photochemical reactions of NO_x, SO_x, and ammonia released from motor vehicles, industrial combustion, and agricultural activities, respectively, as secondary PM (Valavandis et al., 2008). This gas-to-particle chemical conversion occurs within water droplets and aerosols in the atmosphere and produces ammonium nitrate as a nucleation step for PM formation. The ammonium nitrate core eventually grows and ages together with other constituents to form mature PM (K. M. Zhang et al., 2005). In certain regions, ammonium nitrate could take up over 50% of all chemical mass in PM (Kelly et al., 2013).

PM, also referred to as aerosol when present as a mixture in the air, includes a wide variety of microscopic liquid or solid matter in the atmosphere. Particulate contaminants can include biological elements such as pollen, bacteria, viruses, and spores, and suspended non-biological solids such as dust and smoke. Exact composition varies considerably based on its size, location, weather, the season, time of day, and a multitude of other factors. The major components of airborne particulates worldwide are sulfates, nitrates, ammonium, chlorides, elemental and organic carbon, biological materials, and minerals and dust (Harrison & Yin, 2000; Valavandis et al., 2008). The US EPA primarily divides PM into an “ultrafine” designation for PM <100 nm (PM_{0.1}), a “fine” fraction of PM of diameter 2.5 microns or less (PM_{2.5}), and a “coarse” fraction of PM between 2.5 and 10 microns (PM₁₀) (US EPA, 2004). While most components of PM can be found in all size fractions, the smaller PM fractions generally contain higher amounts of toxic metals, black carbon, gases, and other products of combustion while the coarse fraction contains more organic debris, road dust, dust from mechanical processes, and other resuspended materials (Geller et al., 2002; Sardar et al., 2005) (Table 1).

Table 1: Particulate Matter Size Fractions

Size Fraction	Designation	Diameter range (μm)	Major Constituents	Minor Constituents
Coarse PM	PM ₁₀	2.5 - 10	Metals, inorganic ions	Organic matter
Fine PM	PM _{2.5}	0.1 - 2.5	Inorganic ions	Metals, organic matter
Ultra-Fine PM	PM _{0.1}	≤ 0.1	Organic matter	Metals, inorganic ions

Table 1 shows the three common size fractions of PM as designated by the US EPA. Major (>25%) and minor constituents (<25%) are estimated by particle constituent mass from USC studies (Geller et al., 2002; Sardar et al., 2005); note that composition of PM can vary considerably with time and location, and that this is only a general estimate of the components of each size fraction.

The outlined size classifications are commonly used at least in part as the size and weight of the particles plays a major role in determining inhalability and particle deposition in the respiratory tract. While larger particles tend to deposit in and affect the upper respiratory tract, it is largely PM_{2.5} and ultrafine PM that deposit in the lungs (Brauer et al., 2001; Churg & Brauer, 2000). Once in the lung, the soluble components of fine PM are taken in by cells in the respiratory system (Bermudez et al., 2004; A. K. Müller et al., 2004; Stearns et al., 2001) and enter the blood stream (Kreyling et al., 2002; Nemmar et al., 2002)(Fig. 1). PM uptake to the lung cells and blood may act as a shuttle for other chemicals on the surface of the PM to penetrate to these areas (Seaton et al., 1995). PM has additionally been shown to impair the function of macrophages in the lung (Lundborg et al., 2001). While making up only a small percent of total PM by weight, ultrafine PM accounts for a majority of the total particle number and available surface area of PM (M. Chang et al., 2001; S. Kim et al., 2001; K. M. Zhang et al., 2005). In part due to these traits, which increase reaction surface and ability to carry other agents, ultrafine

PM is generally considered the most toxic form of PM (S. Kim et al., 2001; Valavandis et al., 2008). The ultrafine fraction causes increased oxidative stress and mitochondrial damage over larger sizes in macrophages and epithelial cells (N. Li et al., 2003). Evidence suggests that the ultrafine PM can directly infiltrate to the brain through olfactory nerves, and potentially penetrate to the CNS via systemic uptake (Block & Calderón-Garcidueñas, 2009; González-Maciel et al., 2017). Once in the CNS, PM may lead to inflammation response and oxidative damage, similar to what is seen in macrophages and the lungs (Calderón-Garcidueñas, Solt, et al., 2008; Kleinman et al., 2008). Vehicle exhaust is one of the most significant human contributions to $PM_{2.5}$ and $PM_{0.1}$ levels (Schauer et al., 1996; Viana et al., 2008). As PM tends to aggregate and increase in size over time (Zhu et al., 2002), sources of $PM_{2.5}$ to which people are immediately exposed, such as vehicle exhaust in traffic, have a higher impact on human exposure than more distant sources.

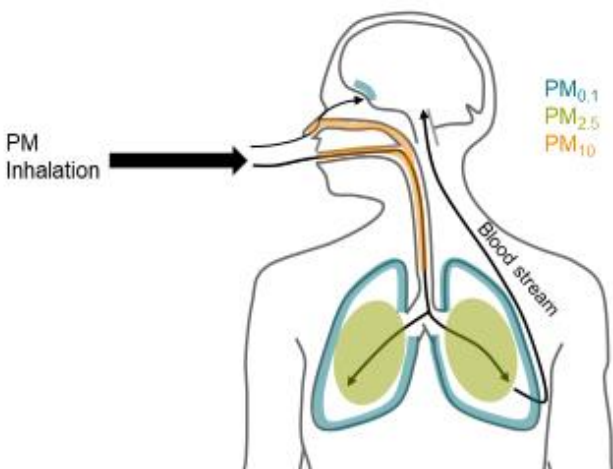


Figure 1: A depiction of primary deposition areas of particulate matter (PM) in the body and potential routes to affect the CNS. Larger particles (PM_{10} , orange) are trapped in the upper respiratory tract, while the fine ($PM_{2.5}$, green) and ultra-fine ($PM_{0.1}$, blue) fractions can penetrate deeply into the lung tissues. $PM_{0.1}$ deposit in the alveoli and can cross into the interstitium and blood, where they may cause systemic effects. $PM_{0.1}$ can also directly cross the olfactory epithelium into the CNS

In the U.S., it is estimated that over 43 million people live in areas where the air concentration of PM_{2.5} exceeds the EPA's 24 hour ambient air quality standard limit of 35 µg/m³, and 20 million people in the US live with exposure levels higher than the EPA long-term exposure standard of 12 µg/m³ year round average (ALA, 2018). These areas include major metropolitan regions such as the Los Angeles basin, which had 2015 average PM_{2.5} of 12.4 µg/m³, with 24 hour averages up to 70 µg/m³ (SCAQMD, 2016). Worldwide, the WHO estimates that 92% of the population lives in areas where WHO air quality guidelines (10 µg/m³ year average, 25 µg/m³ 24 hour average) are not met (WHO, 2016). WHO attributed an estimated 3 million premature deaths to ambient air pollution in 2012. PM levels in developing countries are still rising (van Donkelaar et al., 2014), leaving many people at risk of being exposed to unhealthy levels. In highly polluted areas such as Delhi, India, and Xingtai, China, experienced annual average PM_{2.5} level of over 120 µg/m³. Together, these data indicate the importance of exploring and understanding of the health ramifications of PM exposure.

1.5.2 Epidemiological Studies of PM and General Air Pollution Neuronal Disease Risk

It has been well-documented that exposure to polluted air and particulates is associated with cardiopulmonary mortality and morbidity since major incidents during the 20th century, such as the 1952 London Great Smog event (Khafaie et al., 2016; Pope & Dockery, 2006). It is only in the 21st century that epidemiological studies have begun to uncover a correlation between air pollution and accelerated intellectual and cognitive decline, including AD.

The adverse effect of polluted air on cognition can be caused by exposure as early as *in utero*. Exposure to polycyclic aromatic hydrocarbons (PAHs), a component of the PM organic carbon fraction, during pregnancy correlates with reduced Bayley scale of infant development (BSID-II) scores in the children at 3 years old and reduced verbal and full IQ at 5 years (Perera et al., 2006,

2009), and decreased non-verbal IQ scores at 5 years of age and verbal IQ at 7 years of age (Edwards et al., 2010; Jedrychowski et al., 2015). These studies suggest that PAH exposure during development is associated with delayed impairment of performance during childhood, as in all cases negative cognitive effects were not observed at earlier time points.

In addition to PAH, traffic associated gases are also commonly associated with decreased cognitive ability of children if exposed *in utero* (Guxens et al., 2014; Lertxundi et al., 2015; Porta et al., 2016). NO₂ exposure, PM_{2.5} exposure, and traffic intensity, but not PM₁₀, benzene, or reduced distance to roadways during pregnancy is correlated with reduced IQ performance in children (Lertxundi et al., 2015; Porta et al., 2016). A meta-analysis of six other European studies examining the effects of PM_{2.5}, PM₁₀, and NO₂ exposure during pregnancy on children 1 to 6 years old found the only significant association to be between NO₂ levels and psychomotor development deficit (Guxens et al., 2014). On the other hand, exposure to high levels of SO₂ and non-methane hydrocarbons, but not NO₂ and other pollutants, during 2nd or 3rd trimester pregnancy are found to be associated with reduced motor skills in infants at 6 and 18 months of age in Taiwan (C.-C. Lin et al., 2014). Overall, these studies show that exposures to certain constituents of polluted air during pregnancy likely exhibit adverse effect on cognitive performance of infants. However, the inconsistency between studies of whether a given active constituent causes impaired cognitive functions requires further investigation. Differences in study populations, the concentrations of pollutants seen in the studies, and times of exposure and endpoint testing may account for many the discrepancies. Another interesting possibility raised is that the overall mixture of air pollutants, depending on the constituents and concentrations, may elicit a complex and novel toxicity in the body.

Adverse effect of air pollution on cognition is not limited to *in utero* exposures. Increasing levels of NO₂ are associated with decreased gross motor skills at 5 years and memory span in 9 to 11 year old schoolchildren (Freire et al., 2010; van Kempen et al., 2012). Levels of black carbons are inversely associated with various intellectual performances including vocabulary, composite intelligence, and visual skills of learning and memory in children (Chiu et al., 2013; Suglia et al., 2008). Measuring performance of children living in areas with very high levels of air pollution, versus rural areas with relatively little pollution indicates that children in polluted areas are behind age normalized levels of multiple intelligence subscales, including full scale IQ and vocabulary, and have increased risk of poor psychomotor stability, motor coordination, and response time tests (Calderón-Garcidueñas et al., 2011; Calderón-Garcidueñas, Mora-Tiscareño, et al., 2008; S. Wang et al., 2009). Data using the Project Viva cohort in the U.S. indicated decreased non-verbal IQ in 8 year olds whose mothers lived in residences nearer to major roadways at the time of birth to child age 6 as compared to children of mothers who lived further from major roadways (Harris et al., 2015). These studies provide strong evidence that air pollution exposures, especially those related to PM levels such as black carbon and roadway distance, can negatively impact cognition during youth. The findings of reduced memory ability show that exposure to air pollutants can impact brain functions also affected by AD, and potentially has neurotoxic effect in the regions associated with those functions. Long term studies following from childhood to senescence are highly challenging, but it is interesting to consider that early life PM exposure extends its adverse effect in later life and triggers neurodegenerative diseases like AD.

Elderly adults who are exposed to polluted air also experience cognitive impairment. In China, Mexico and the U.S., elderly residents over 65 years old who live in areas with high air pollution

generally performed significantly worse on a mini-mental state examination (MMSE), one of common cognitive tests to assess dementia, than those living in cleaner areas (Sánchez-Rodríguez et al., 2006; Wellenius et al., 2012; Zeng et al., 2010). Black carbon, and PM_{2.5} are particularly associated with poor performance on MMSE among the elderly (Gatto et al., 2014; Power et al., 2011). It is estimated that every 10 µg/m³ annual average increase to black carbon exposure is equivalent to an extra two years of cognitive decline by aging (Power et al., 2011). A strong association between increased rate of errors in tests of working memory and orientation was observed in adults age 55 or older exposed to high levels of PM_{2.5} (J. A. Ailshire & Clarke, 2014), and with reduced episodic memory as compared to the group with low PM_{2.5} exposure (J. A. Ailshire & Crimmins, 2014; Younan et al., 2020). Elderly women exposed to high PM_{2.5-10} or PM_{2.5} levels for up to 14 years, as estimated by modeling of US EPA environmental data, have greater decline in global cognitive function than those in the lowest exposure level (Weuve et al., 2012). PM_{2.5} exposure was also linked to increase in cognitive disability, as determined by the World Health Organization Disability Assessment Schedule, in a study of populations from lower income countries (H. Lin et al., 2017). Other population-based studies identify PM_{2.5} and PM₁₀ levels associating with reduced memory scores in multiple tests (J. Ailshire et al., 2017; Tonne et al., 2014). Interestingly, PM_{2.5} and cognitive decline are much better correlated when neighborhood stressor factors, such as empty lots and abandoned buildings, are added (J. Ailshire et al., 2017). This study raises the important point that a combination of environmental factors may synergize in modulating the effects and must be considered when determining the impact of PM on cognition. It is also of note that a study focusing on younger adults, mean age approximately 37, found no significant association between PM₁₀ exposure levels and reduced cognition (J.-C. Chen & Schwartz, 2009). This could indicate that PM exposure is a more

significant risk factor in vulnerable populations, such as the elderly or children, than it is in healthy adults, though additional research in this age group is required to be sure they are not vulnerable.

Recent works demonstrate a correlation between airborne particulate matter exposure and risk for neurological disease outcomes, including AD and vascular dementia (VaD). A European study cohort of elderly women (<75 years) in Germany reveals that living within 50 meters of a busy roadway and PM exposure are correlated with lower executive function, olfactory function, and reduced cognitive performance relevant to AD by the Consortium to Establish a Registry for Alzheimer's Disease (CERAD) neuropsychological test battery (Ranft et al., 2009; Schikowski et al., 2015). A similar trend is observed in a Canadian cohort of ages 55-85, showing a significant adjusted hazard ratio (HR) for incident dementia at 1.07 for those living within 50 meters of the nearest major roadway compared to those living at a further distance (H. Chen, Kwong, Copes, Hystad, et al., 2017; H. Chen, Kwong, Copes, Tu, et al., 2017). PM_{2.5} exposure specifically is significantly associated with increased overall mild cognitive impairment (MCI) incidence and incidence of amnesic MCI in Germany (Tzivian et al., 2015), as well as AD, Parkinson's disease, and VaD risk in the U.S. and Taiwan (Jung et al., 2015; Kioumourtzoglou et al., 2016; Y.-C. Wu et al., 2015). Together, these studies show consistent evidence that AD risk is increased with exposure to higher levels of PM. As VaD and general dementia are also shown to be linked to PM exposure, it remains an open question whether AD risk is elevated more than other forms of dementia.

Genetic predisposition may play an important role in air pollution dementia risk. The *APOE* gene remains the strongest known genetic risk factor, and a few studies have examined whether air pollutant exposure risk is modulated by *APOE* allele status. Elderly women living in areas

with high PM_{2.5} concentrations, greater than the EPA recommended long term exposure limit of 12 µg/m³, are found to have increased risk of dementia which is exacerbated by *APOE ε4* status, with increasing risk when exposed to high levels PM in carriers of one copy of the allele and the highest risk with two copies (Cacciottolo et al., 2017). Similarly, traffic pollutant exposure was linked to impaired visuospatial function, but only in *APOE ε4* allele carriers (Schikowski et al., 2015). In a younger population, children with *APOE ε4* carrier status and in higher air pollution areas showed greatly increased risk of cognitive impairment compared to either factor alone (Calderón-Garcidueñas et al., 2016). The ability of *APOE* status to modulate risk of dementia and impaired cognition strongly suggests a gene-environment interaction in determining the likelihood of developing dementia.

1.5.3 Animal Studies of the effects of PM in the CNS

Growing bodies of epidemiological studies have unveiled pathological link between PM exposure and AD related cognitive decline. Underlying cellular and molecular mechanisms are being investigated using *in vivo* and *in vitro* models to provide powerful insight into understanding the etiopathogenesis of AD. In relatively the same environmental conditions as humans, dogs living in Mexico City with high levels of ambient air pollution develop white matter lesions, damage to the blood-brain barrier, degenerating neurons, oxidative damage, glial activation and neuroinflammation, as well as diffused Aβ plaques and neurofibrillary tangles, two key pathological hallmarks of AD, while dogs living in rural and less polluted areas of Mexico do not (Calderon-Garciduenas et al., 2003; Calderón-Garcidueñas, Mora-Tiscareño, et al., 2008). These studies suggest that PM adversely impacts neuroanatomical and neuropathological changes in the brain, leading to the development of AD-like pathology via

multifactorial mechanisms, including neurodegeneration, altered glial cell levels, amyloid processing, and immune response. However, as in the similarly structured epidemiological studies, the lack of tight control on the exposure paradigm leaves considerable room to question which components of air pollution are critical in these processes.

In the laboratory environment and under controlled exposure settings, different rodent models can exhibit various degrees of neuropathological signs and cognitive decline following PM exposure. These variances may be in part due to different strain background, varying PM concentrations and constituents, or exposure paradigm differences; however, these *in vivo* studies still provide significant insights into the neurotoxic effects of PM exposure and may allow us to decipher underlying mechanisms linking to the development of dementia and AD. High levels of ultrafine PM for short durations (2-6 weeks) in mice elicit significant increases in pro-inflammatory cytokines interleukin-1 α (IL-1 α) and tumor necrosis factor- α (TNF α), glial responses, activation of NF- κ B and AP-1 transcriptional factors in brain tissue, and glutathione redox imbalance (Campbell et al., 2005; Kleinman et al., 2008; Park et al., 2020). Increased brain inflammation, measured by IL-1 α , IL-1 β , TNF α , heme oxygenase-1 (HO-1), glial fibrillary acidic protein (GFAP), CD14, or CD68 mRNA, is also observed in C57BL/6 mice and Wistar rats exposed to nanoscale PM, ultra-fine PM, or PM_{2.5} after 6 to 10 weeks of exposure (Cheng et al., 2016; Guerra et al., 2013; Morgan et al., 2011). Long term exposure (30-39 weeks) to concentrated PM_{2.5} in young mice induces similar changes in inflammatory responses, as measured by TNF α , IL-10, IL-13, eotaxins, and HO1 mRNA or protein in the brain (Bhatt et al., 2015; Fonken et al., 2011). *Ex vivo* hippocampal slices from mice treated with PM had buildup of A β and NMDA receptor mediated neurotoxicity, and media taken from PM treated glial cells impaired neurite outgrowth (Morgan et al., 2011). These data strengthen the hypothesis that

immune activation may be a critical pathway for air pollutants to affect the CNS and establish a role for glial cells and oxidative damage in the brain in response to PM exposure.

Exposed mice develop multiple AD related pathologies and changes in the CNS. Long term PM exposure leads to a significant loss of dendritic spine density and dendrite length in the CA1 region of the hippocampus, which correlates with impaired cognitive outcomes (Fonken et al., 2011), and increases β -secretase (BACE) expression (Bhatt et al., 2015). Upregulation of BACE is suspected to promote amyloidogenic pathway of APP processing and increase the production of A β in the exposed mice. Exposure to very concentrated (1 mg/m³) PM_{2.5} or nickel nanoparticles can increase the A β ₄₂ and tau load in the CNS (S. H. Kim et al., 2012; Levesque et al., 2011), as did a lower level exposure to ultrafine PM (Park et al., 2020). Levels of hyperphosphorylated tau also increase in mice exposed to PM (Calderón-Garcidueñas et al., 2018, 2020). These findings bridge the association between chronic exposure to PM and inflammation and the development of AD-like neuropathology coupled with cognitive decline, demonstrating that PM and other inhaled exposures can lead to neuronal loss similar to what is seen in AD and other neurodegenerative diseases in animal models over longer exposures.

Although there is strong epidemiological evidence that developmental and early life PM exposures can have significant effects on cognitive function, there are currently limited animal model studies examining pre-natal and post-natal during development exposures. Rats exposed to PM_{2.5} for 24 hours per day either during gestation, post-natal until testing and sacrifice at 5 months of age, or both, showed changes in oxidative damage indicated by MDA, SOD, and tGSH protein levels, and reduced short-term discriminative memory and habituation, but only with both exposures (Zanchi et al., 2010). This suggests early life exposure as a possible potentiating factor to effects of exposure later in life. Mice exposed to concentrated ambient

ultra-fine particulates either during post-natal days 4-7 and 10-13, post-natal days 56-60, or both showed deficiencies in the novel object recognition (NOR) and Fixed-interval schedule control performance tasks at 10 weeks of age (Allen et al., 2013; Allen, Liu, Pelkowski, et al., 2014; Allen, Liu, Weston, et al., 2014). Levels of multiple neurotransmitters, cytokines, and GFAP were also altered with exposures, though there was considerable variance in which exposure groups saw significant changes and large variance between sexes. As the tissues were not harvested until 9 months, it is difficult to directly compare the protein changes in the brain with behavior performance. Mice exposed to PM_{2.5} during gestation exhibited decreased spatial memory in the cross maze task and higher anxiety as assessed by a light-dark box, as well as changes in COX2 and synaptophysin levels (Kulas et al., 2018). In all, these studies suggest that exposure during development causes both immediate and long-term molecular changes in the CNS that need to be further investigated.

Studies of PM exposure effects in AD model animals are limited but indicate PM's role in exacerbating AD pathology. 5xFAD mice with either the $\epsilon 3$ or $\epsilon 4$ allele of *APOE* exposed to ultra-fine ambient concentrated PM from the Los Angeles, CA area (Cacciottolo et al., 2017). Cerebral cortex sections showed significant increases in A β plaques, thioflavin S staining, and A β oligomers, but only with the $\epsilon 4$ allele. Decreases in the AMPA receptor subunit GluR1 and CA1 neurite density were also observed but were not dependent on *APOE* allele status. These findings demonstrate pathological changes that may explain the link between *APOE* $\epsilon 4$ carrier status and increased risk for cognitive impairment seen in epidemiological studies (Cacciottolo et al., 2017; Calderón-Garcidueñas et al., 2016; Schikowski et al., 2015). 12 month old triple transgenic mice (3xTg-AD) exposed to ultrafine PM had decreased performance in spatial learning and memory tasks, but the decrease was not significantly different from what is

observed in wild type animals (Jew et al., 2019); A β pathology was not assessed. Ex vivo hippocampal tissue slices from 3xTg-AD mice cultured with PM show increased A β load, glial activation, and PARP-1 activation (Jang et al., 2018). Inhibition of PARP-1 reduced the effects, suggesting the involvement of DNA repair pathways in PM mediated AD exacerbation. Since exacerbation of A β load has also been shown in wild type mice as described above (Bhatt et al., 2015; S. H. Kim et al., 2012; Levesque et al., 2011), determining whether PM acts through any AD specific pathways in addition to inflammation response, ROS generation, and PARP-1 is of interest.

1.5.4 Human Studies of PM Effects on the Central Nervous System

Studies in humans primarily consist of studies in younger age group performed by comparing Mexico City residents to those living in less polluted areas of Mexico. MRI scans showed increased white-matter hyperintensity in Mexico City children and young adults compared to controls, and minor decreases in bilateral and parietal temporal lobe white matter volume, while necropsy tissue shows white matter lesions and disruption of the blood-brain barrier based on staining of tight junctions (Calderón-Garcidueñas et al., 2011; Calderón-Garcidueñas, Mora-Tiscareño, et al., 2008; Calderón-Garcidueñas, Solt, et al., 2008). Blood, urine, and necropsy tissue sample from children and adults showed increases in multiple cytokines, inflammatory response markers, and oxidative stress markers, including COX2, IL-1 β , IL-12, NF- κ B, CD14, TNF α , and down regulation of prion-related protein PrPC in multiple brain tissues for those living in Mexico City (Calderón-Garcidueñas et al., 2004; Calderón-Garcidueñas, Mora-Tiscareño, et al., 2008). Children and young adults living in the high pollution area exhibited greater amounts of A β ₄₂ immunoreactivity, A β diffuse plaques, and hyperphosphorylated tau pre-tangles in the olfactory bulb, hippocampus, and cortical neurons than subjects in low

pollution areas (Calderón-Garcidueas, Kavanaugh, et al., 2012; Calderón-Garcidueñas et al., 2004, 2020; Calderón-Garcidueñas, Solt, et al., 2008). Critically, subjects homozygous for *APOE* $\epsilon 4$ had more A β plaque pathology, A β_{42} immunoreactivity, and hyperphosphorylated tau, and performed worse in olfaction tests, than those with the $\epsilon 3$ allele (Calderón-Garcidueas, Kavanaugh, et al., 2012; Calderón-Garcidueñas, Solt, et al., 2008). A separate group performed a MRI study of children ages 8-12 and found a correlation between higher levels of PM_{2.5} elemental carbon and NO₂ with indications of slower maturation (Pujol et al., 2016). In older patients, MRI scans showed increasing similarity to patterns seen in AD patients with increasing PM_{2.5} exposure (Younan et al., 2020). These studies indicate that the animal model and *in vitro* findings that PM exposure can affect amyloid processing and inflammation response are also present in humans and help validate further use of those models in further investigations. They also demonstrate overt neurotoxicity and vascular damage in the brain similar to what the group observed in canines, suggesting a potential mechanism for cognitive impairment due to pollution exposure in humans. However, as the majority of this work has been performed by one group in the same area and populations, additional studies with expanded scope may be required for extrapolation to the population at large. These findings further strengthen the epidemiological and animal model evidence that environmental exposure may particularly exacerbate pathology in tandem with AD risk genes, emphasizing the importance of studying these interactions.

Summarizing the current information on PM effects in the CNS, studies *in vitro* and *in vivo*, both animal model and human, show PM exposure involvement in inflammatory pathways, oxidative stress, and amyloidogenesis, as well as negative effect on cognition and behaviors in animals, providing potential mechanisms by which PM exposure can increase AD risk (Fig. 2). Additional research is required to determine which of these pathways, if any, are the major

factors in increasing AD risk, and whether the risk association between PM exposure and AD is specific to AD, or largely caused by general insult.

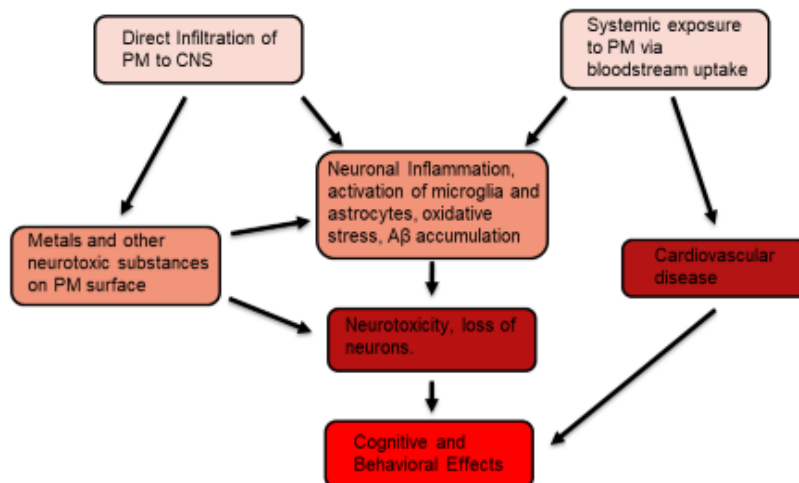


Figure 2: Proposed pathways by which PM exposure leads to neurotoxicity and cognitive deficits. Direct infiltration of PM into the brain can provide a pathway for metals and other neurotoxic chemicals to accumulate in neural tissues, and potentially provide a reactive surface. Systemic effects from PM infiltrating the blood via the alveoli include cardiovascular disease, which can lead to impaired cognition and promote AD pathology. Both pathways potentially contribute to the inflammatory, glial, and amyloid pathology responses observed in animal models and human studies. The cascade from these responses to neurotoxicity and cognitive loss is well documented, and consistent with results showing neuronal toxicity and behavioral effects observed with PM exposure.

1.6 Hypothesis

Exposure to the ultrafine fraction of airborne particulate matter exacerbates memory loss by increasing inflammation and A β pathology build up in the humanized APP animal model of AD.

1.7 Dissertation Contribution

- ❖ Adult and *in utero* exposure to ultrafine particulate matter impairs memory in adult wild-type and *App*^{NL-G-F/+} mice.
- ❖ UF PM exposure at adult age in mice:

- Increases amyloid plaque burden, but only after plaque pathology onset in the AD model
- Does not increase astrocyte or microglia activation
- Decreases total protein levels of the astrocytic glutamate transporter GLT-1 in both wild-type and the AD model
- Memory impairment in the adult AD model due to UF PM exposure occurs without changes in glia activation and before effects on amyloid pathology.
- Glutamate transport disruption is implicated as a potential mechanism
- ❖ UF PM exposure *in utero* effects in adult mice:
 - Increases astrocyte response when paired with the $App^{NL-G-F/+}$ genotype
 - Increases Iba1+/CD68+ microglia only in the wild-type
 - Increases amyloid plaque build up in the AD model
 - Early life exposure to UF PM can impact AD like pathology at later life in mice
- ❖ In a *Drosophila* tauopathy model:
 - increase or loss of GLT-1 homolog dEaat1 directionally modulates lifespan loss and geotaxic response.
 - Direct neuronal excitation increases tau propagation.

1.8 Conclusion

Exposure to airborne ultra-fine particulates exacerbates memory loss and AD like pathology in $App^{NL-G-F/+}$ -KI mouse model of AD. However, adult and *in utero* exposure may impact adult neuropathology through different pathways. Glutamate transport may be impacted, which suggests a connection to tau pathology, requiring further study.

Chapter 2: Exposure to ultra-fine particulate matter impairs memory function and exacerbates amyloid pathology in the *App*^{NL-G-F} knock-in mouse model

2.1 Abstract:

Exposure to traffic-related air pollution consisting of particulate matter (PM), nitrogen oxides, and volatile organic compounds, is associated with cognitive decline and memory impairment in wide spectrum of age groups. Among elderly, growing evidence suggests that PM contributes to accelerated onset of Alzheimer's disease (AD) and other forms of dementia. Here, we examined the impact of PM exposure on cognition and neuropathology in wild-type mice and a knock-in mouse model of AD (*App*^{NL-G-F/+}-KI). Three-month exposure to concentrated ultrafine PM from ambient air resulted in a marked impairment of memory tasks in young, pre-pathological *App*^{NL-G-F/+}-KI mice without measurable changes in amyloid- β (A β) pathology, synaptic degeneration, and neuroinflammation. The same duration of exposure in older mice, both wild-type and *App*^{NL-G-F/+}-KI, showed similar decline in memory tasks without overt changes in synaptic proteins or inflammation. However, A β plaque burden was significantly increased in the *App*^{NL-G-F/+}-KI mice exposed to ultrafine PM. Both age groups also exhibit a decrease in the astrocytic glutamate transporter, which may suggest future experiments to determine the mechanisms behind the reduction in memory performance with ultrafine PM exposure.

2.2 Introduction:

Generation and dispersion of fine and ultrafine particulate matter (PM) from automobiles and other anthropogenic activities constitutes a major part of air pollution (Karagulian et al., 2015; Mazzei et al., 2008), which in turn contributed substantially to the global public health concern and disease burden (Cohen et al., 2017). While exposure to PM and other toxic constituents in

polluted air are well known to increase morbidity and mortality from cardiovascular and cardiopulmonary diseases (Khafaie et al., 2016; Pope & Dockery, 2006), growing evidence from multiple epidemiological studies worldwide unveils a strong association between exposure to air pollution and accelerated cognitive decline and memory impairment across a wide spectrum of ages, from infants to the elderly (Freire et al., 2010; Guxens et al., 2014; Jedrychowski et al., 2015; X. Zhang et al., 2018). Among elderly populations, exposure to traffic-related pollution, which consists primarily of fine and ultrafine PM, nitrous oxides, carbon monoxide and dioxide, hydrocarbons, and volatile organic compounds (Westerdahl et al., 2009; Zavala et al., 2013), significantly increases the risk of dementia including Alzheimer's disease (AD) and other neurological disorders (Cacciottolo et al., 2017; H. Chen, Kwong, Copes, Hystad, et al., 2017; Jung et al., 2015; Oudin et al., 2016). However, the precise neurotoxic mechanisms of PM and other constituents leading to cognitive decline and potential neurodegeneration remain largely unknown.

In animal models, ultrafine PM (UF PM, aerodynamic diameter $\leq 0.1 \mu\text{m}$) can infiltrate the central nervous system (CNS) via the olfactory epithelium (Block & Calderón-Garcidueñas, 2009; González-Maciel et al., 2017), and its chronic exposure recapitulates certain aspects of cognitive decline, synaptic loss, and/or buildup of amyloid- β ($A\beta$) species (Bhatt et al., 2015; Cacciottolo et al., 2017; Durga et al., 2015; Fonken et al., 2011). These studies suggest that PM perturbs inflammatory homeostasis by increasing levels of the inflammatory cytokines, such as interleukin (IL)-6, IL-1 β , and tumor necrosis factor- α (TNF- α) (Fonken et al., 2011; Guerra et al., 2013). Total $A\beta$ load (Bhatt et al., 2015; Cacciottolo et al., 2017) and pathogenic $A\beta_{42}$ (Durga et al., 2015) are also increased due to PM exposure, suggesting a possible connection between PM and AD. Age-related inflammatory dyshomeostasis and perturbed microglia

functions associated with increased cytokine levels- similar to what is seen with PM exposure- have been linked to pathological buildup of A β and loss of synapses and neuronal integrity (Heppner et al., 2015; W. Y. Wang et al., 2015). It remains unclear if the pathways leading to A β buildup and increased inflammatory cytokines operate independently in relation to PM exposure. Here, we hypothesized that chronic exposure to concentrated fine and ultrafine PM from ambient air accelerates cognitive decline through aberrant neuroinflammation and buildup of AD-like neuropathology in the brain. We tested this hypothesis using a recently generated *App* knock-in mouse model of AD (*App*^{NL-G-F-KI}) (Saito et al., 2014). We examined the effect of PM exposure in young, pre-pathological, mice as well as in older mice in order to determine whether early-life exposure substantially accelerates age-related pathological changes in the brain of these mice.

2.3 Methods:

2.3.1 Animals

All experiments were performed in accordance with the Institutional Animal Care and Use Committee at University of California. Mice were housed on a 12 hour light-dark cycle with feed and water ad libitum. Humanized APP with the Swedish, Arctic, and Iberian mutations (*App*^{NL-G-F-KI}) mice in the C57BL/6 background (Saito et al., 2014) were obtained from the RIKEN Institute (Japan) and maintained as heterozygous *App*^{NL-G-F/+}-KI by crossing with C57BL/6J mice. *App*^{NL-G-F/+}-KI animals were either 3 or 9 months of age at the start of exposure start and animal were sacrificed at 6 or 12 months of age, respectively. C57BL/6J male and female mice were obtained from Jackson Laboratory (Bar Harbor, ME). In total 60 *App*^{NL-G-F/+}-KI mice and 36 C57BL/6J mice were used in this experiment. 24 *APP*^{NL-G-F/+}-KI animals, 12 male and 12 female, were used at the 6 month time point. 20 *App*^{NL-G-F/+}-KI mice and 20

C57BL/6J mice, divided evenly at 10 male and 10 female mice per group, were used for the 12 month time point.

2.3.2 Exposure Paradigm

Ambient particles in the area around the UC Irvine area in Orange County, California with particle diameters smaller than 180 nm (quasi-ultra-fine particles) were concentrated using a versatile aerosol concentration and enrichment system (VACES) as previously described (S. Kim et al., 2001). The VACES consists of size selective inlets, saturator/chiller modules that supersaturate the aerosol with water vapor causing ultrafine particles to grow to a size that can be inertially separated using a virtual impactor, and a diffusion drier module that removes excess water vapor and returns the aerosol to a size distribution similar to the ambient air. The system can enrich the concentration of particles in the 0.03 - 2.0 μm size range by a factor of up to of 30x ambient, depending on output flow rate. The VACES system is located adjacent to a major roadway in Irvine, CA, and exposure occurs over morning commute hours to emphasize motor vehicle associated PM. Starting at 3 or 9 months of age, *App*^{NL-G-F/+}-KI mice were exposed to either air filtered to remove particulate matter or concentrated UF PM. Animals were exposed 4 days per week (Tuesday – Friday), for 5 hours per day, for 12 weeks, from 07:30-12:30 local time, which captured the period of maximum PM concentration during the day. Our concentrated PM exposure regimen was still within the range of environmentally-relevant concentrations in those highly polluted areas (Moreno et al., 2008). The 4 days/wk exposure paradigm reflects typical air pollution episodes (Kleinman et al. 2005, Kleinman et al. 2007). Animals were sacrificed immediately following exposure end for tissue collection. Particulate mass and particle counts were obtained using a DustTrak aerosol monitor with DustTrak Pro

software (TSI) and a Condensation Particle Counter with Aerosol Instrument Manager software (TSI).

2.3.3 Cognitive Assessments

Animals in the were tested in Object Location Memory (OLM) and Object Recognition Memory (ORM) tasks. OLM was performed 3 weeks from exposure end. ORM was run following a 1 week break period after OLM testing. These tasks were performed based on a previously described protocol (Vogel-Ciernia & Wood, 2014). For both tests, animals were habituated to the test arena for 6 days, 5 minutes per day, and then exposed to two identical objects for 10 minutes for training. Different base objects were used for ORM and OLM acquisition. Testing occurred 24 hours following training. In the OLM task one of the two objects was moved to a new location, while for ORM one of the objects was replaced with a novel object. Replaced or moved objects alternated between mice. Mice were allowed to explore during the test for 5 minutes. Both test and training exploration were recorded, with the video used to score animal performance. Total time spent exploring each object- determined as time with the animal's nose within 1 cm of the object and pointing directly at the object- was recorded. Time exploring each of the two objects was summed to obtain total exploration time. Animals showing a strong preference for exploring one object over the other during the acquisition phase were removed from the final analysis pool. The discrimination index was calculated as the difference between time spent exploring the novel object or location and time spent exploring the familiar object or location expressed as a percentage of the total time spent exploring during the test phase.

2.3.4 Protein Extraction and Western Blot Analysis

Half brain cortical tissue and hippocampi were homogenized in T-PER buffer with protease and phosphatase inhibitor cocktails (Thermo Fisher). Protein extract was then centrifuged at 100,000

x g for 1 hour at 4°C and the supernatant was taken as the detergent soluble fraction. The pellet was resuspended in 88% formic acid and centrifuged again at 100,000 x g for 1 hour at 4°C and the supernatant from this step was taken as the formic acid soluble fraction. For the vascular enriched protein samples, half brains were homogenized in sucrose buffer (0.32M sucrose, 3mM HEPES, Fisher) using a glass Dounce homogenizer. Samples were centrifuged at 1,000 x g for 10 minutes at 4°C. This process was repeated for the resultant pellet. The pellet was then re-homogenized and centrifuged at 100 x g for 30 seconds with the supernatant kept, and this process repeated once. The supernatant fractions were pooled and spun for 2 minutes at 200 x g, and this final pellet was resuspended in 0.1% BSA (ThermoFisher) as the vascular enriched protein fraction. Protein concentration was determined by the Bradford protein assay. Protein samples were run on Bio-Rad Mini-PROTEAN® TGX™ gels (Bio-Rad) at 150V and transferred to Immobilon®-FL PVDF membranes (Millipore). After 1 hour blocking in Li-Cor Odyssey® Blocking Buffer in TBS (Li-Cor Biosciences), membranes were immunoblotted with the following antibodies overnight at 4°C: Glyceraldehyde-3-phosphate dehydrogenase (GAPDH, 1:1,000, Santa Cruz Biotechnology), tubulin (1:25,000 Abcam), post synaptic density protein 95 kDa (PSD95, 1:1,000, Cell Signaling Technology), synaptophysin (1:1,000, Cell Signaling Technology), glial fibrillary acidic protein (GFAP, 1:1000, DAKO), Iba1 (1:1,000, Abcam), GLT-1 (1:500, a gift from Dr. Jeffery Rothstein at Johns Hopkins University), amyloid precursor protein, c-terminal (751-770) (CT-20, 1:1000, EMDMillipore), CD31 (1:1,000, Abcam), or Claudin-5 (1:500, Thermo Fisher). Membranes were then washed, incubated for 1 hour at room temperature with secondary antibodies Goat anti Rabbit or Goat anti Mouse IRDye® 680 and 800 (1:20000 Li-Cir Biosciences), washed again and read. Blots were read using the Li-Cor Odyssey system and Image Studio software version 5 (Li-Cor Biosciences) to obtain band signal intensity.

Signal is expressed relative to tubulin or GAPDH levels, which were used for protein loading control, before statistical analysis. GLT-1 levels were expressed relative to GFAP levels to account for potential changes due to astrocyte activation or loss.

2.3.5 Immunofluorescent Staining

Frozen brain hemispheres sectioned into 40 μ m slices coronally using a microtome and stored in phosphate buffered saline with 0.05% sodium azide. Sections were mounted on standard glass microscope slides (Fisher) before staining. For antibody staining sections were permeabilized with 0.1% triton-x 100 in tris buffered saline (TBS) for 15 minutes and blocked with 3% bovine serum albumin (Fisher), 5% normal goat serum (Vector), and 0.1% triton-x 100 in TBS for one hour. For A β plaque staining sections were treated with 88% formic acid for 7 minutes before other treatments. After pre-treatment and blocking, the sections were incubated with primary antibodies against ZO-1 (1:100, Thermo Fisher), PSD95 (1:1,000, Cell Signaling Technology), synaptophysin (1:1,000, Cell Signaling Technology), GFAP (1:1000, DAKO), Iba1 (1:1,000, Abcam), CD68 (1:1000, Bio-Rad) Lectin (1:500, Sigma Aldrich) or anti amyloid 82E1 (1:1000, Immuno-Biological Laboratories) overnight at 4°C. Sections were washed with TBS and treated for 1 hour at room temperature the following day in 3% BSA, 5% normal goat serum, and 0.1% triton-x 100 in TBS with secondary antibodies conjugated with Alexa Fluor 488, 555, or 633 (Fisher). For Thioflavin S staining sectioned were rehydrated with ethanol at 100%, 95%, 70%, and 50% and then treated with Thioflavin S (Sigma) in 50% ethanol for 10 minutes. Slides were mounted with Fluoromount-G (Fisher). Images were taken with either a Leica TCS SPE confocal microscope for A β plaque staining and GFAP and IBA1 staining. Plaque burden was assessed as the percent of total measured area occupied by amyloid beta plaques from the cortex

and hippocampus CA1 region. Vascular width was determined by the average of 5 measurements across the vessel. ImageJ version 1.52 was used to analyze images.

2.3.6 Real-Time Polymerase Chain Reaction

RNA was isolated from *App*^{NL-G-F/+}-KI mouse hippocampal and cortical brain tissue in TRI Reagent and extracted using the Direct-Zol RNA MiniPrep kit (ZYMO Research Corp) used according to manufacturer instructions. RNA concentration in the extract was quantified using a NanoDrop Lite (ThermoFisher). 1 µg of total RNA was used in a single cycle reverse transcriptase reaction of 5 minutes at 25°C, 20 minutes at 46°C, 1 minute at 95°C to make cDNA using iScript reaction mix and reverse transcriptase (Bio-Rad). 2 µL of cDNA were used per reaction using iTaq Universal SYBR Green Supermix (Bio-Rad) for detection of *Il1β*, *Il6*, and *App*. Expression levels were normalized with *Gapdh* mRNA levels. Primer sequences are as follows: *Il1β* forward 5'- TGGACCTTCCAGGATGAGGACA-3' reverse 5'- GTTCATCTCGGAGCCTGTAGTG-3' (Origene NM_008361), *Il6* forward 5'- TACCACTTCACAAGTCGGAGGC-3' reverse 5'-CTGCAAGTGCATCATCGTTGTTC-3' (Origene NM_031168), *Gapdh* forward 5'-AACTTTGGCATTGTGGAAGG-3' reverse 5'- ACACATTGGGGGTAGGAACA-3' (Origene NM_010277), *App* 5'- TCCGTGTGATCTACGAGCGCAT-3' reverse 5'-GCCAAGACATCGTCGGAGTAGT-3' (Origene NM_007471). The PCR cycle parameters are listed: denaturing step (95°C for 15 seconds), annealing step (60°C for 60 seconds), and extension step (72°C for 30 seconds). Bio-Rad CFX Manager software version 3.1 was used to determine Cq values. ΔCq values were determined as determined by the difference between the gene of interest Cq and *Gapdh* Cq. ΔCq values between filtered air exposed and UF PM exposed animals were compared to obtain relative expression values, with the filtered air group set to 1.

2.3.6 A β Quantitation

Detergent soluble and formic acid soluble A β ₁₋₄₀ and A β ₁₋₄₂ levels were measured using the V-PLEX A β Peptide Panel with 6E10 capture antibody used as recommended by the manufacturer and read on a MESO QuickPlex SQ 120 (Meso Scale Discovery) for the 6 month group. For the 9 and 12 month groups A β levels were quantified using Human β Amyloid (1-40) ELISA kit and Human β Amyloid (1-42) ELISA kit (Wako). Protein sample extracts were obtained and quantified as described under Protein Extraction and Western Blots. 100 μ L of protein was loaded per well for each sample. Bradford protein assay concentration readings were used to adjust for total protein loaded per sample.

2.3.7 Statistical Analysis

Immunoblots were quantified using Image Studio Software version 5. Immunofluorescent images were quantified using ImageJ version 1.52. All other data were analyzed using Microsoft Excel (Microsoft Office 365 ProPlus) or Prism version 3 (GraphPad Software). Statistics were carried out using unpaired t-test or two-way analysis of variance with Tukey's post hoc test. p values ≤ 0.05 were considered significant. Sex differences were generally not observed, and data are presented as mixed groups.

2.4 Results:

Initial experiments were performed in the 3 month old *App*^{NL-G-F/+}-KI exposed to concentrated UF PM for 3 months. To test our hypothesis, we examined cognitive decline with the ORM and OLM tasks and assessed synaptic density, glial neuroinflammation, and A β levels. As all of these have previously been linked to both PM exposure (Bhatt et al., 2015; Cacciottolo et al., 2017; Kleinman et al., 2008; Morgan et al., 2011) and AD (Cleary et al., 2005; Shankar et al.,

2008; Stephenson et al., 2018), they are likely pathways to connect UF PM exposure to AD. At 6 months the *App*^{NL-G-F/+}-KI model is at a pre to early stage in A β pathology (Saito et al., 2014), ideally making determination of acceleration of A β pathology clearer compared to animals with already advanced pathology as ascertained by Cacciottolo et al (Cacciottolo et al., 2017).

2.4.1 Concentration of ambient particulates

Quasi-ultrafine PM was concentrated 7-fold by particle count and 5-fold by weight over the ambient levels over the course of the experiment (Fig. 1A, B). Average particulate concentration during the experiment for the UF PM exposed animals was 131 $\mu\text{g}/\text{m}^3$, which was still environmentally relevant to highly polluted areas, such as Mexico City (Moreno et al., 2008). In addition, considering human heterogeneity of sensitivity to exposure, animal-to-human extrapolation, and the differences in exposure durations in humans (lifetime) and animal models (less than a lifetime), exposing mice to higher concentrations than average human exposure is still translatable (Rees & Hattis, 2004).

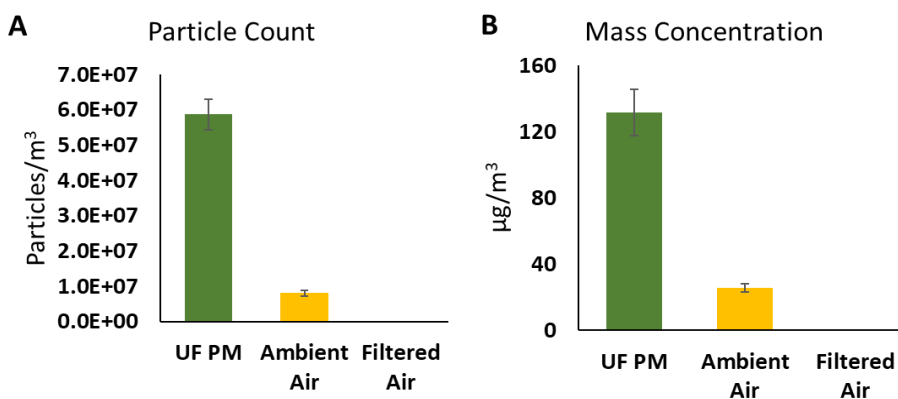


Figure 1: Exposure particle concentration.

(A) Average particle count per cubic meter during the exposure period of *App*^{NL-G-F/+}-KI mice. (B) Average particle mass concentration during exposure for concentrated quasi-ultrafine PM (UF PM), total ambient air, and filtered air using the VACES system. Bars represent mean values, with error bars expressed as standard error of the mean.

2.4.2 UF PM exposure impairs cognition in young *App*^{NL-G-F/+}-KI mice

Beginning after week 9 of exposure, 6 month old *App^{NL-G-F/+}-KI* mice were tested with the OLM and ORM behavior tasks (Vogel-Ciernia & Wood, 2014). In the younger animals PM-exposed *App^{NL-G-F/+}-KI* mice significantly performed worse in both tasks as compared to *App^{NL-G-F/+}-KI* mice exposed to filtered air (Fig. 2). The discrimination index was 20.3% less in OLM ($p < 0.05$) (Fig. 2A) and 8.9% less in ORM ($p < 0.05$) (Fig. 2B).

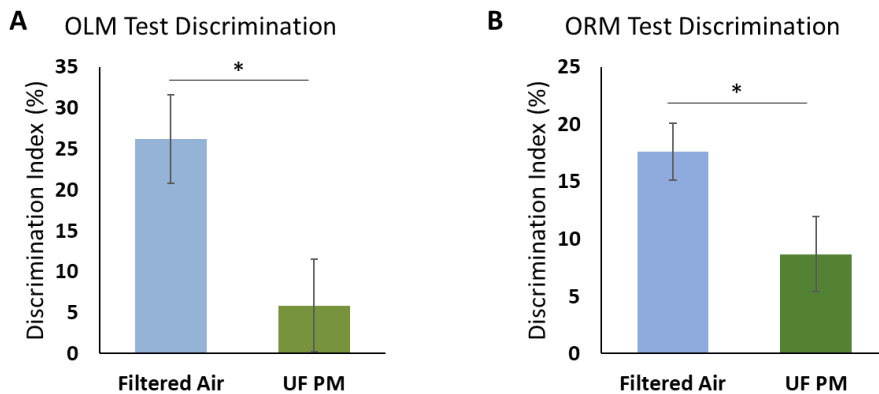


Figure 2: UF PM exposure reduces memory task performance in young *APP^{NL-G-F/+}-KI* mice.

Object location memory (OLM) and object recognition memory (ORM) task results for *App^{NL-G-F/+}-KI* mice and synaptic marker quantification. Discrimination index is the difference between time spent exploring the novel object or object in novel place and the familiar as a percentage of the total time. (A) Discrimination index for OLM test. Quasi ultrafine particulate matter (UF PM) exposed mice exposed mice showed significantly decreased ability to discriminate the novel object location compared to those exposed to filtered air. (B) Discrimination index for ORM. UF PM exposed mice showed decreased ability to discriminate the novel object compared to animals exposed to filtered air. Bars represent mean values, with error bars expressed as standard error of the mean (N = 10 animals per group). * denotes p -value < 0.05 .

After sacrifice at 6 months of age, cortical and hippocampal tissues were analyzed for synaptic markers to determine if synaptic loss due to UF PM exposure could explain the observed memory performance reductions. Despite the significant decrease in memory performance levels of the synaptic proteins PSD95 or synaptophysin did not vary with PM exposure status, indicating that the observed cognitive loss is not resultant from gross synaptic loss (Fig. 3). Neither protein varied due to UF PM exposure using immunofluorescent quantification of the cortex and CA1 region of the hippocampus (Fig. 3A, 3B) or by western blot protein quantification of whole cortex or hippocampus homogenate (Fig. 3C, 3D).

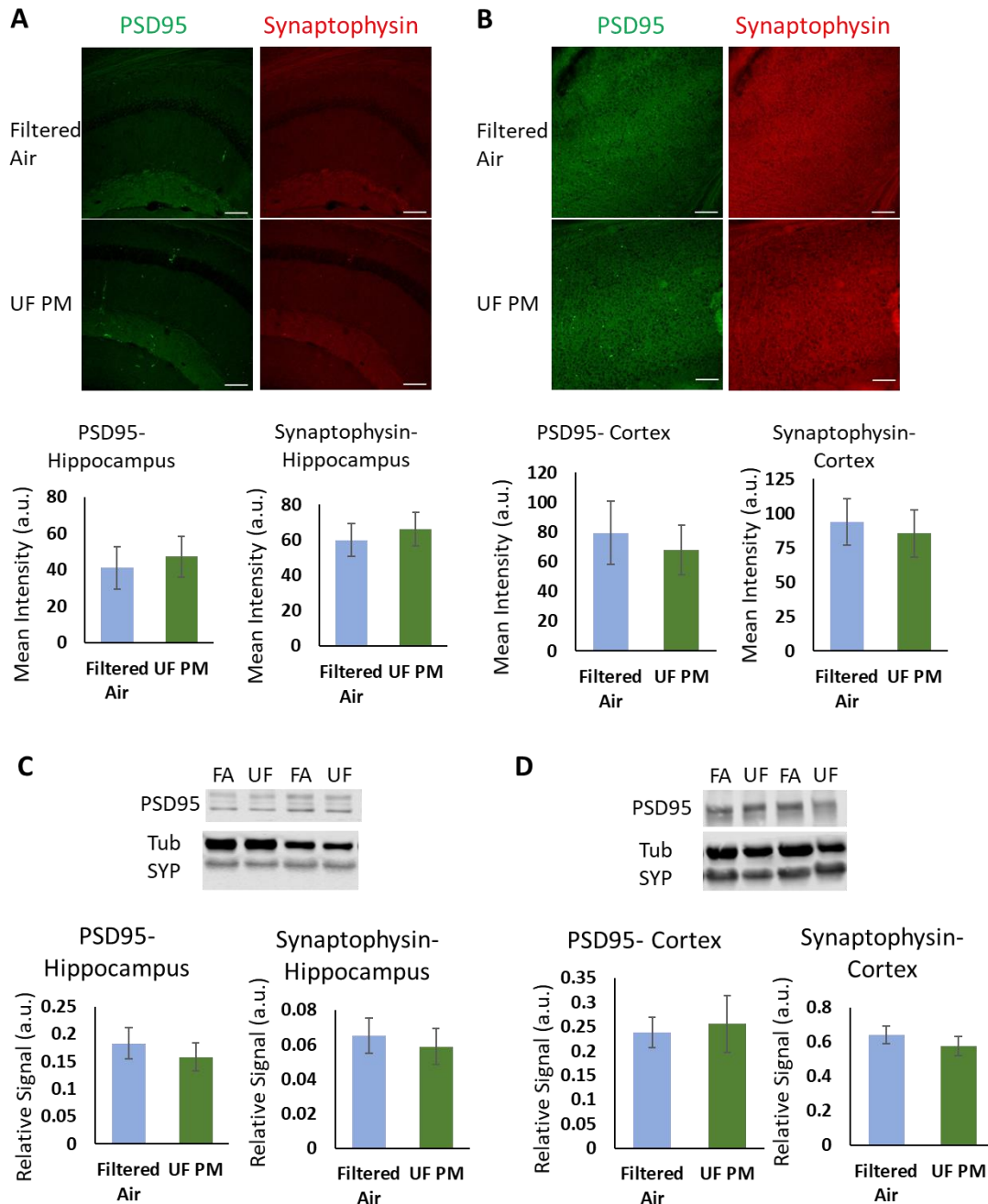


Figure 3: UF PM exposure does not induce changes in synaptic markers in young *APP^{NL-G-F/+}-KI* mice.

Quantification of synaptic markers PSD95 and synaptophysin by immunofluorescence and western blot. (A) Representative images of PSD95 (green) and synaptophysin (red) immunofluorescent staining and fluorescent intensity quantification for the CA1 region of the hippocampus. (B) Representative images of PSD95 (green) and synaptophysin (red) immunofluorescent staining taken from the parietal and somatosensory cortex and fluorescent intensity quantification from the whole cortex. (C) Representative western blot of synaptophysin and PSD95 from hippocampal tissue samples with band intensity relative to tubulin. FA- Filtered Air, UF- UF PM, Tub- Tubulin. (D) Representative western blot of synaptophysin and PSD95 from cortical tissue with band intensity relative to tubulin. Bars represent mean values, with error bars expressed as standard error of the mean (N = 8 animals per group for immunostaining and N = 10 animals per group for immunoblot. Scale bars = 100 μ m). * denotes p value < 0.05.

2.4.3 UF PM exposure does not affect Amyloid β burden or glial inflammation in young

App^{NL-G-F/+}-KI mice

Heterozygous *App*^{NL-G-F/+}-KI mice at 6 months do not develop extensive plaque pathology (Saito et al., 2014), and exposure to concentrated PM did not significantly accelerate the buildup of plaques or A β peptides (Fig. 4). Only a few A β plaques were present in the cortex (Fig. 4A), and nearly no plaques were observed in the hippocampus (Fig. 4B). Virtually no dense core plaques were detected in either group by Thioflavin S staining (data not shown). The steady-state levels of full-length APP protein did not significantly increase with exposure, and *App* mRNA levels in the cortex and hippocampus were unaffected by the PM exposure (Fig. 4C, 4D). Similarly, no significant difference in soluble A β ₄₂ peptide levels was detected between exposed and unexposed animals (Fig. 4E); A β ₄₀ peptides and insoluble A β ₄₂ peptides were not detectable (data not shown).

As previous studies in non-Alzheimer's model animals have shown altered central nervous system (CNS) inflammation with PM exposure (Allen, Liu, Pelkowski, et al., 2014; Campbell et al., 2005; Guerra et al., 2013; Kleinman et al., 2008), we also investigated whether UF PM exposure increased markers of inflammation in the CNS in the current model (Fig. 5). No clear upregulation of either Iba1 positive microglia or GFAP positive astrocytes was evident with exposure to PM in either the cortex or hippocampus (Fig. 5A, 5B). mRNA levels of the cytokines interleukin-6 (*Il6*) and interleukin 1 β (*Il1 β*) similarly did not significantly vary with PM exposure status (Fig 5C).

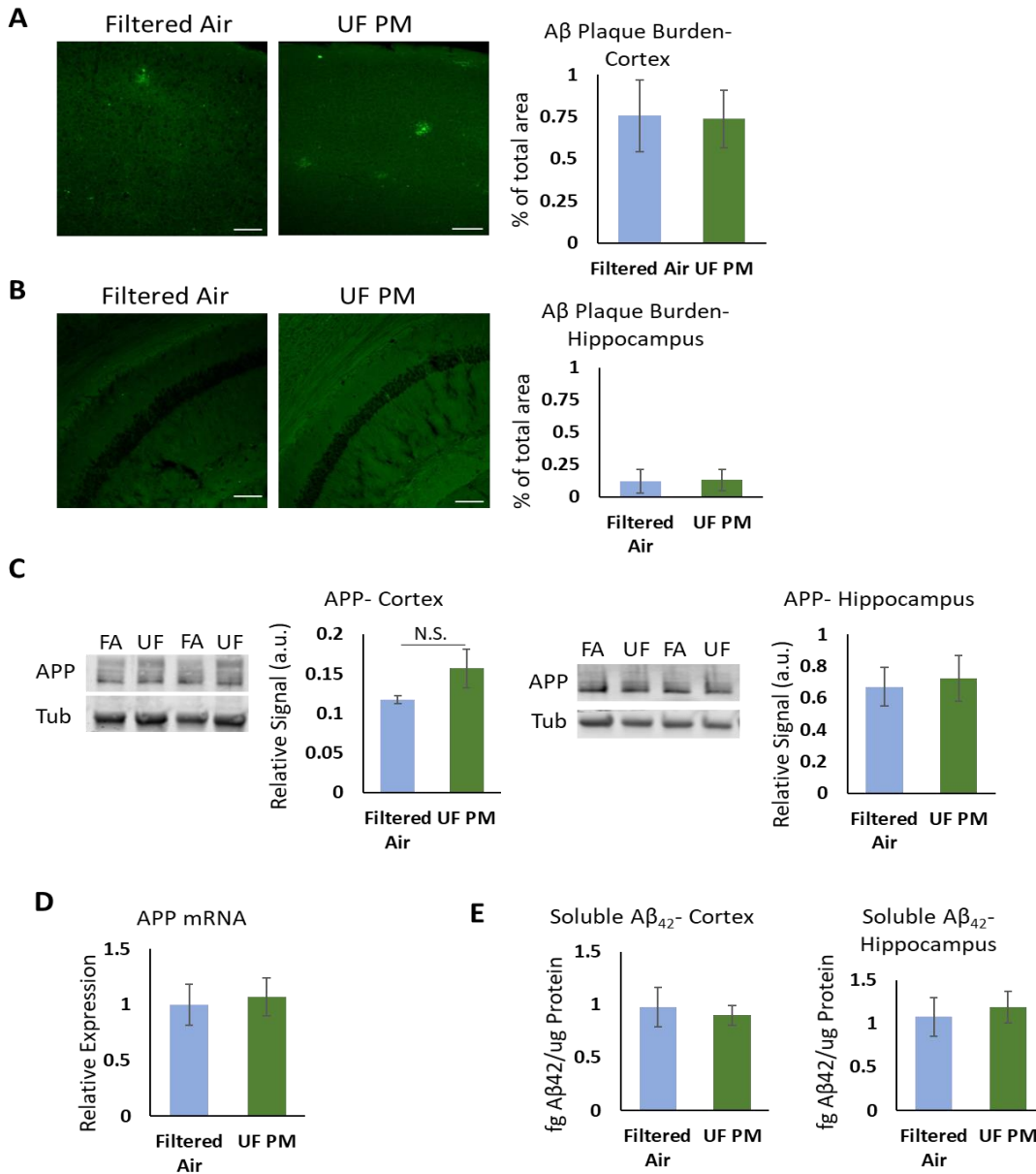


Figure 4: Aβ deposition and protein load is unaffected by UF PM exposure in the 6 month old *App*^{NL-G-F/+}-KI mouse model

Brain sections were stained with 82E1 antibody to detect Aβ plaques in *App*^{NL-G-F/+}-KI mice. (A) Representative images of cortical Aβ plaque burden from the parietal cortex in *App*^{NL-G-F/+}-KI mice exposed to filtered air or UF PM (left), and quantification of plaque burden expressed as percentage of the total area measured occupied by plaques (right). (B) Representative images of hippocampal Aβ plaque burden in *App*^{NL-G-F/+}-KI mice exposed to filtered air or UF PM from the hippocampal CA1 region (left), and quantification of plaque burden expressed as percentage of the total area measured occupied by plaques (right). In neither region was total plaque load increased. (C) Steady-state levels of full-length APP in tissue homogenates extracted from cortical and hippocampal tissues were not significantly affected by the PM exposure. FA- Filtered Air, UF- UF PM, Tub- Tubulin. (D) mRNA levels of *App* normalized to *Gapdh* mRNA. *App* mRNA levels from cortical tissue were also unaffected by the exposure. (E) No differences in soluble Aβ₄₂ levels were found in the brain. Bars represent mean values, with error bars expressed as standard error of the mean (N = 8 animals per group for immunofluorescent staining and quantification, and N = 6 animals per group for immunoblot, V-PLEX, and qPCR. Scale bars = 100 μm).

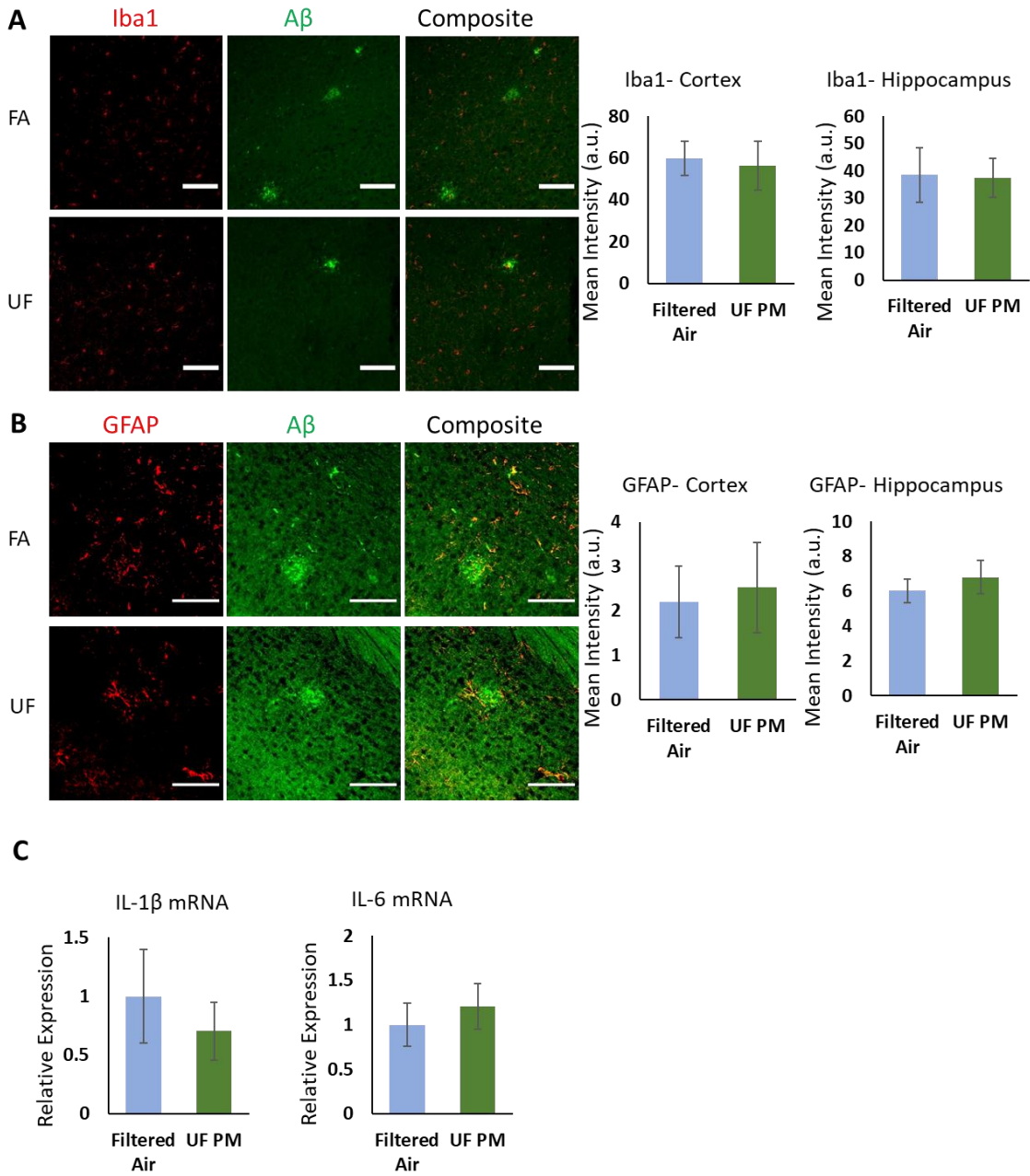


Figure 5: Glia markers GFAP and Iba1 do not increase with exposure to UF PM in 6 month old *App^{NL-G-F/+}-KI* mice

(A) Representative images of microglial marker Iba1 (red) and A β (green) staining taken from the parietal cortex (top) and CA1 region of the hippocampus (bottom), as well as quantification of the mean fluorescent intensity of Iba1 staining for the cortex and hippocampus. Exposure to UF PM does not increase the levels of Iba1 in the brain. FA- Filtered Air, UF- UF PM. (B) Representative images of astrocytic marker GFAP (red) and A β (green) staining taken from the parietal cortex (top) and CA1 region of the hippocampus (bottom), as well as quantification of the mean fluorescent intensity of GFAP staining for the cortex and hippocampus. UF PM exposure does not change the levels of GFAP observed. (C) mRNA levels of cytokines *Il6* and *Il1 β* normalized to *Gapdh* mRNA. Neither *Il1 β* or *Il6* mRNA levels from cortical tissue were significantly affected by the exposure status. (N = 8 animals per group for immunofluorescent staining and quantification, and N = 6 animals per group for immunoblot and qPCR. Scale bars = 100 μ m).

2.4.4 UF PM exposure in aged *App*^{NL-G-F/+}-KI and wild-type mice

As UF PM exposure induced little change in the pre-to-early pathology 6 month old *App*^{NL-G-F/+}-KI model, we next sought to examine whether UF PM exposure exacerbates A β pathology, inflammation, and other markers of neurodegeneration in *App*^{NL-G-F/+}-KI mice at a more advanced aged with greater existing A β pathology. 9 month old *App*^{NL-G-F/+}-KI mice were exposed to concentrated UF PM for 3 months to determine whether inflammation and A β pathology are affected in aged animals with established pathology. Behavior results in the younger group in absence of altered A β pathology indicate some functional change without A β perturbation, so wild-type animals of the same background and age were included in this second cohort to better investigate A β independent effects of UF PM. Given the lack of effect seen in the younger cohort in inflammation or A β , we additionally expanded our scope to include other targets linked to AD progression, PM exposure, and memory function. Previous reports indicating damage to the blood brain barrier (BBB) in association with air pollution exposure (Calderón-Garcidueñas, Solt, et al., 2008; MohanKumar et al., 2008) and in AD pathology (Sweeney et al., 2018; Van De Haar et al., 2016) lead us to assess tight junction makers in the brain. We also investigated the reelin positive neuronal subset in the entorhinal cortex, as they have been shown to be involved in pyramidal neuron synaptogenesis and memory function (Chameau et al., 2009; Stranahan et al., 2011) and have an affinity for early A β accumulation and may be vulnerable before general A β pathology changes (Kobro-Flatmoen et al., 2016). Finally, based on reports showing glutamate receptor dyshomeostasis with PM exposure (Cacciottolo et al., 2017; Morgan et al., 2011) we examined levels of the glutamate transport protein GLT-1, which has known roles in AD progression, long term potentiation, and memory

ability (Katagiri et al., 2001; Kobayashi et al., 2018; Meeker et al., 2015; Mookherjee et al., 2011).

2.4.5 Concentration of ambient particles in the 12 month old animal cohort

UF PM levels were concentrated 7-fold by count and 9-fold by weight on average over the course of this exposure (Fig. 6). The concentrated particle count was approximately 124 million particles per cubic meter (Fig. 6A), while the concentration by mass was at a similar level as in the younger cohort at 126 μg per cubic meter of air (Fig. 6B). The increase in total particle count compared to the younger cohort exposure while maintaining a similar concentration by mass indicates a smaller average PM size in this second exposure.

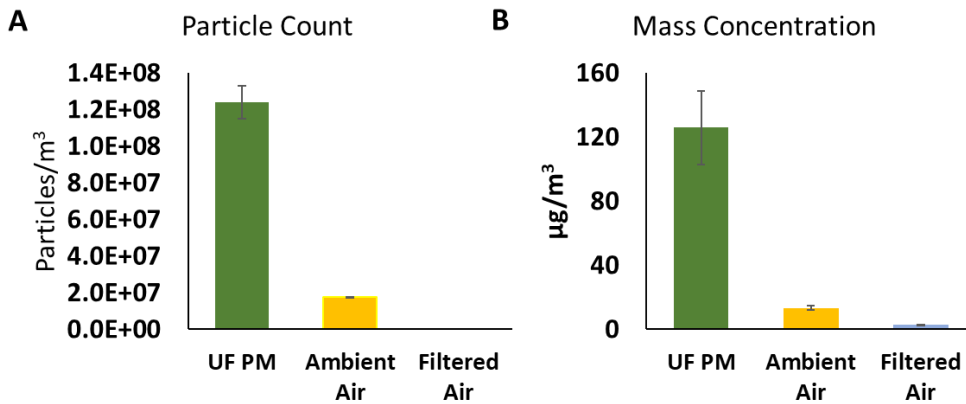


Figure 6: Aged exposure particle concentration.

(A) Average particle count per cubic meter during the exposure period of *App*^{NL-G-F/+}-KI and wild-type mice. (B) Average particle mass concentration during exposure for concentrated quasi-ultrafine PM (UF PM), total ambient air, and filtered air using the VACES system. Bars represent mean values, with error bars expressed as standard error of the mean.

2.4.6 UF PM exposure impairs cognition in 12 month old wild- type and *App*^{NL-G-F/+}-KI mice

In the 12 month old group, memory performance was decreased both by *App*^{NL-G-F/+} genotype and by UF PM exposure (Fig. 7). For OLM only the performance difference between the air exposed wild-type and UF PM exposed *App*^{NL-G-F/+}-KI mice was significant (14.3% decrease in discrimination index, $p < 0.01$) (Fig. 7A). In the ORM task object discrimination decreased by

11% ($p < 0.05$) with UF PM exposure within the wild-type group, 12% ($p < 0.05$) when comparing air exposed wild-type animals to air exposed $App^{NL-G-F/+}$ -KI animals, and the largest decrease, 22.6% ($p < 0.001$), was observed comparing the air wild type group to the UF PM exposed $App^{NL-G-F/+}$ -KI group (Fig. 7B); the difference between within the $App^{NL-G-F/+}$ -KI mice with UF PM exposure did not reach significance. These results indicate an additive effect of UF PM exposure and amyloid genotype on cognitive impairment.

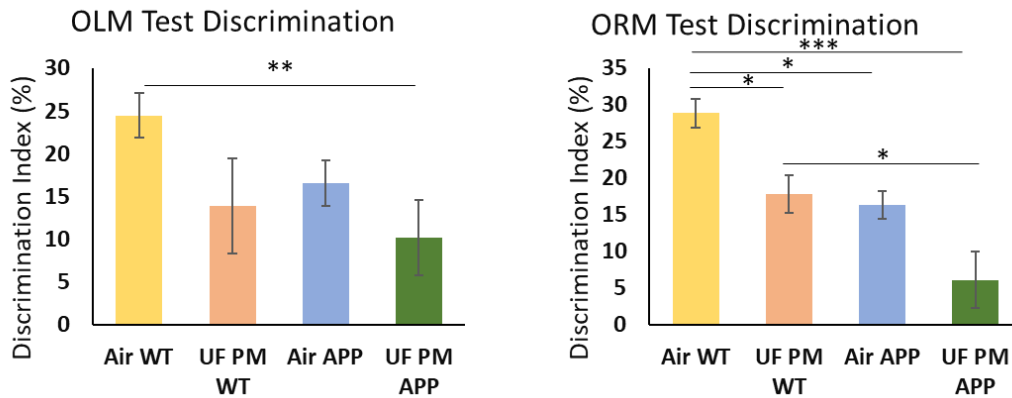
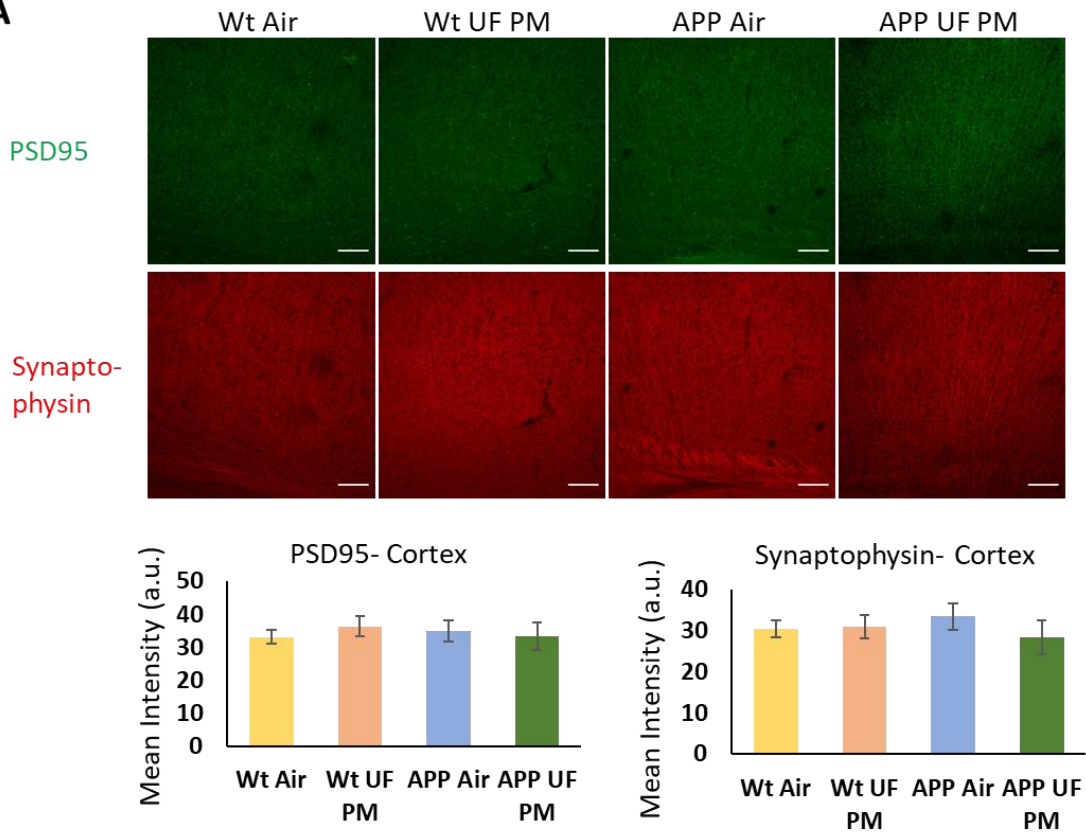
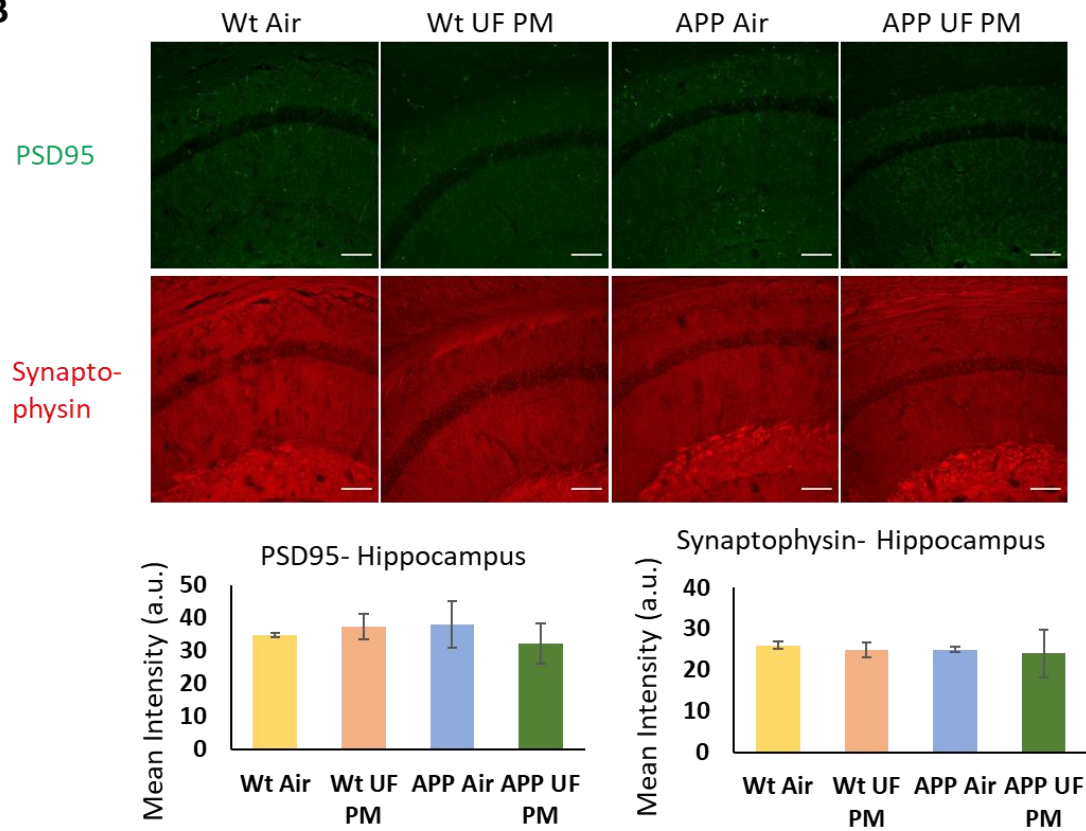


Figure 7: UF PM exposure impairs memory in aged wild-type and $App^{NL-G-F/+}$ -KI mice.

Object location memory (OLM) and object recognition memory (ORM) task results for $App^{NL-G-F/+}$ -KI (APP) and wild-type (Wt) mice. Discrimination index is the difference between time spent exploring the novel object or object in novel place and the familiar as a percentage of the total time. (A) Discrimination index for OLM test. Quasi ultrafine particulate matter (UF PM) exposed mice exposed mice showed significantly decreased ability to discriminate the novel object location compared to those exposed to filtered air. (B) Discrimination index for ORM. UF PM exposed mice showed decreased ability to discriminate the novel object compared to animals exposed to filtered air. (N = 10-12 animals per group. Scale bars = 100 μ m). * denotes p value < 0.05 , ** denotes $p < 0.01$, and *** denotes $p < 0.001$.

As in the younger group, there were no detectable changes in synaptic density markers synaptophysin and PSD95 in either the hippocampus or cortex either between genotypes or due to UF PM exposure status by immunofluorescent quantification or western blot analysis (Fig. 8A-D).

A**B**

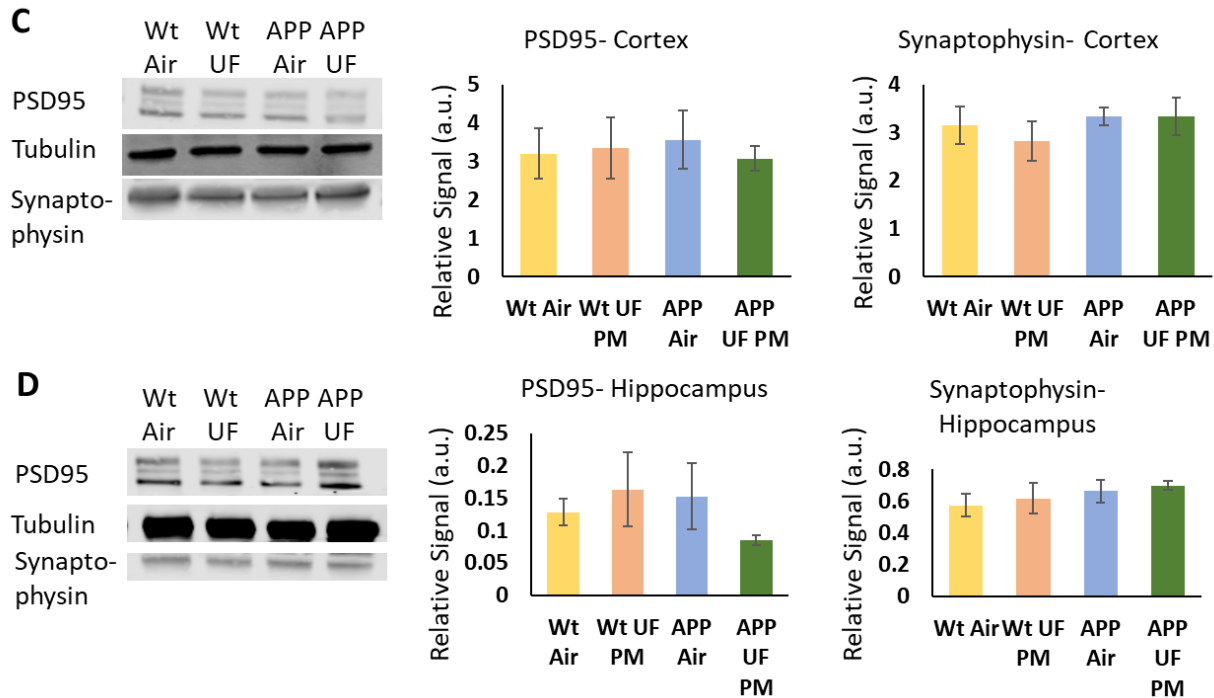
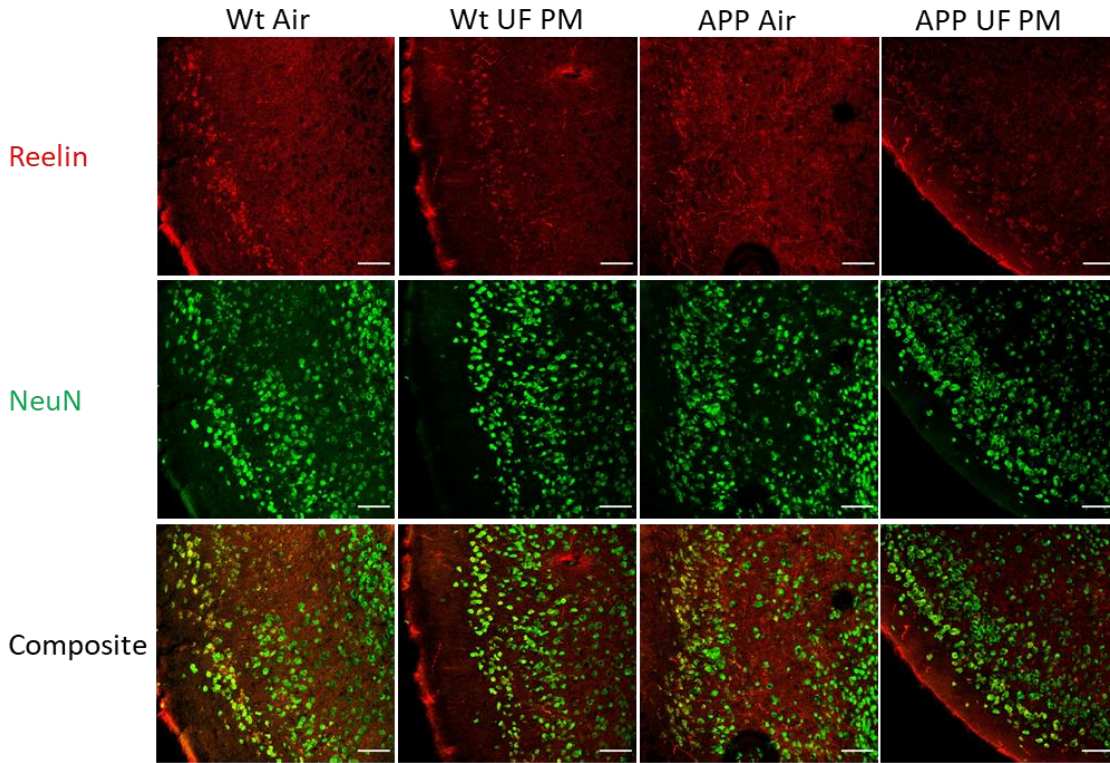


Figure 8: Synaptic markers do not change with UF PM exposure in aged *App*^{NL-G-F/+}-KI and wild-type mice. (A) Representative images of PSD95 (green) and synaptophysin (red) immunofluorescent staining and fluorescent intensity quantification from the parietal and somatosensory cortex and fluorescent intensity quantification from the whole cortex in aged *App*^{NL-G-F/+}-KI (APP) and wild-type (Wt) mice. (B) Representative images of PSD95 (green) and synaptophysin (red) immunofluorescent staining taken from CA1 region of the hippocampus and quantification. (C) Representative western blot of synaptophysin and PSD95 from cortical tissue samples with band intensity relative to tubulin. UF- UF PM. (D) Representative western blot of synaptophysin and PSD95 from hippocampal tissue with band intensity relative to tubulin. Bars represent mean values, with error bars expressed as standard error of the mean (N = 4 animals per group for immunostaining and quantification and N = 4-6 animals per group for immunoblot. Scale bars = 100 μ m).

The reelin positive neuron subpopulation in the entorhinal cortex was also assessed to determine if UF PM exposure may be specifically toxic to certain subsets of neurons that may account for observed cognitive deficits. However, the number of reelin positive neurons in the entorhinal cortex did not vary significantly with UF PM exposure or genotype (Fig. 9), indicating that loss of the reelin positive neuronal subset is not responsible for the cognitive impairment seen.



Reelin Positive Neurons- Entorhinal Cortex

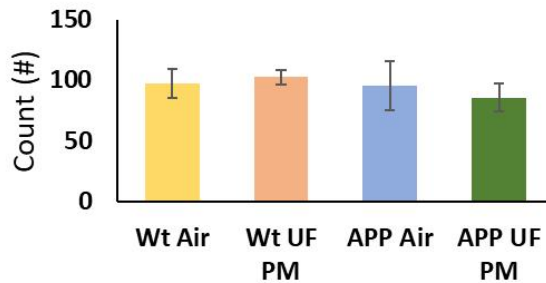


Figure 9: Entorhinal cortex reelin positive neurons are not reduced by UF PM.

Representative images of reelin (red), NeuN (green), and merged staining in the entorhinal cortex and reelin positive neuron count in 12 month old wild-type (Wt) and *App*^{NL-G-F/+}-KI (APP) exposed to filtered air or quasi ultrafine PM. Bars represent mean values, with error bars expressed as standard error of the mean (N = 10 animals per group for behavior tests, N = 8 animals per group for immunostaining and quantification, and N = 10 animals per group for immunoblot. Scale bars = 100 μm).

2.4.6 UF PM exposure increases A β plaque load in *App*^{NL-G-F/+}-KI mice with established pathology

In the 12 month group plaque pathology is more advanced in the heterozygous animals (Fig. 10). Plaque load as detected by 82E1 was increased in the cortex of *App*^{NL-G-F/+}-KI mice exposed to UF PM as compared to the air group, with a percent of area covered by plaques at 2.2% versus 1.4% ($p < 0.01$) (Fig. 10A). In the hippocampus, 82E1 plaques did not increase with exposure. UF PM exposure also increased Thioflavin S stained dense core plaque load in the cortex (0.48% compared to 0.83% of total area, $p < 0.05$) and hippocampus (0.26% compared to 0.59%, $p < 0.05$) (Fig. 10B). Despite increases in plaque load, as in the younger group no significant differences were seen in APP protein levels or *App* mRNA (Fig. 10C, 10D). Due to concerns about the efficacy of the binding antibody used in the MSD V-Plex kit used in the younger group, A β peptide levels in this group were measured using WAKO ELISA kits. A β peptide levels were not detectable in the soluble fraction (data not shown) and were not altered with PM exposure status in the detergent insoluble fraction (Fig. 10E).

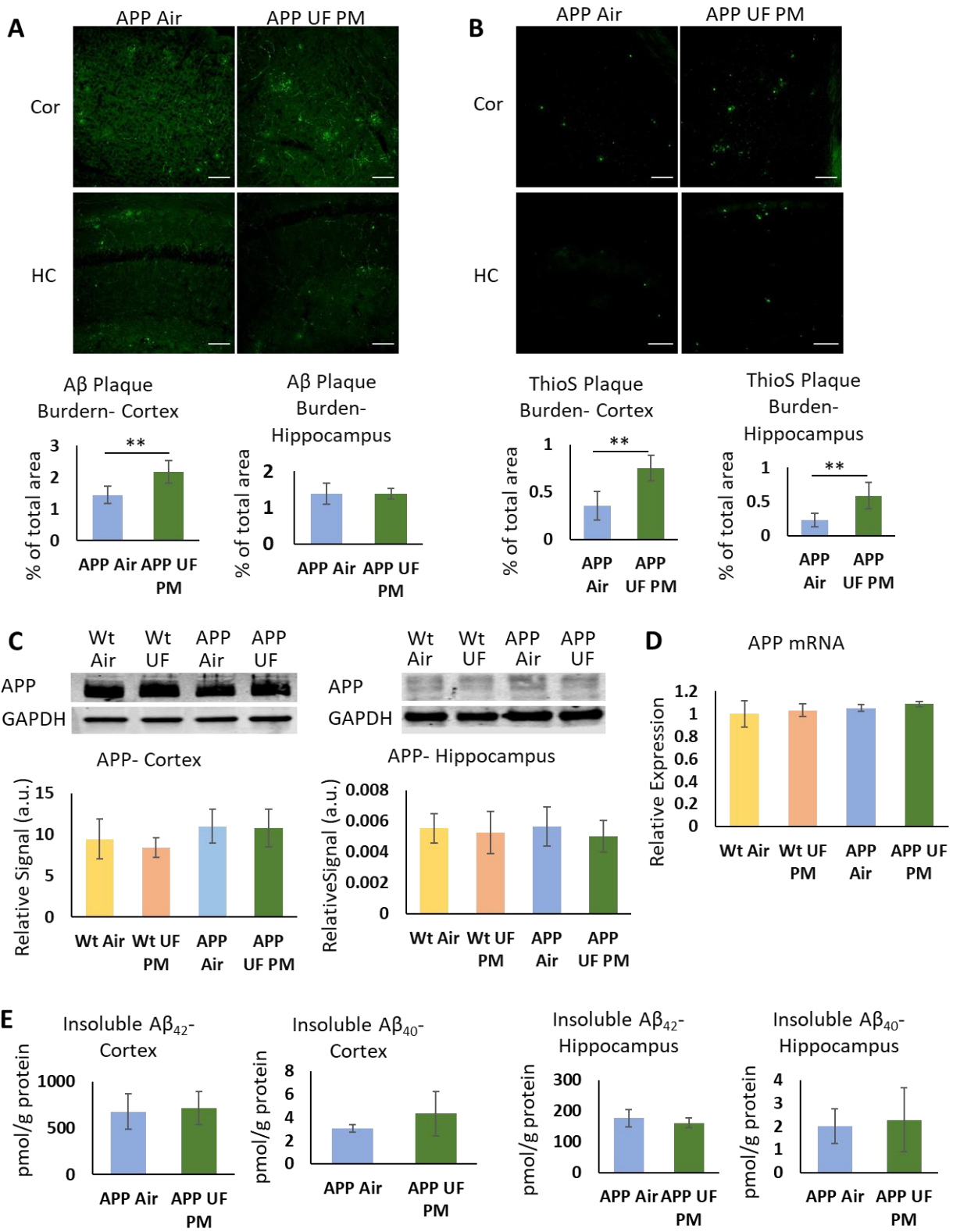


Figure 10: A β plaque burden is increased by UF PM exposure in the 12 month old *App*^{NL-G-F/+}-KI mouse model

Brain sections were stained with 82E1 antibody and ThioflavinS to detect diffuse and dense core A β plaques in 12 month old *App*^{NL-G-F/+}-KI (APP) mice. (A) Representative images of A β plaque burden detected by 82E1 from the parietal cortex (Cor) and CA1 region of the hippocampus (HC) in *App*^{NL-G-F/+}-KI mice exposed to filtered air or UF PM (top), and quantification of plaque burden expressed as percentage of the total area measured occupied by plaques (bottom). Area % covered by plaques increases with UF PM exposure in the cortex but not hippocampus. (B) Representative images of A β dense core plaque burden from the parietal cortex (Cor) and CA1 region of the hippocampus (HC) (top) and quantification of plaque burden (bottom). Dense core plaque burden in the cortex and hippocampus also increases with UF PM exposure. (C) Steady-state levels of full length APP in tissue homogenates extracted from cortical and hippocampal tissues were not significantly affected by the PM exposure. UF- UF PM. (D) mRNA levels of *App* normalized to *Gapdh* mRNA. *App* mRNA levels from cortical tissue were also unaffected by the exposure. (E) No differences in insoluble A β ₄₀ or A β ₄₂ levels were found in the cortex or hippocampus by ELISA. Bars represent mean values, with error bars expressed as standard error of the mean (N = 6 animals per group for immunofluorescent staining and quantification, and N = 4 animals per group for immunoblot, V-PLEX, and qPCR. Scale bars = 100 μ m). * denotes p value < 0.05, ** denotes p < 0.01.

No increase in glia markers Iba1 or GFAP was detected with UF PM exposure in the 12 month old group (Fig. 11). Iba1 positive microglia non-significantly trended toward a decrease with exposure and Iba1 levels did not change with genotype (Fig. 11A). Microglia co-expressing IBA1 and CD68, which indicates a reactive state (Muhleisen et al., 1995), were not observed in the younger cohort or the wild-type animals in this older cohort (data not shown). However, in the *App*^{NL-G-F/+}-KI mice microglia expressing both Iba1 and CD68 were observed in areas around amyloid plaques; the number of observed microglia expressing Iba1 and CD68 was not significantly different between the UF PM and air exposed groups by count (Fig. 11A). GFAP levels increased in the *App*^{NL-G-F}-KI animals as compared to wild-type but did not change with UF PM exposure status (Fig. 11B). *Ili β* and *Ii6* mRNA levels were not different between the exposure groups within each age group (Fig. 11C). These results indicate that amyloid pathology and glial inflammation in the CNS are not responsible for the cognitive decline observed in either the 6 month or 12 month groups. While increased amyloid plaque load may contribute some to the decreased memory performance seen in the older *App*^{NL-G-F}-KI animals, it cannot explain the deficits in the younger group or the wild-type animals in the older group.

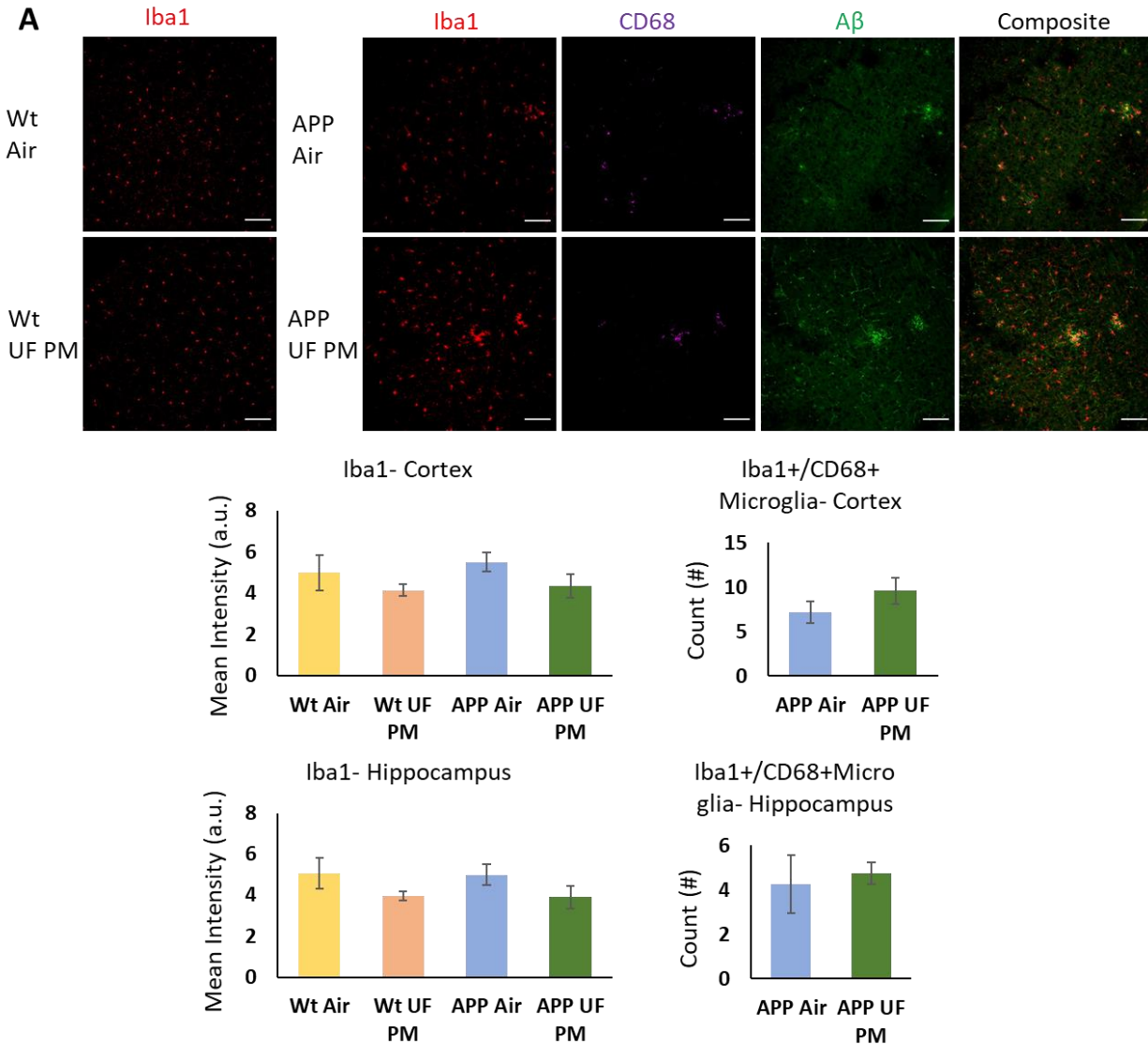
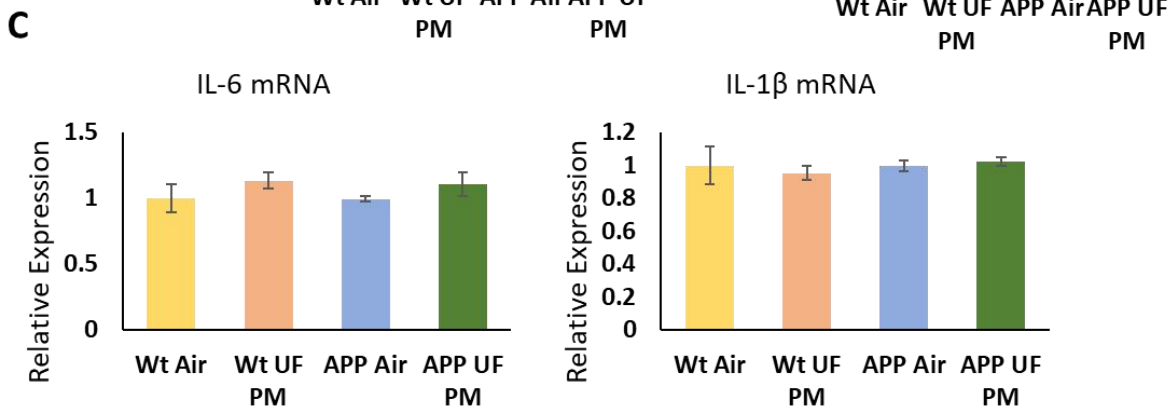
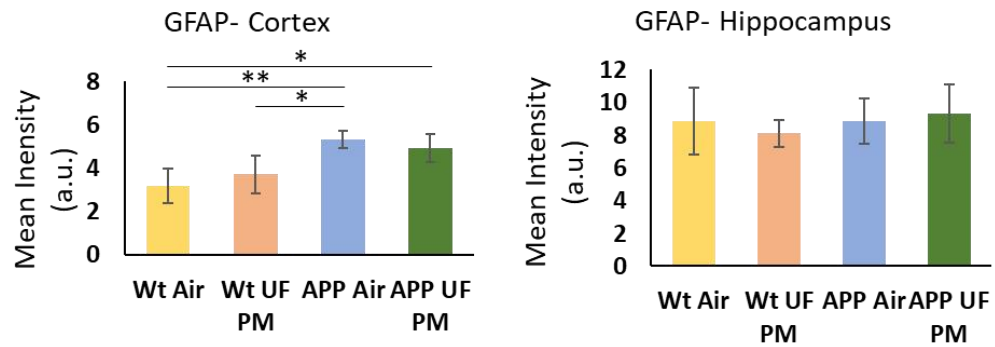
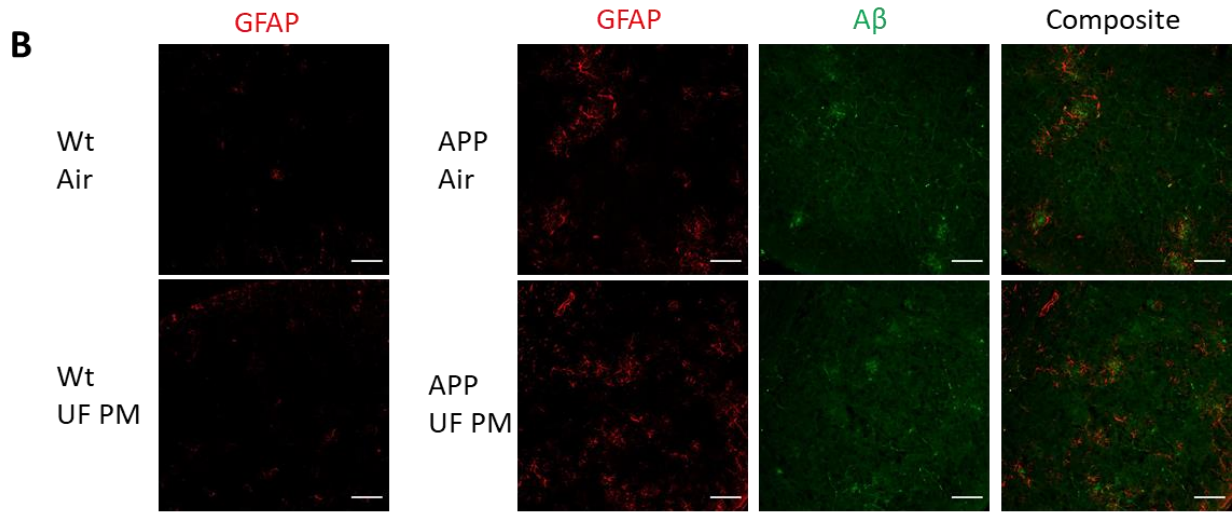


Figure 11: Glia markers GFAP and Iba1 do not increase with exposure to UF PM in 12 month old *App^{NL-G-F/+}*-KI mice

(A) Representative images of microglial marker Iba1 (red), CD68 (purple), and Aβ (green) staining from the parietal cortex (top) of wild-type (Wt) and *App^{NL-G-F/+}*-KI (APP) mice exposed to filtered air or ultra-fine PM and quantification of the mean fluorescent intensity of Iba1 staining for the cortex and hippocampus from all mice and total count of Iba1 and CD68 positive microglia in *App^{NL-G-F/+}*-KI mice (bottom). Exposure to UF PM does not increase the levels of Iba1 or Iba1+/CD68+ microglia in the brain in either group. (B) Representative images of astrocytic marker GFAP (red) and Aβ (green) staining from the parietal cortex (top) and quantification of the mean fluorescent intensity of GFAP staining for the cortex and hippocampus (bottom). UF PM exposure does not change the levels of GFAP observed in either group. (C) mRNA levels of cytokines *Il6* and *Il18* normalized to *Gapdh* mRNA. Neither *Il18* or *Il6* mRNA levels from cortical tissue were significantly affected by the exposure status or genotype. Bars represent mean values, with error bars as standard error of the mean (N = 6 animals per group for immunofluorescent staining and quantification, and N = 4 animals per group for immunoblot and qPCR. Scale bars = 100 μm).



2.4.7 UF PM exposure does not impact tight junction markers in the blood-brain barrier in 12 month *App*^{NL-G-F/+}-KI or wild-type mice

We next sought to investigate whether the BBB integrity was impacted by the current exposure in the 12 month old wild-type and *App*^{NL-G-F}-KI group (Fig. 12). Using tight junction marker ZO-1, cerebral vasculature width was assessed with immunofluorescent staining (Fig. 12A). No differences were seen in the width of the blood vessels due to either exposure status or genotype. We also assessed total albumin protein levels in the cortex by western blot, as a leaky BBB could cause a build up of albumin in brain tissue, but again saw no significant changes between the groups (Fig. 12B). Finally, using a vascular enriched whole brain protein fraction, we assessed the levels of two other tight junction proteins, Claudin-5 and CD31 (Fig. 12C, 12D). Once more there were no differences between either treatment status or genotype. Overall, we observed no indications of BBB disruption with exposure to UF PM.

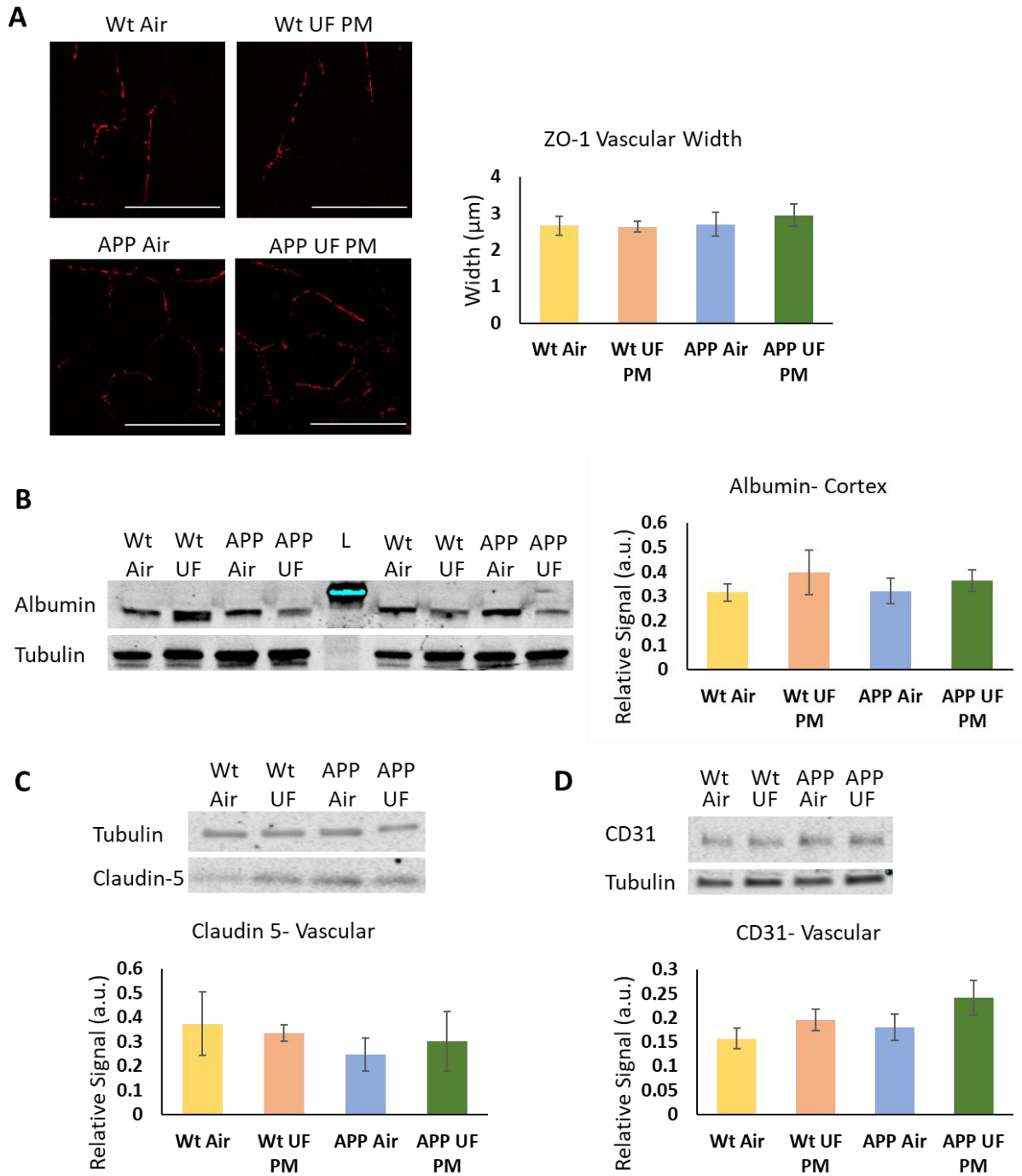


Figure 22: Tight junction markers do not decrease in wild-type or *App*^{NL-G-F/+}-KI mice exposure to UF PM (A) Representative images of ZO-1 staining of cerebral vasculature from the cortex in wild-type (Wt) and *App*^{NL-G-F/+}-KI (APP) mice exposed to filtered air or UF PM (left) and quantification of vascular width (right). No differences are seen across treatment or genotype. (B) Representative western blot of albumin in cortical protein extract. Differences between groups are not significant. (C) Representative western blot of tight junction marker Claudin-5 and (D) intercellular junction marker CD31 from vascular enriched protein samples. Neither genotype nor exposure status shows significant differences. Bars represent mean values, with error bars expressed as standard error of the mean (N = 4-5 animals per group for all assays. Scale bars = 100 μm).

2.4.8 UF PM exposure reduces total protein level of GLT-1 in both wild-type and $App^{NL-G-F/+}$ -KI mice

Glutamatergic neuron dysfunction has been shown with nano-scale particulate matter *in vitro* (Morgan et al., 2011) and is suggested in a rodent model of AD (Cacciottolo et al., 2017). We sought to determine if the astrocytic glutamate transporter 1 (GLT-1), which is implicated strongly in AD pathology (Kobayashi et al., 2018; Mookherjee et al., 2011; Zumkehr et al., 2015), is also affected by exposure to airborne particulates. Using western blot total protein assays of GLT-1 levels relative to levels of the astrocytic marker GFAP, we found that GLT-1 is decreased in the hippocampus of mice exposed to UF PM, which we also confirmed in the younger exposure cohort (Fig. 13). In the 6 month group, a 41% decrease of GLT-1 is observed in the hippocampus of UF PM exposed App^{NL-G-F} -KI animals compared to the filtered air exposed group $p < 0.05$, (Fig. 13A). This change is not evident in the cortex of those animals. In the 12 month old group wild-type and App^{NL-G-F} -KI UF PM exposed animals again show decreased levels of GLT-1 in the hippocampus as compared to the wild-type air exposed group, 44% and 47% respectively, $p < 0.05$ for both (Fig. 13B). Within the APP^{NL-G-F} -KI group there is a smaller non-significant decrease, as the $App^{NL-G-F/+}$ -KI air group itself shows a non-significant decrease compared to the wild-type air group. These results indicate that region specific GLT-1 loss is associated with UF PM exposure. Whether GLT-1 loss is involved in the pathway leading to cognitive decline in these animals is unknown.

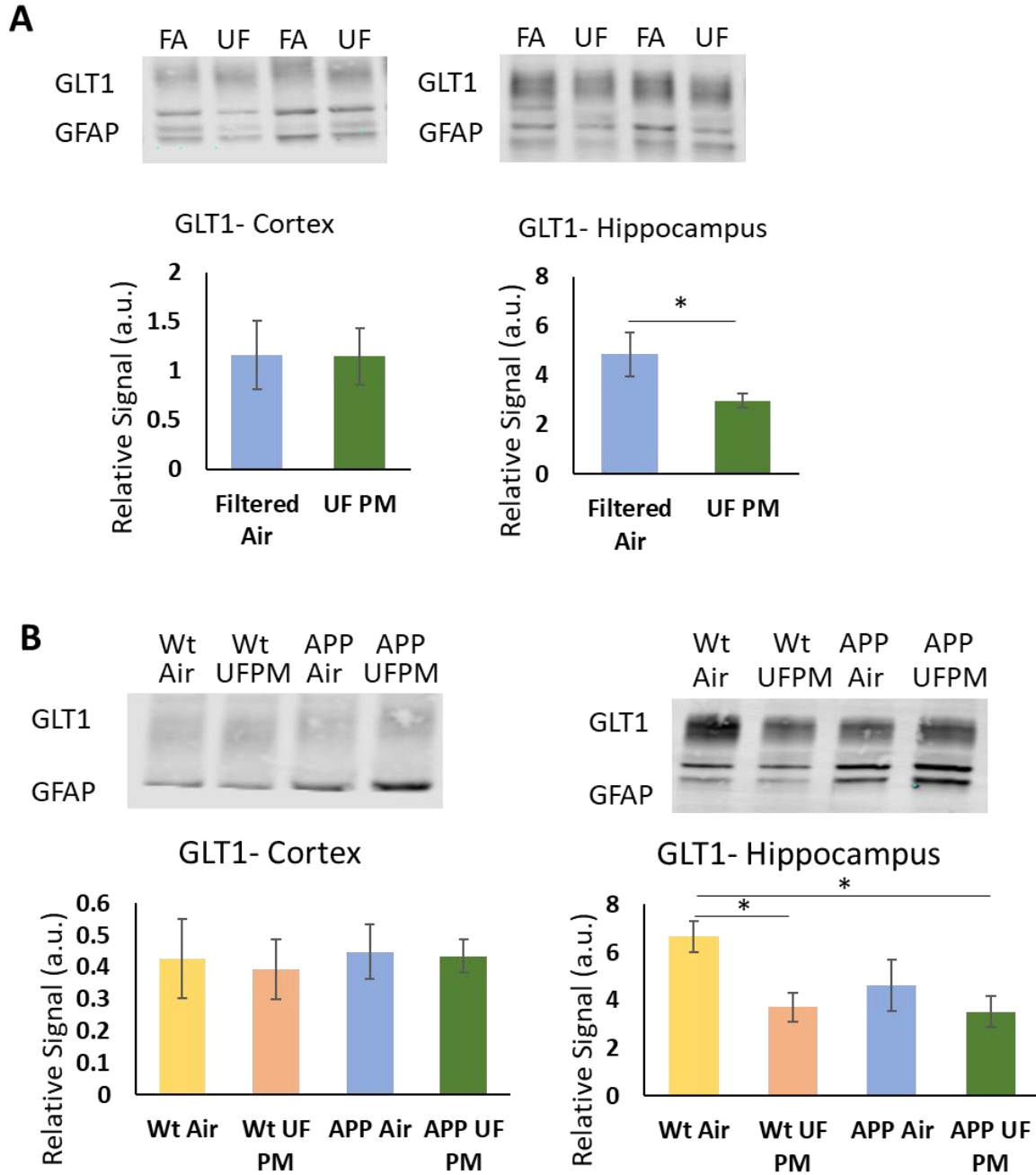


Figure 13: Levels of astrocytic glutamate transporter GLT-1 decrease in the hippocampus of mice exposed to UF PM

(A) Representative western blots of GLT-1 protein levels relative to GFAP in the cortex (left) and hippocampus (right) from 6 month old *App^{NL-G-F/+}-KI* mice exposed to either filtered air or UF PM, with quantification of western blot band intensity (below). GLT-1 levels decrease in the hippocampus, but not cortex, of UF PM exposed animals. FA- Filtered air UF- UF PM. (B) Representative western blots of GLT-1 protein levels relative to GFAP in the cortex (left) and hippocampus (right) from 12 month old wild-type (Wt) or *App^{NL-G-F/+}-KI* (APP) mice exposed to either filtered air or UF PM with quantitation (below). GLT-1 is decreased in UF PM exposed animals compared to wild-type air exposed animals, but not within the *App^{NL-G-F/+}-KI* group. Bars represent mean values, with error bars expressed as standard error of the mean (N = 8 animals per group). * denotes $p < 0.05$.

2.5 Discussion:

We report that chronic exposure to concentrated UF PM was associated with decreased performance in spatial and object recognition memory tasks in both a young *App^{NL-G-F/+}-KI* mouse model and older wild-type and *App^{NL-G-F/+}-KI* mice, which recapitulates the adverse impact of PM in cognition observed at multiple ages in humans (Harris et al., 2015; Jedrychowski et al., 2015; H. Lin et al., 2017; X. Zhang et al., 2018). We also show that 12-week PM exposure exacerbated AD-related neuropathology, particularly A β burden, in older heterozygous *App^{NL-G-F/+}-KI* mice, while no significant change was observed in younger *App^{NL-G-F/+}-KI* mice with pre-to-early plaque pathology. These changes in memory tasks and A β plaque load with UF PM exposure are not accompanied by gross loss of synaptic proteins, increases in glial inflammatory markers, or BBB integrity. However, we observe a decrease in the protein levels of the astrocytic glutamate transporter GLT-1 in both *App^{NL-G-F/+}-KI* and wild-type animals exposed to UF PM, which has not been previously reported.

Our current findings on increased A β plaque load in *App^{NL-G-F/+}-KI* mice following UF PM exposure are not only consistent with previous reports in different mouse models (Bhatt et al., 2015; Cacciottolo et al., 2017; Durga et al., 2015), but also adding new knowledge that UF PM exposure exacerbates plaque development even in the brain with physiological expression of APP, and that advancing age and pathology may be more susceptible to such change. However, the absence of increased A β pathology with exposure to concentrated PM in the 6 month old group, as well as the impairment of behavior in the wild-type animals in the aged group, suggests that the mechanisms by which PM exposure impairs cognitive function is not primarily reliant on A β pathology. Additionally, while both inflammation and the loss of BBB integrity are associated with PM exposure in other models (Block & Calderón-Garcidueñas, 2009; Calderón-

Garcidueñas, Solt, et al., 2008; Fonken et al., 2011; Kleinman et al., 2008), we do not see changes in those areas in the current model. Differences in exposure paradigms as well as the composition of exposure may account for the discrepancy. Determination of the precise mechanisms leading to cognitive decline in this model may also provide insight into whether the changes in inflammation and BBB integrity seen elsewhere would potentially be caused by the same pathway, or if they are separate pathologies.

GLT-1 loss is well associated with neurodegenerative outcomes (Colangelo et al., 2014; Pajarillo et al., 2019). The observed loss of GLT-1 in the hippocampus with UF PM exposure here indicates glutamate transport disruption as a possible pathway linking to the cognitive deficits observed. Previous PM exposure studies mice show changes in the glutamate receptor subunit GRIA1 with exposure *in vivo* (Cacciottolo et al., 2017; Morgan et al., 2011) as well as *in vitro* effects on neurite outgrowth and NMDA toxicity (Morgan et al., 2011). Together with our finding of decreased GLT-1, these results form a basis to further investigate the role of glutamate dyshomeostasis in PM induced cognitive decline. Glutamate excitotoxicity (Lewerenz & Maher, 2015) of particular neuronal subsets may in part account for our observed memory task decline, and bears inquiry. As glutamate transport dyshomeostasis and excitotoxicity are known to be involved in tau pathology progression, both by increasing phosphorylation and encouraging tau propagation (Dabir et al., 2006; Hunsberger et al., 2015; Kilian et al., 2017; J. W. Wu et al., 2016), the loss of GLT-1 here indicates a possible mechanism linking tau pathology and air pollution exposure. Numerous reports have shown an increase in total tau as well as phosphorylated tau in humans, dogs, and mice exposed to air pollution (Calderón-Garcidueñas, Mora-Tiscareño, et al., 2012; Calderón-Garcidueñas et al., 2018, 2020; Levesque et al., 2011; Park et al., 2020), providing a clear connection between exposure and tau pathology. Further

study in a human tau transgenic model may provide insight into possible non-amyloid based mechanisms linking air pollution exposure and AD risk, as well as potential involvement in other tauopathies.

The current study, however, has several shortfalls limiting the ability to fully ascertain the mechanisms at play connecting UF PM, cognitive decline, and amyloid pathology. As mentioned previously, despite strong existing evidence showing neuroinflammation and A β changes with PM exposures, we found no evidence of either in the younger animal cohort, and only A β plaque accumulation in the older *App*^{NL-G-F/+}-KI but not wild-type animals, providing no clear mechanism for the memory task impairment seen in these groups. The finding of GLT-1 loss in the hippocampus suggests possible mechanisms, but without additional evidence of LTP impairment, synapse dysfunction, or neuronal damage, it does not fully explain the changes either. While the younger cohort was intended as a pilot group to study A β changes in an AD model and was thus performed with only *App*^{NL-G-F/+}-KI animals, the lack of wild-type animals there limits our ability to determine whether the cognitive changes observed are at all related to the *App*^{NL-G-F/+}-KI genotype or were entirely independent. Similar findings in the older cohort, as well as a lack of change in any observed amyloid markers, suggests an amyloid independent pathway. It is, however, feasible that even the low levels of A β present interacted with PM toxicity. In both the ORM task and GLT-1 protein assays in the older cohort we observe a decrease with UF PM exposure in the wild-type group, but not the *App*^{NL-G-F/+}-KI. In both cases, the *App*^{NL-G-F/+}-KI and wild-type UF PM groups have similar reported values, while the *App*^{NL-G-F/+}-KI air group shows a non-significant decrease compared to the wild-type air group. It may be that UF PM exposure toxicity and amyloid toxicity act in the same pathway in such a way that the additional insult has limited impact, but that cannot be determined from the current data.

Finally, the particle number in the UF PM exposure in the older study is nearly twice the value as in the younger cohort study but the mass concentrations are relatively close, which suggests a smaller average particle size in the older cohort exposure. As PM is typically considered more toxic and better able to infiltrate the body the smaller the size (S. Kim et al., 2001; Valavandis et al., 2008), it is unknown to what degree this influenced the changes observed in A β plaques in *App*^{NL-G-F/+}-KI animals with exposure in the older cohort compared to the younger cohort.

Investigation of potential metal accumulation in the brain may provide additional insights into the pathways by which cognitive impairment occurs and the degree of PM infiltration to the CNS. PM is highly heterogeneous and consists of various compounds and metals (Hand et al., 2012; Kleeman et al., 2000; Perrone et al., 2013). Exposure to nickel through inhalation has been shown to increase A β load in wild-type mice (S. H. Kim et al., 2012). PM associated metals appear to deposit in multiple areas of the body following exposure (Q. Li et al., 2015) and it is known that the smaller PM size fractions can both infiltrate to the blood (Kreyling et al., 2002; Nemmar et al., 2002) and to the CNS directly via the olfactory nerves (Block & Calderón-Garcidueñas, 2009; González-Maciel et al., 2017). Manganese exposure has been linked to impaired glutamate transport (Erikson et al., 2002; Hazell & Norenberg, 1997), including loss of GLT-1 protein (Mulkus et al., 2005) as observed here, and leads to dopaminergic neuronal loss (Pajarillo et al., 2018) which could potentially explain the observed cognitive deficits. However, whether manganese or any other metals accumulate in the brain with PM exposure in the current model remains purely speculative and requires investigation.

In summary, we find reduction of memory function in both wild-type and the *App*^{NL-G-F/+}-KI mouse model with exposure to concentrated UF PM. This is accompanied by a reduction of the astrocytic glutamate transporter GLT-1, but not changes in glial inflammatory markers. A β

plaque burden is increased in aged animals but is not accelerated at a pre-pathological age, indicating that PM exposure is sufficient to increase amyloid burden, but also that cognitive decline due to PM exposure cannot be only due to amyloid pathology. Further investigation into the mechanisms linking PM exposure to memory impairment, particularly the extent of glutamate transport disruption and whether it plays a causative role in this impairment, in the model is required.

Chapter 3: *In Utero* exposure to ultra-fine particulate matter impairs cognition and increases neuroinflammation in aged mice and increases Amyloid β plaque load in AD model mice.

3.1 Abstract:

Accelerated cognitive decline and increased risk for Alzheimer's disease (AD) have recently emerged as a direct consequences of chronic exposure to airborne particulate matter (PM) in elderly populations, and its exposure during the prenatal period has been associated with decreased intellectual performance in children and young adults. However, little is known about the neurotoxic impact of early-life exposure to PM on cognition and late-life neurological disorders, despite the fact that life-long exposure to PM is inevitable particularly for individuals residing highly polluted areas. Here, we examined the impact of *in utero* PM exposure on cognition and neuropathology in adult wild-type mice and the amyloid precursor protein knock-in ($App^{NL-G-F/+}$ -KI) model of AD. Two-week exposure to concentrated quasi-ultrafine PM (UF PM) collected from ambient air resulted in decreased performance in the object location memory task in both groups as compared to animals exposed to filtered air, while the object recognition task was only decreased when comparing the wild-type air exposed group to the App^{NL-G-F} -KI UF PM group. Markers of glial neuroinflammatory response, astrocytic GFAP and microglia expressing Iba1 and CD68, were also increased with UF PM exposure. Exposure to UF PM also increased amyloid- β plaque load pathology in the App^{NL-G-F} -KI animals. Overall, these results show that developmental exposure to UF PM can affect cognition, neuroinflammation, and AD pathology progression in adult animals in a murine model. The molecular mechanisms altered during the exposure period leading to these changes remain to be elucidated.

3.2 Introduction:

There is substantial and increasing evidence that exposure to air pollution is linked negatively to cognitive function in a wide range of ages. Particulate matter (PM), a heterogeneous mixture of small solids and liquids suspended in the air, comprises a significant portion of traffic related air pollution and has been specifically linked to some of these outcomes in exposures as early as *in utero*. Exposure to polycyclic aromatic hydrocarbons (PAHs), a component of PM, during pregnancy correlates with reduced verbal and non-verbal IQ in adolescence (Edwards et al., 2010; Jedrychowski et al., 2015; Perera et al., 2006, 2009). More generally, exposure to fine particulate matter (PM_{2.5}) is correlated with reduced IQ performance in children as well (Lertxundi et al., 2015; Porta et al., 2016). In the elderly exposure to PM is associated with reduced working and episodic memory (J. A. Ailshire & Clarke, 2014; J. A. Ailshire & Crimmins, 2014; Younan et al., 2020) as well as significantly increased risk of dementias, including Alzheimer's disease (AD) (Cacciottolo et al., 2017; H. Chen, Kwong, Copes, Hystad, et al., 2017; Jung et al., 2015; Oudin et al., 2016). While there is significant evidence of a link between PM exposure and accelerated cognitive decline in humans, the molecular mechanisms driving this are still incompletely understood. Additionally, there is limited research investigating whether the cognitive changes and presumed underlying molecular changes with developmental PM exposure persist into adulthood and affect the risk of developing AD and other dementias in later life.

Experiments in rodent models exposed to ultra-fine PM (UF PM, a diameter of 100 nm or less) have demonstrated cognitive decline, synaptic loss, and inflammation in the CNS (Bhatt et al., 2015; Durga et al., 2015; Fonken et al., 2011; Guerra et al., 2013). UF PM exposure in adult animals increases levels of inflammatory cytokines and glia activation in wild type animals (Bhatt et al., 2015; Fonken et al., 2011; Guerra et al., 2013; Kleinman et al., 2008), and in an AD

model increases amyloid- β (A β) levels (Cacciottolo et al., 2017), suggesting possible mechanisms by which PM exposure may impact cognitive function. Studies of the effects of PM exposure during development in adult animal models are limited, but available reports indicate that such an exposure can alter memory function and neuroimmune state in adult mice (Allen et al., 2013; Allen, Liu, Pelkowski, et al., 2014; Allen, Liu, Weston, et al., 2014; Kulas et al., 2018; Zanchi et al., 2010). Currently no studies have examined whether exposure to PM during development in AD model animals can influence AD pathology progression later in life. Here, we hypothesized that exposure to concentrated ultrafine PM from ambient air during development accelerates cognitive decline later in adult mice through aberrant neuroinflammation and/or accelerated buildup of AD-like neuropathology in the brain. To test this hypothesis, we designed an *in utero* exposure using pregnant wild-type females mated with either wild-type males or homozygous *App* knock-in (*App*^{NL-G-F/NL-G-F}-KI) male mice (Saito et al., 2014), which carried wild-type or heterozygous *App*^{NL-G-F/+}-KI offspring, respectively. The use of wild-type females also allowed us to eliminate maternal genetic variances that may impact on the development of fetus. We aged offspring until 12 months of age and examined the effect of *in utero* PM exposure in order to determine whether developmental exposure substantially accelerates age-related cognitive and pathological changes in these mice.

3.3 Methods:

3.3.1 Animals

All experiments were performed in accordance with the Institutional Animal Care and Use Committee at University of California. Mice were housed on a 12 hour light-dark cycle with feed and water ad libitum. Humanized APP with the Swedish, Arctic, and Iberian mutations (*App*^{NL-G-F/+}-KI) mice in the C57BL/6 background (Saito et al., 2014) were obtained from the

RIKEN Institute (Japan). C57BL/6J male and female mice were obtained from Jackson Laboratory (Bar Harbor, ME). A total of 16 female C57BL/6J mice were bred to either male C57BL/6J or *App*^{NL-G-F/NL-G-F}-KI mice and exposed to concentrated particulates during pregnancy. Of 80 pups 11 were wild-type air exposed, 19 were wild-type UF PM exposed, 23 were *App*^{NL-G-F/+}-KI air exposed, and 27 were *App*^{NL-G-F/+}-KI UF PM exposed.

3.3.2 Exposure Paradigm

Ambient particulates in the area around the UC Irvine campus in Orange County, California with particle diameters smaller than 180 nm (quasi-ultra-fine particles) were concentrated using a versatile aerosol concentration and enrichment system (VACES) as previously described (S. Kim et al., 2001). The VACES is composed of size selective inlets, saturator and chiller modules that supersaturate the aerosol with water vapors to grow them to a size that can be inertially separated using a virtual impactor, and a diffusion drier module that removes excess water vapor and returns the aerosol to a size distribution similar to the ambient air. The system can enrich the concentration of particles in the 0.03 - 2.0 μm size range by a factor of 30x ambient, depending on output flow rate. The VACES system is located adjacent to a major roadway in Irvine, CA, and exposure occurs over morning commute hours to emphasize motor vehicle associated PM. Upon observation of a vaginal plug, female wild type mice bred with either *App*^{NL-G-F/NL-G-F}-KI or wild-type male mice were transferred to the facility housing the VACES to begin exposure. Presumed pregnant dams were exposed to either air filtered to remove particulate matter or concentrated UF PM. Animals were exposed 4 days per week (Tuesday – Friday), for 5 hours per day, for approximately 2.5 weeks, from 07:30-12:30 local time, which captures the period of maximum PM concentration during the day. Average particulate concentration during the experiment for the UF PM exposed pregnant mothers was 206 $\mu\text{g}/\text{m}^3$, or 42.9 $\mu\text{g}/\text{m}^3$ per day if

weighted for 24 hours, and $0 \mu\text{g}/\text{m}^3$ for the filtered air exposed mothers. The UF PM exposure is within values that are seen in highly polluted areas (WHO, 2016), and accounting for heterogeneity of sensitivity to exposure in humans as well as animal-to-human extrapolation exposing mice to is translatable to potential human exposure during pregnancy (Rees & Hattis, 2004). The 4 days/wk exposure paradigm reflects typical air pollution episodes (Kleinman et al. 2005, Kleinman et al. 2007). Pups were allowed to age under normal condition with no additional air pollution exposure until 12 months of age. At 12 months, the pups were sacrificed for tissue collection. Particulate mass and particle counts were obtained using a DustTrak aerosol monitor with DustTrak Pro software (TSI) and a Condensation Particle Counter with Aerosol Instrument Manager software (TSI).

3.3.2 Cognitive Assessments

Animals in the were tested in Object Location Memory (OLM) and Object Recognition Memory (ORM) tasks. OLM was performed 3 weeks from sacrifice, at approximately 11.5 months of age. ORM was run following a 1 week break period after OLM testing. These tasks were performed based on a previously described protocol (Vogel-Ciernia & Wood, 2014). Animals were habituated to the test arena for 6 days, 5 minutes per day, and then exposed to two identical objects for 10 minutes for training. Different base objects were used for ORM and OLM acquisition. Testing occurred 24 hours following training. In the OLM task one of the two objects was moved to a novel location, while for ORM one of the objects was replaced with a novel object. Objects replaced or moved were alternated between mice. Mice were allowed to explore during the acquisition for 10 minutes and the test for 5 minutes. Both test and training exploration were recorded, with the video used to score performance. Total time spent exploring each object- set as the time with the animal's nose within 1 cm of the object and pointing directly

at the object- was recorded. Time exploring each of the two objects was summed to obtain total exploration time. Animals showing a strong preference for exploring one object over the other during the acquisition phase were removed from the final analysis pool. The discrimination index was calculated as the difference between time spent exploring the novel object or location and time spent exploring the familiar object or location expressed as a percentage of the total time spent exploring during the test phase.

3.3.3 Protein Extraction and Western Blot Analysis

Half brain cortical tissue and hippocampi were homogenized in T-PER buffer with protease and phosphatase inhibitor cocktails (Thermo Fisher). Protein extract was then centrifuged at 100,000 x g for 1 hour at 4°C and the supernatant was taken as the detergent soluble fraction. The pellet was resuspended in 88% formic acid and centrifuged again at 100,000 x g for 1 hour at 4°C and the supernatant from this step was taken as the formic acid soluble fraction. Protein concentration was determined by the Bradford protein assay. Protein samples were run on Bio-Rad Mini-PROTEAN® TGX™ gels (Bio-Rad) at 150V and transferred to Immobilon®-FL PVDF membranes (Millipore). After 1 hour blocking in Li-Cor Odyssey® Blocking Buffer in TBS (Li-Cor Biosciences), membranes were immunoblotted with the following antibodies overnight at 4°C: Glyceraldehyde-3-phosphate dehydrogenase (GAPDH, 1:1,000, Santa Cruz Biotechnology), tubulin (1:25,000 Abcam), post synaptic density protein 95 kDa (PSD95, 1:1,000, Cell Signaling Technology), synaptophysin (1:1,000, Cell Signaling Technology), glial fibrillary acidic protein (GFAP, 1:1000, DAKO), Iba1 (1:1,000, Abcam), GLT1 (1:500, a gift from Dr. Jeffery Rothstein at Johns Hopkins University), or amyloid precursor protein, c-terminal (751-770) (CT-20, 1:1000, EMDMillipore). Membranes were then washed, incubated for 1 hour at room temperature with secondary antibodies Goat anti Rabbit or Goat anti Mouse

IRDye® 680 and 800 (1:20000 Li-Cor Biosciences), washed again and read. Blots were read using the Li-Cor Odyssey system and Image Studio software version 5 (Li-Cor Biosciences) to obtain band signal intensity. Signal is expressed relative to tubulin or GAPDH levels, which were used for protein loading control, before statistical analysis. GLT1 levels were additionally expressed relative to GFAP levels to account for potential changes due to astrocyte activation or loss.

3.3.4 Immunofluorescent Staining

Frozen brain hemispheres sectioned into 40µm slices coronally using a microtome and stored in phosphate buffered saline with 0.05% sodium azide. Sections were mounted on standard glass microscope slides (Fisher) before staining. For antibody staining sections were permeabilized with 0.1% triton-x 100 in tris buffered saline (TBS) for 15 minutes and blocked with 3% bovine serum albumin (Fisher), 5% normal goat serum (Vector), and 0.1% triton-x 100 in TBS for one hour. For Aβ plaque staining sections were treated with 88% formic acid for 7 minutes before other treatments. After pre-treatment and blocking, the sections were incubated with primary antibodies against PSD95 (1:1,000, Cell Signaling Technology), synaptophysin (1:1,000, Cell Signaling Technology), GFAP (1:1000, DAKO), Iba1 (1:1,000, Abcam), CD68 (1:1000, Bio-Rad), or anti amyloid 82E1 (1:1000, Immuno-Biological Laboratories) overnight at 4°C.

Sections were washed with TBS and treated for 1 hour at room temperature the following day in 3% BSA, 5% normal goat serum, and 0.1% triton-x 100 in TBS with secondary antibodies conjugated with Alexa Fluor 488, 555, or 633 (Fisher). For Thioflavin S staining sectioned were rehydrated with ethanol at 100%, 95%, 70%, and 50% and then treated with Thioflavin S (Sigma) in 50% ethanol for 10 minutes. Slides were mounted with Fluoromount-G (Fisher).

Images were taken with a Leica TCS SPE confocal microscope for Aβ plaque staining and

GFAP and Iba1 staining. Plaque burden was assessed as the percent of total measured area occupied by amyloid beta plaques from the cortex and hippocampus CA1 region. Vascular width was determined by the average of 5 measurements across the vessel. ImageJ version 1.52 was used to analyze images.

3.3.5 A β Quantitation

Detergent soluble and formic acid soluble A β ₁₋₄₀ and A β ₁₋₄₂ levels were measured using the Human β Amyloid (1-40) ELISA kit and Human β Amyloid (1-42) ELISA kit (Wako). Protein sample extracts were obtained and quantified as described under Protein Extraction and Western Blots. 100 μ L of protein was loaded per well for each sample. Bradford protein assay concentration readings were used to adjust for total protein loaded per sample.

3.3.6 Statistical Analysis

Immunoblots were quantified using Image Studio Software version 5. Immunofluorescent images were quantified using ImageJ version 1.52. All other data were analyzed using Microsoft Excel (Microsoft Office 365 ProPlus) or Prism version 3 (GraphPad Software). Statistics were carried out using unpaired t-test or two-way analysis of variance with Tukey's post hoc test. p values ≤ 0.05 were considered significant. Sex differences were generally not observed, and data are presented as mixed groups.

3.4 Results:

3.4.1 UF PM exposure in utero impairs cognition in 12 month old wild-type and *App*^{NL-G-F/+}-

KI mice

Beginning at 11.5 months the *App*^{NL-G-F/+}-KI and wild-type mice born from the exposed mothers were tested for memory function with object recognition memory (ORM) and object location memory (OLM) tasks following established protocols (Vogel-Ciernia & Wood, 2014) (Fig. 1).

In the spatial memory OLM task no genotype effect was detected but UF PM exposure significantly decreased performance in both the wild-type and *App*^{NL-G-F/+}-KI groups (Fig. 1A). In the wild-type group the discrimination index was 29.1% for air exposed animals versus 13.4% for the UF PM exposed group (p<0.01), and 24.1% compared to 16.2% respectively in the *App*^{NL-G-F/+}-KI group (p<0.05). For the ORM task the wild-type air exposed group performed best at a 25.9% discrimination index, with the wild-type UF PM exposed and *App*^{NL-G-F/+}-KI air exposed mice both at 21.4%, and the *App*^{NL-G-F/+}-KI UF PM group the worst at 16.3% (Fig.1B). Only the wild-type air to UF PM *App*^{NL-G-F/+}-KI comparison was significantly different (p<0.05). Together these results indicate that exposure to UF PM during development can impact memory function in adult mice, and that the *App*^{NL-G-F/+}-KI genotype and *in utero* UF PM exposure may have additive effects on memory impairment.

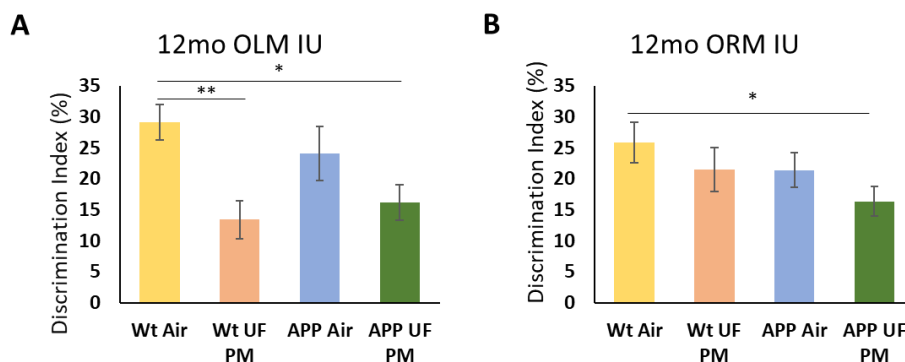


Figure 1: UF PM exposure *in utero* impairs memory in aged wild-type and *App*^{NL-G-F/+}-KI mice.

Object location memory (OLM) and object recognition memory (ORM) task results for wild-type (Wt) and *App*^{NL-G-F/+}-KI (APP) mice. Discrimination index is the difference between time spent exploring the novel object or object in novel place and the familiar as a percentage of the total time. (A) Discrimination index for the OLM task. UF PM exposed mice of either genotype mice showed significantly decreased ability to discriminate the novel object location compared to wild-type mice exposed to filtered air. (B) Discrimination index for ORM. *App*^{NL-G-F/+}-KI UF PM exposed mice showed decreased ability to discriminate the novel object compared to wild-type animals exposed to filtered air. (N = 8-12 animals per group. Scale bars = 100 μ m). * denotes p value < 0.05 and ** denotes p < 0.01.

3.4.2 In utero UF PM exposure decreases synaptic marker PSD95 and increases glia

inflammation in combination with the *App*^{NL-G-F/+}-KI genotype

A previous report examining *in utero* fine PM exposure on adult mice found increases in both synaptic marker synaptophysin and astrocytic marker GFAP in the exposed group (Kulas et al., 2018). We first examined synaptic density markers PSD95 and synaptophysin (SYP) in the cortex and hippocampus and found that PSD95 decreased by 30% in the cortex and 35% in the hippocampus comparing the wild-type air exposed group to the *App^{NL-G-F/+}*-KI UF PM group ($p < 0.05$ for both, Fig. 2A, B). However, we failed to detect a significant difference in PSD95 between filtered air and UF PM exposed groups within the same genotype. There was no significant difference in synaptophysin in any of the groups tested in either area (Fig. 2A, B).

PM exposure has been associated with increased inflammatory reactions in the CNS (Calderón-Garcidueñas, Mora-Tiscareño, et al., 2008; Calderón-Garcidueñas, Solt, et al., 2008; Kleinman et al., 2008; Kulas et al., 2018). While we did not observe inflammatory reactions with UF PM exposure of adults in the *App^{NL-G-F/+}*-KI (Chapter 2), development may be a time of particular vulnerability. PM_{2.5} exposure in pregnant rats causes cognitive deficits in the pups which are ameliorated by administration of anti-inflammatory compounds reducing microglia and oxidative stress (Tseng et al., 2019). An exposure paradigm similar to the current experiment in developing mice has also shown an increase in astrocyte presence in adult mice (Kulas et al., 2018), which play important roles in both inflammation response and synaptic signaling function.

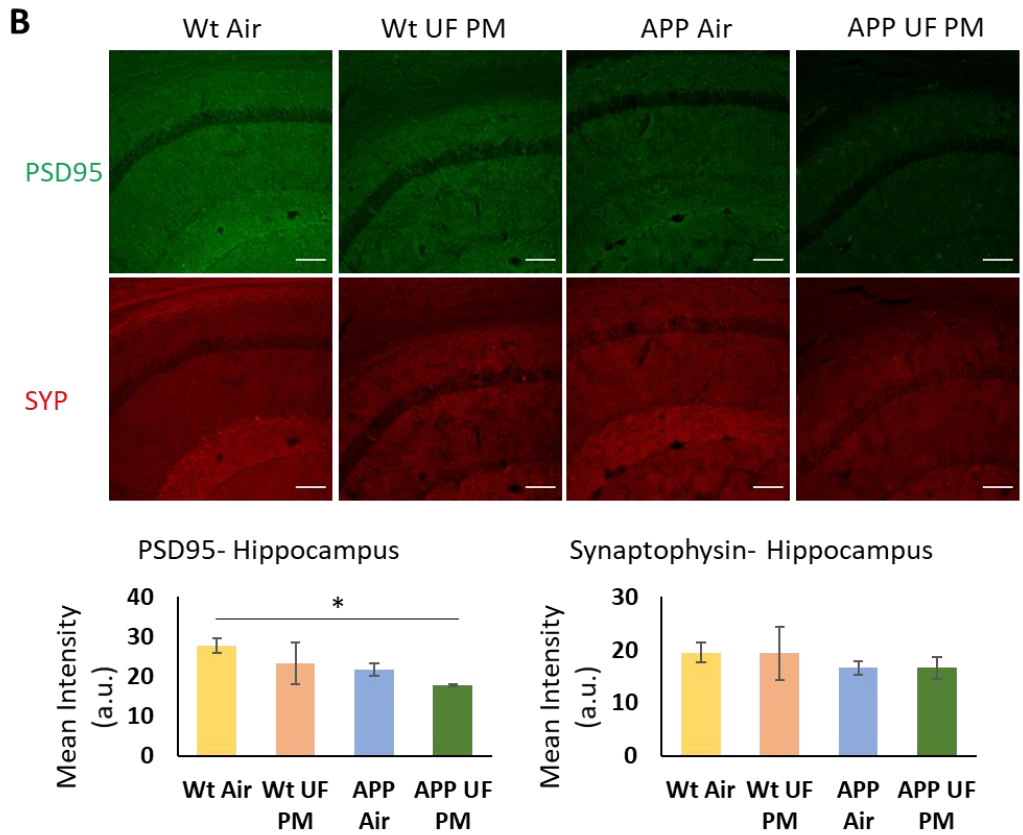
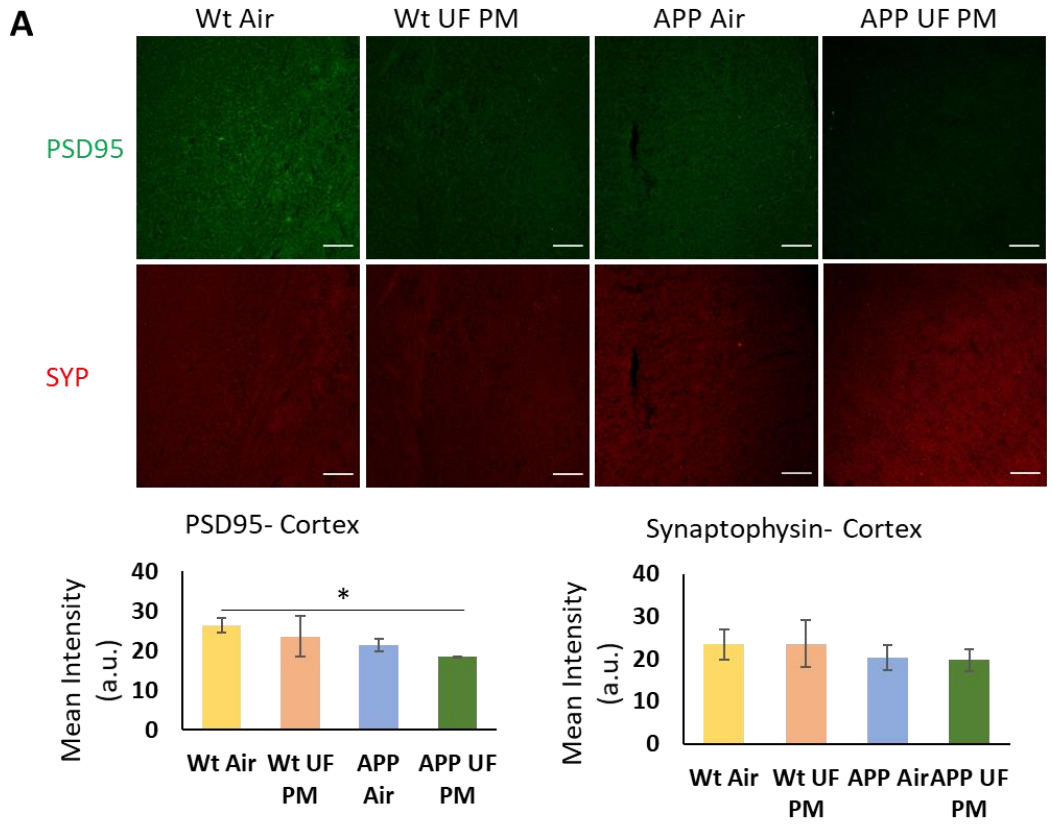
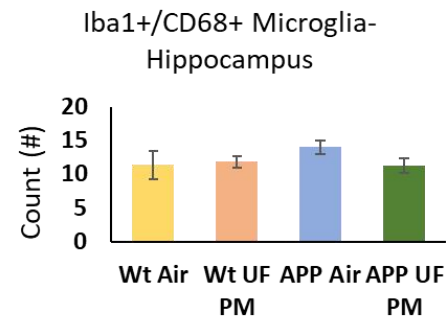
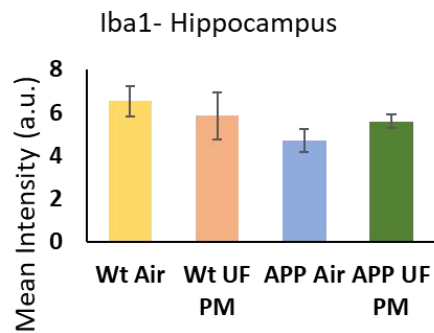
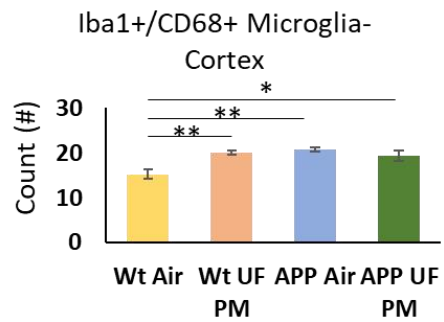
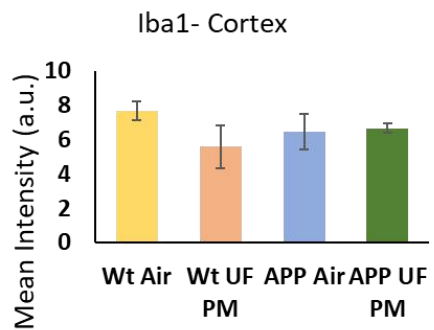
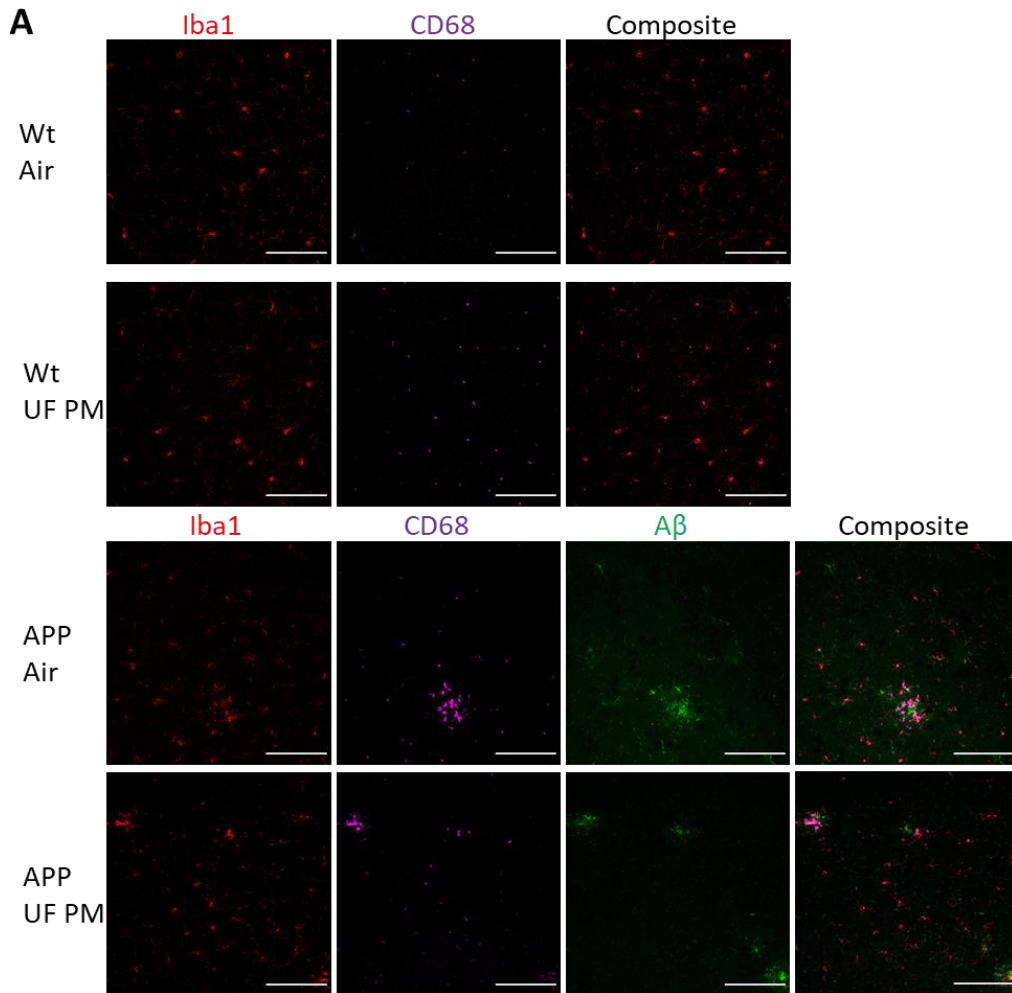


Figure 2: Synaptic marker PSD95 decreases in 12 month old mice with joint *in utero* UF PM exposure *App*^{NL-G-F/+}-KI genotype. (A) Representative images of PSD95 (green) and synaptophysin (red) immunofluorescent staining taken from the parietal cortex with fluorescent intensity quantification from the whole cortex. PSD95 is decreased in the *App*^{NL-G-F/+}-KI (APP) animals exposed to UF PM *in utero* as compared to wild-type (Wt) animals exposed to filtered air. (B) Representative images of PSD95 (green) and synaptophysin (red) immunofluorescent staining and fluorescent intensity quantification for the CA1 region of the hippocampus. As in the cortex, PSD95 is decreased in the *App*^{NL-G-F/+}-KI animals exposed to UF PM *in utero* as compared to wild-type animals exposed to filtered air. (C) Representative western blot of synaptophysin and PSD95 from cortical tissue samples with band intensity relative to tubulin. (D) Representative western blot of synaptophysin and PSD95 from hippocampal tissue with band intensity relative to tubulin. Bars represent mean values, with error bars expressed as standard error of the mean (N = 4 animals per group. Scale bars = 100 μ m). * denotes p value < 0.05.

We examined neuroinflammation by detecting GFAP+ astrocytes, Iba1+ microglia, and CD68 as a marker of autophagosomes to quantify the phagocytic capacity of microglia in the brain (Fig. 3). Total Iba1 signal was not significantly changed by genotype or exposure status in the cortex or hippocampus, however the count of reactive microglia, described here as microglia with co-expression of CD68 and Iba1, was increased comparing the wild-type air exposed animals to the other three groups in the cortex (Fig. 3A). In the cortex the number of reactive microglia increased by 31% comparing exposure groups within the wild-type genotype ($p < 0.01$), 36% comparing air exposed wild-type to the *App*^{NL-G-F/+}-KI group ($p < 0.01$), and 27% comparing the wild-type air group to the *App*^{NL-G-F/+}-KI UF PM group ($p < 0.05$); there were no changes in reactive microglia count in the hippocampus. Total GFAP signal was increased 74% comparing the wild-type air exposed group to the UF PM exposed *App*^{NL-G-F/+}-KI animals in the cortex ($p < 0.05$) and showed non-significant trends to increase comparing exposure status within genotype in the cortex (Fig. 3B). In the hippocampus there were no significant changes in GFAP signal. We also examined the total protein level of the astrocytic glutamate transporter GLT-1 in the hippocampus of these mice, as it was shown to be decreased with UF PM exposure in adult mice (Chapter 2 Fig. 13). However, in this study hippocampal GLT-1 levels were not significantly decreased with UF PM exposure (Fig. 3C). Both the PSD95 and GFAP results indicate that an additive effect may exist between UF PM exposure *in utero* and *App*^{NL-G-F/+}-KI genotype, supporting the result of the behavior data from the ORM task.



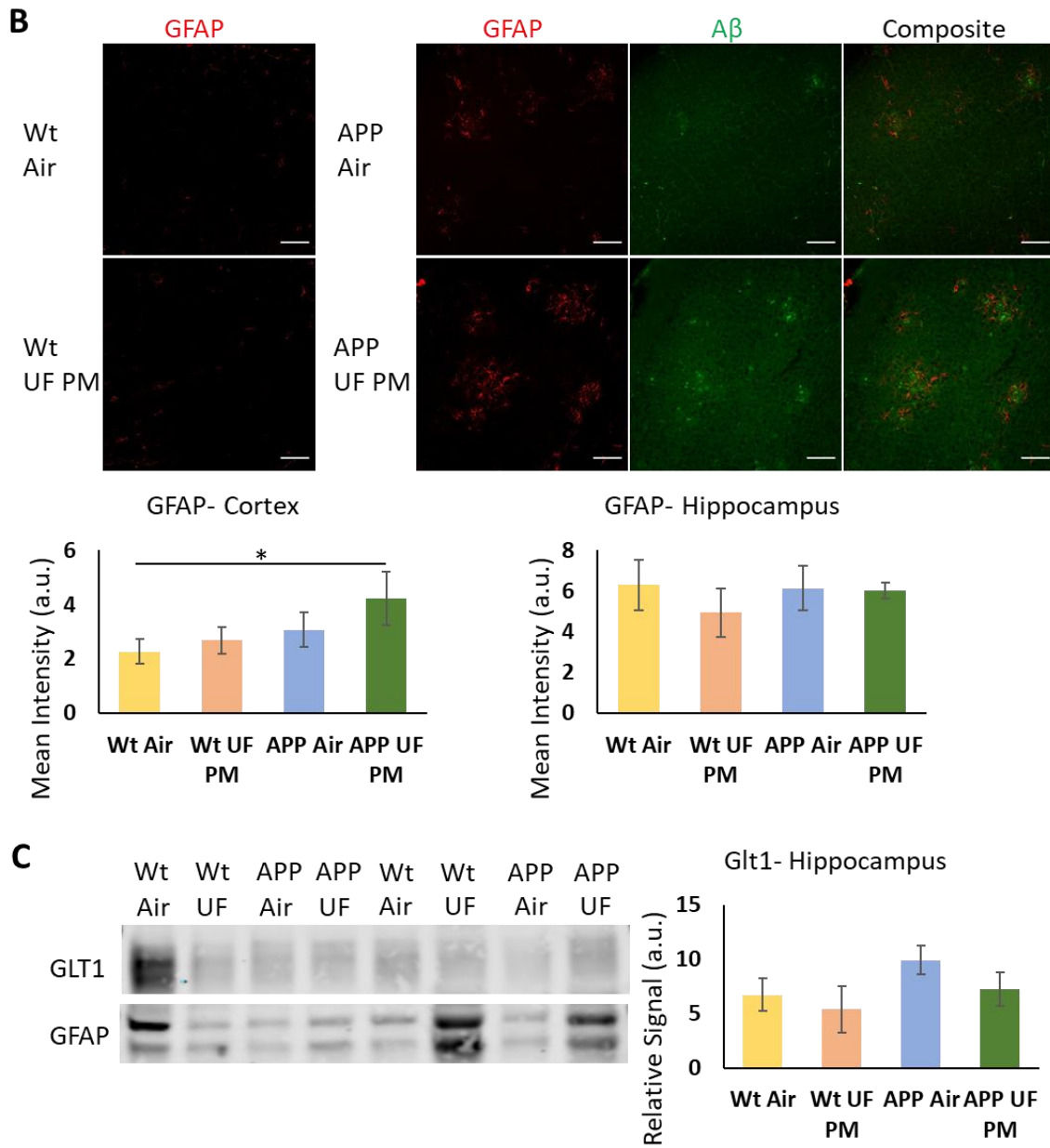


Figure 3: Glial marker GFAP increases with *in utero* exposure to UF PM in 12 month old $App^{NL-G-F/+}$ -KI mice. $Iba1+$ /CD68+ microglia increase with *in utero* exposure to UF PM in 12 month old wild-type mice.

(A) Representative images of microglial marker Iba1 (red), CD68 (purple), and A β (green) staining taken from the parietal cortex of wild-type (Wt) and $App^{NL-G-F/+}$ -KI (APP) mice exposed to filtered air or UF PM, as well as quantification of the mean fluorescent intensity of Iba1 staining and total count of Iba1 and CD68 positive microglia in $App^{NL-G-F/+}$ -KI mice from the cortex and hippocampus. Exposure to UF PM increases the number of Iba1+/CD68+ microglia in the cortex of wild-type animals, but not in $App^{NL-G-F/+}$ -KI animals. (B) Representative images of astrocytic marker GFAP (red) and A β (green) staining taken from the parietal cortex as well as quantification of the mean fluorescent intensity of GFAP staining for the cortex and hippocampus. UF PM exposure combined with $App^{NL-G-F/+}$ -KI genotype increases the levels of GFAP compared to wild-type animals exposed to filtered air. (C) Representative western blot of GLT-1 in the hippocampus and quantification. No changes are seen in GLT-1 levels. (N = 4-6 animals per group for immunofluorescent staining and quantification, and N = 6 animals per group for immunoblot. Scale bars = 100 μ m). * denotes p value < 0.05 and ** denotes p < 0.01.

3.4.3 UF PM exposure in utero increased amyloid β plaque load in adult $App^{NL-G-F/+}$ -KI mice

We additionally sought to determine whether UF PM exposure *in utero* might affect amyloid pathology in the $App^{NL-G-F/+}$ -KI AD model animals, which does not occur in the heterozygous model until 6-7 months of age (Saito et al., 2014) and is thus significantly removed temporally from the exposure. We found that *in utero* UF PM exposure increases the total amyloid plaque load in the cortex of 12 month $App^{NL-G-F/+}$ -KI mice, but otherwise does not increase amyloid burden (Fig. 4). The total area occupied by A β plaques as detected by 82E1 antibody increased 90% in UF PM exposed $App^{NL-G-F/+}$ -KI mice as compared to the filtered air exposed group ($p < 0.05$), but was did not significantly increase in the hippocampus (Fig. 4A). Dense core plaque area, as detected by Thioflavin-S, did not increase in either the cortex or hippocampus (Fig. 4B). Total APP protein detected by western blot was also not significantly affected by UF PM exposure in either the wild-type or $App^{NL-G-F/+}$ -KI groups (Fig. 4C). Finally, there were no changes in the detergent insoluble A β_{1-40} or A β_{1-42} peptide levels with UF PM in the cortex exposure either (Fig. 4D), while hippocampal insoluble and the detergent soluble fraction were below detection limits (data not shown). Together these data indicate that the changes due to *in utero* UF PM exposure may increase A β aggregation, but do not affect total production of APP protein or peptides.

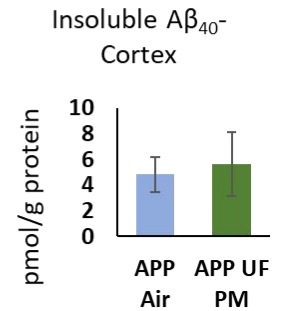
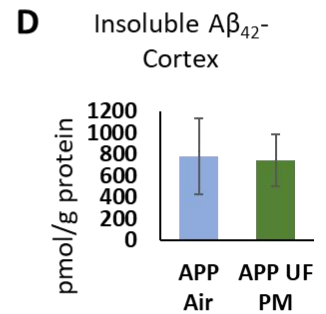
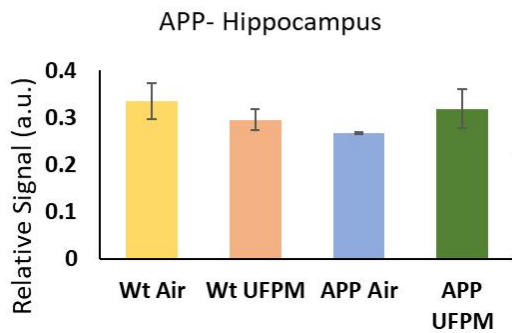
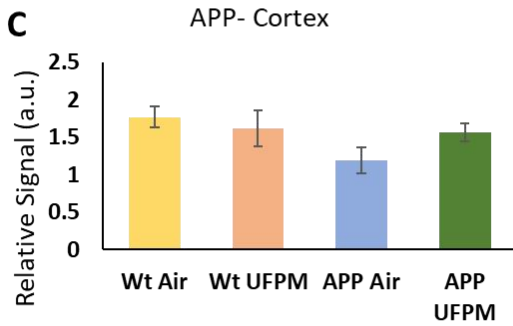
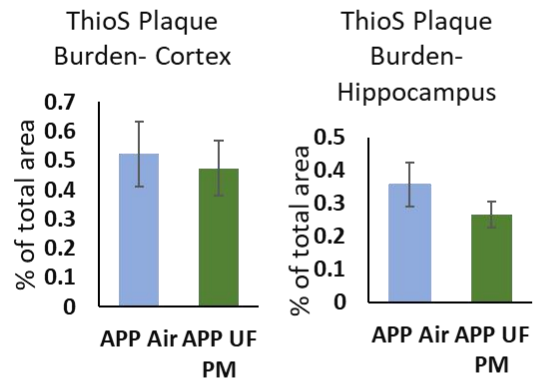
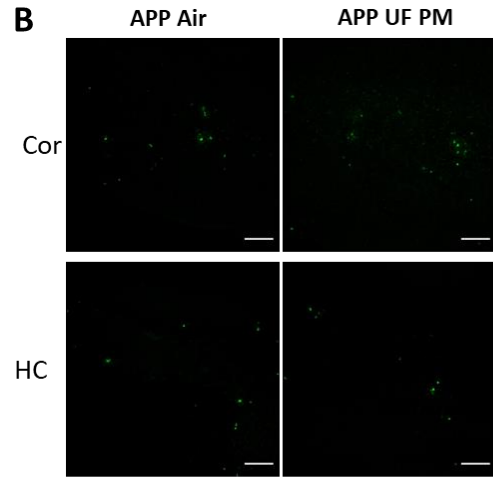
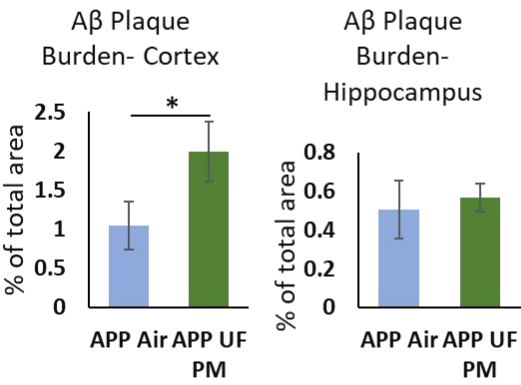
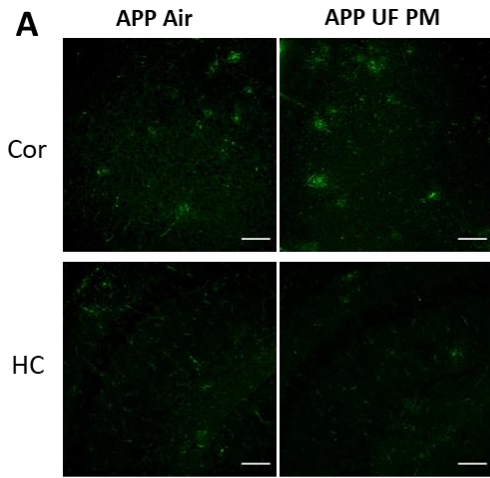


Figure 4: A β plaque burden is increased in the cortex by *in utero* UF PM exposure in the 12 month old *App^{NL-G-F/+}-KI* mice

Brain sections were stained with 82E1 antibody and Thioflavin-S to detect diffuse and dense core A β plaques in 12 month old *App^{NL-G-F/+}-KI* mice. (A) Representative images and quantification of total area of A β plaque burden detected by 82E1 from the parietal cortex (Cor, top) and CA1 region of the hippocampus (HC, bottom) in *App^{NL-G-F/+}-KI* (APP) mice exposed to filtered air or UF PM. Area % covered by plaques increases with UF PM exposure in the cortex, but not hippocampus. (B) Representative images of cortical and hippocampal A β dense core plaque burden from the parietal cortex (Cor, top) and CA1 region of the hippocampus (HC, bottom) and quantification of plaque burden for both. Dense core plaque burden does not increase with UF PM exposure. (C) Representative western blots and quantification. Steady-state levels of full length APP in tissue homogenates extracted from cortical and hippocampal tissues were not significantly affected by PM exposure *in utero*. (D) Quantification of A β peptides. No differences in insoluble A β_{40} or A β_{42} levels in *App^{NL-G-F/+}-KI* mice were found in the brain by ELISA. Bars represent mean values, with error bars expressed as standard error of the mean (N = 6 animals per group for immunofluorescent staining and quantification, and N = 4 animals per group for immunoblot, V-PLEX, and qPCR. Scale bars = 100 μ m). * denotes p value < 0.05.

3.5 Discussion:

This is the first report examining the long-term adverse effects of *in utero* exposure to quasi ultrafine particulate matter on adult neuropathology and behavior in a knock-in mouse model of AD. We find that *in utero* exposed mice impair spatial memory and object recognition memory, and that synaptic proteins are decreased while markers of glial inflammation are increased. In both behavior and neuropathological changes, we find the greatest effect with joint UF PM exposure and *App^{NL-G-F/+}-KI* genotype compared to either alone. However, it remains unanswered whether this effect is due to exacerbation of the AD pathology by UF PM, or simply an additive effect of two independent insults. We additionally report that *in utero* exposure can increase A β plaque build-up in adult AD model mice. This result is of interest as A β pathology does not start in the *App^{NL-G-F/+}-KI* model until 6-7 months of age, indicating the PM exposure during development can impact processes that do not even begin until adult life. Whether this is mediated by the abnormal inflammatory activation remains to be determined. Regardless, this result suggests that early life exposure to UF PM in AD model mice affects AD outcomes in later life.

Comparing to the other known work examining *in utero* exposure on CNS changes in adult wild-type mice (Kulas et al., 2018), there are several notable differences. Kulas et al found no change in the synaptic marker PSD95 and an increase in synaptophysin when examining FVB mice. Conversely, we find no change in synaptophysin and a decrease in PSD95, but only when comparing wild-type C57BL/6J animals exposed to filtered to *App*^{NL-G-F/+}-KI mice exposed to UF PM. In both studies astrocyte marker GFAP is increased, but again only with both *App*^{NL-G-F/+}-KI genotype and UF PM exposure together in the current study. In both studies no changes were seen in total Iba1. While Iba1 and CD68 co-expressing microglia were found to be increased here with UF PM exposure in both the wild-type and *App*^{NL-G-F/+}-KI groups, they were not assessed in the Kulas et al paper. Memory impairment is associated with exposure both here and in Kulas et al, though working memory was assessed in that study compared to spatial and recognition memory in the present study. As the Kulas et al study did not use an AD model, they were unable to assess amyloid plaque pathology, but both here and in that study mouse APP protein levels were unaffected by exposure. The discrepancies between the two studies may be accounted for in the different models used or differences in exposure length, severity, and particulates. The Kulas et al study had a lower average concentration by weight at 46.7 $\mu\text{g}/\text{m}^3$ as compared to 206 $\mu\text{g}/\text{m}^3$ here, but with a longer exposure period of 30 hours per week versus 20 hours per week here. Additionally, we use UF PM of diameter less than 180 nm, while they used the fine PM fraction- PM of diameter 2.5 μm or less. Finally, the composition of airborne particulates is highly variable (Harrison & Yin, 2000; Valavandis et al., 2008), and differences in composition may account for some of the differences seen. Overall, however, these studies agree that *in utero* exposure to particulate matter can impair cognitive function and increase

inflammation in adult mice and together form a strong foundation to encourage further examination the effects of such exposure of neuropathology in disease models.

The current study is intended as a pilot to determine whether *in utero* exposure to airborne particulates can impact neuropathology that develops later in life rather than a comprehensive examination of molecular pathways. There are several limitations regarding determination of the mechanisms by which this neuropathological impact occurs. Most critically, we do not have data from the pregnant dams and the fetuses being exposed to particulates at the time of exposure. Additional research at this critical time point is required to understand which pathways are being altered and how such changes might persist into adult mice. Whether these changes are occurring by direct PM influence in the fetus or indirectly by effects on the mother, or both, is also unknown currently. Examination of the model at multiple time points is required to determine if the inflammatory changes seen are persistent starting at exposure, or only occur in aged animals. Similarly, behavioral testing at multiple ages may reveal whether the *in utero* exposure only potentiates memory deficits later in life, or if the animals are impaired at young ages as is seen in human exposure (Lertxundi et al., 2015; Porta et al., 2016). Finally, the health of the mice outside of the CNS was not assessed. Other works have indicated that *in utero* exposure can have effects in the cardio-pulmonary system and may induce high blood pressure in adult mice (Morales-Rubio et al., 2019; Rychlik et al., 2019; Tanwar et al., 2018; Ye et al., 2018), which in turn potentially affects memory ability and AD pathology (Cifuentes et al., 2015; Tucsek et al., 2017). Thus, with the current findings we are unable to determine whether the effects seen are the primary driving factors or simply derivative from potential systemic effects in the body.

Despite these shortcomings, this study provides preliminary evidence for further investigation into the effects of exposure to particulates during development on later life neuropathological outcomes in the mouse model of AD. We observe behavior deficits concurrent with changes in synaptic proteins, glial response, and A β build up in 12 month old adult mice with *in utero* UF PM exposure. Further study to determine the causative molecular pathways of the memory deficits in the current model, whether other dementia animal models exhibit the same vulnerability to early-life PM exposure, and whether this relationship translates to humans will help determine the contribution of *in utero* PM exposure to dementia risk later in life.

Chapter 4: Astrocyte transport of glutamate and neuronal activity reciprocally modulate tau pathology in *Drosophila*

4.1 Preamble

This work was completed at University of California, Merced, in the Quantitative and Systems Biology program and published in *Neuroscience*, vol. 348 April 2017 as Kilian et al “Astrocyte transport of glutamate and neuronal activity reciprocally modulate tau pathology in *Drosophila*” prior to transfer to University of California, Irvine and the Environmental Health Sciences program. As such, this work does not directly continue the work in air pollution and mouse models of AD presented in chapters 2 and 3. However, the nature and findings of this work focusing on glutamate transport connect directly to loss of GLT-1 seen in the adult exposure model (Chapter 2), and inform future directions I suggest in Chapter 5. Thus, I feel this work has value to be presented in the current thesis.

4.2 Abstract

Glutamate homeostasis disruption is increasingly implicated in Alzheimer’s disease (AD) progression and cognitive decline. Particularly, the loss of the major astrocytic glutamate transporter, GLT-1, accelerates cognitive decline and AD pathology accumulation. Previously, we demonstrated that a restoration of GLT-1 ameliorated a buildup of tau pathology and rescued cognition in a mouse model of AD. Abnormal buildup of the microtubule associated protein tau is a major pathological hallmark of Alzheimer’s disease and various tauopathies. The mechanisms by which pathological tau accumulates and spreads throughout the brain remain largely unknown. We hypothesized that aberrant extracellular glutamate and abnormal neuronal excitatory activities promoted tau pathology. In the present study, we investigated genetic interactions between tau and the GLT-1 homolog dEaat1 in *Drosophila melanogaster*.

Neuronal-specific overexpression of human wildtype tau markedly shortened lifespan and impaired motor behavior. RNAi depletion of dEaat1 in astrocytes worsened these phenotypes, whereas overexpression of dEaat1 improved them. However, the synaptic neuropil appeared unaffected, and we failed to detect any major neuronal loss with tau overexpression in combination with dEaat1 depletion. To mimic glutamate-induced aberrant excitatory input in neurons, repeated depolarization of neurons via transgenic TrpA1 was applied to the adult *Drosophila* optic nerves, and we examined the change of tau deposits. Repeated depolarization significantly increased the accumulation of tau in these neurons. We propose that increased neuronal excitatory activity exacerbates tau-mediated neuronal toxicity and behavioral deficits.

4.3 Introduction

Alzheimer's disease (AD) is the most common neurodegenerative disease associated with dementia (Reitz et al., 2011). The main pathological hallmarks of AD are the formation of amyloid plaques and neurofibrillary tangles (NFTs), respectively composed of amyloid beta (A β) peptides and hyperphosphorylated microtubule associated protein tau. Mutations that cause familial AD are either in the amyloid precursor protein gene or in genes of proteins critical for APP processing, supporting the hypothesis that A β buildup is the major upstream factor in familial AD pathogenesis (De Strooper et al., 1998; Reitz et al., 2011; Scheuner et al., 1996). Abnormal buildup of A β alone may not be sufficient to cause AD dementia, however, suggesting that other pathological changes, such as inflammation, tauopathy, and synaptic dysfunction are essential to development of AD (Hämäläinen et al., 2007; Jacob et al., 2007; Jay et al., 2015; Kimura et al., 2013; Roberson et al., 2007; Shipton et al., 2011; Vom Berg et al., 2012). Disruption of glutamate homeostasis is implicated in the development of AD pathology and cognitive decline (Masliah et al., 1996; Meeker et al., 2015; Mookherjee et al., 2011). Glutamate

is the main excitatory neurotransmitter of the central nervous system. Its clearance from the extracellular space and its recycling is regulated by five glutamate transporters in humans. Excitatory amino acid transporter 2 (EAAT2), expressed in astrocytes, is responsible for roughly 90% of glutamate uptake in the synaptic cleft (Danbolt et al., 1992; Tanaka et al., 1997). Reduced *EAAT2* expression in AD patients and transient hyperactivation of neurons in the hippocampus and medial temporal lobe suggest functional impairment of glutamate clearance in synapses (Bookheimer et al., 2000; Hämäläinen et al., 2007; Jacob et al., 2007; S. Li et al., 1997). In addition, decreased activity of EAAT2 correlates with neuronal and synaptic loss in AD (Masliah et al., 1996). Impairment of synaptic glutamate uptake may lead to sustained excitatory neuronal activities and abnormal cellular signaling through extrasynaptic NMDA receptors in neurons (Parsons & Raymond, 2014). These findings suggest glutamate-based excitotoxicity as a potential cellular mechanism promoting AD neuropathology. In a mouse model of AD decreased expression of GLT-1 (the mouse homolog of EAAT2) accelerates the onset of cognitive deficits, increases pathological A β , and alters brain metabolic pathways (Meeker et al., 2015; Mookherjee et al., 2011). Pharmacological upregulation of GLT-1 rescues AD pathology, reducing amyloid plaques, pathological tau accumulation, synaptic loss, and cognitive deficiency (Takahashi et al., 2015; Zumkehr et al., 2015). The connection between GLT-1 loss and tau may be self-reinforcing, as astrocytic expression of human tau in a mouse model reduces GLT-1 function and GLT-1 levels, and vesicular glutamate transport is altered in human tau expressing mice (Dabir et al., 2006; Hunsberger et al., 2015). Additionally, non-AD tauopathies also exhibit neurodegeneration and dementia in humans without A β buildup (Ballatore et al., 2007; Wolfe, 2012), linking synaptic dysfunction and tau pathology as A β independent pathways leading to dementia in AD. The complete underlying molecular

mechanisms by which abnormal synaptic function and tau pathology in AD remain incompletely understood.

To better understand the molecular link between the glutamate transporter and tau pathology we used *Drosophila melanogaster* as a model organism. *Drosophila* provides an alternative to the mouse model for genetic disease studies. *Drosophila* is widely used to identify the molecular basis of neurodegenerative diseases, including AD and tauopathies (Lu & Vogel, 2009; McGurk et al., 2015; Prüssing et al., 2013). Particularly, *Drosophila* has been used to investigate AD-related mechanisms of tau pathology exacerbation, including the role of the GSK-3 β pathway in tau phosphorylation, the negative effects of phosphorylated tau on normal tau, and the AD risk gene *BINI*'s effect in modulating tau pathology (Chapuis et al., 2013; Chatterjee et al., 2009; Cowan et al., 2010; Jackson et al., 2002). *Drosophila* expresses two glutamate transporters, the human EAAT2 homolog dEaat1, and dEaat2, with dEaat1 being the only high affinity glutamate transporter in *Drosophila* (Besson et al., 2000, 2011). Here, we decreased and increased the astrocytic expression of dEaat1 and examined behavioral and pathological impacts on *Drosophila* expressing human wildtype 2N4R tau. Our results provide evidence for a role of astrocytic glutamate transport reduction and glutamate-induced excitatory signal in the overall phenotypes and the progression of tau pathology.

4.4 Materials and Methods:

4.4.1 Fly Stocks: Fly stocks were maintained on cornmeal, molasses, and agar food at 25°C and 70% humidity. cDNA from the 2N4R human tau isoform was subcloned into a modified P{13XLexAop2-IVS-myr::GFP} plasmid (Addgene) (Pfeiffer et al., 2010). Microinjection of the *lexAop-tau^{wt}* 2N4R was carried out by BestGene Inc. (Chino Hills, CA). *UAS-dEaat RNAi* flies have been previously described (Rival et al., 2004). *alrm-Gal4* flies were obtained from

Marc Freeman at the University of Massachusetts Medical School (Doherty et al., 2009). Other transgenic flies were obtained from the Bloomington Drosophila Stock Center (Indiana University, Bloomington, IN): *UAS-tau^{wt}* 1.13 (51362), *nsyb-LexA* (56166), *GMR-Gal4* (1104), *UAS-dEaat1* (8202), and *UAS-dTrpAI* (26263).

4.4.2 Lifespan Analysis: Groups of ten recently eclosed adult male flies were placed in a standard food vial without yeast and kept at 25°C. The flies were transferred to a new vial three times a week without anesthesia, and the number of surviving flies were counted. Each genotype was tested with total n >= 100.

4.4.3 Negative Geotaxis Climbing Assay: To assess motor ability and geotaxis response a climbing assay as described by Ali *et al.* (2011) was used. Ten male flies were placed into food vials via CO₂ anesthesia and allowed to recover for at least 24 hours. A simple apparatus was prepared consisting of two empty polystyrene vials. One vial was marked 8 cm from the bottom using a black marker. Flies were transferred to one of the vials without anesthesia, and the two vials were taped together open end to open end and placed upright. The flies were allowed five minutes to acclimate. Flies were tapped to the bottom of the marked tube, and both the number of flies that reach the 8cm mark within 10 seconds and the total amount of time, in seconds, that was required for half of the flies to cross the 8 cm mark was recorded. This process was performed a total of ten times per cohort, with one minute between trials. All flies were tested three days after eclosion.

4.4.4 Immunohistochemistry: Brains from adult flies 10-12 days after eclosion were dissected in PBT (Phosphate buffered saline + 0.05% Tween-20) and fixed in 2% paraformaldehyde in PBT at 4°C for 16 hours (J. S. Wu & Luo, 2006). After washing in PBT and blocking in PBT plus 0.5% BSA and 5% normal goat serum, primary then secondary antibodies were incubated

with the fixed brains for 24 hours, with PBT washes in between incubations. Brains were mounted in Vectashield (Vector Laboratories). Images were obtained on a Nikon Eclipse Ti C1® confocal microscope using the 40x oil immersion objective or Leica TCS SPE confocal microscope using the 10x objective. Images were analyzed with Image J software version 1.47. Antibodies used were rabbit anti-human tau (Dako) 1:200, mouse PHF-1 (phosphorylated tau at S396/S404; from Dr. Peter Davies, Albert Einstein College of Medicine) 1:1000, rabbit anti-tyrosine hydroxylase (T8700, Sigma) 1:100, and mouse anti-discs large (4F3, Developmental Studies Hybridoma Bank at University of Iowa) 1:100.

4.4.5 Immunoblot: For sarkosyl insoluble protein extraction 200 heads from adult flies 1 and 12 days after eclosion were homogenized in 15 mM NaCl, 25 mM Tris-HCl at pH 7.4, 1mM EGTA, 1 mM EDTA, 1 mM Na₃VO₄, 50 mM NaF, and 1x protease inhibitor cocktail (complete™ Roche). The homogenate was quickly centrifuged to remove debris, and then centrifuged for 1 hour at 100,000 x g. The supernatant was saved as the soluble fraction. The pellet was re-suspended in 10% sucrose, 0.8 M NaCl, 10 mM Tris-HCl at pH 7.4, 1 mM EGTA, 1 mM Na₃VO₄, 50 mM NaF, and 1x protease inhibitor cocktail, and centrifuged for 30 minutes at 15,000 x g. Sarkosyl was added to 1% and incubated at 37°C for 1 hour, then centrifuged for 2 hours at 100,000 x g. The sarkosyl insoluble pellet was resuspended in 15 µL homogenization buffer. Soluble protein fraction concentration was quantified by the Bradford protein assay (Bio-Rad). Antibodies used were mouse AT8 (phosphorylated tau at S202/T205, MN1020, ThermoFisher) 1:2000, mouse CP13 (phosphorylated at S202/T205; from Dr. Peter Davies, Albert Einstein College of Medicine), 1:1000, rabbit anti-human tau antibody (Dako) 1:1000, mouse anti-discs large (4F3, Developmental Studies Hybridoma Bank at University of Iowa) 1:100, mouse anti-alpha-tubulin 1:25000 (T6074, Sigma), and mouse PHF-1 1:1000. Sarkosyl

insoluble fraction extraction was performed as described (Colodner & MB., 2010; Goedert et al., 1992). Band intensities were analyzed with an Odyssey image station and Image Studio software v2.1.10 (Licor).

4.4.6 Eye Morphology: The temperature sensitive cation channel TrpA1 was used to stimulate *Drosophila* optic neurons under the glass multiple reporter (GMR-Gal4) driver. All flies were temperature treated to activate TrpA1 at 31°C for 2 hours/day for five consecutive days. Images were captured with a Nikon SMB-2Z dissecting microscope and digital camera. Images were taken from adult male flies 20-22 days after eclosion. Immunohistochemistry was done on flies aged 20-22 days after eclosion.

4.4.7 Statistical Analysis: Lifespan data were analyzed using the log-rank test, with $p < 0.05$ considered significant. One way ANOVA with Tukey post hoc testing for more than 2 groups and unpaired *t*-test for 2 groups were used to test for significance for negative geotaxis and immunofluorescent intensity data, and $p < 0.05$ was considered to be significant. The chi squared goodness of fit test was used to determine normality.

4.5 Results

4.5.1 dEaat1 expression modulates lifespan and behavioral phenotypes *Drosophila* overexpressing human tau

Flies expressing the longest human tau isoform, 2N4R, were used to assess the effects of human tau in the *Drosophila* brain. The 2N4R isoform contains all terminal inserts and microtubule binding repeats present in the six isoforms of tau, ensuring that domain-specific interactions can be observed. Human wildtype 2N4R tau (*LexAop-htau*) was overexpressed in all neurons using LexA/LexAop binary expression system with *nsyb-LexA*. *nsyb>tau* flies showed reduced life-

span compared to control (*nsyb>+*) flies (Figure 1A), consistent with previous reports for the 0N4R human tau isoform (Wittmann et al., 2001). Deficiency of dEaat1 by RNAi in astrocytes has previously been achieved using the GAL4/UAS binary expression system with the *alrm-Gal4* astrocyte-specific driver (*alrm>Eaat1.IR*), and these flies exhibited reduced lifespan, as previously reported (Rival et al., 2004). Combined neuronal tau overexpression and astrocytic dEaat1 depletion (*alrm>Eaat1.IR;nsyb>tau*) resulted in further reduced survival than expression of either transgene alone. Conversely, overexpression of *dEaat1* in astrocytes (*alrm>Eaat1*) did not affect lifespan (Figure 1A). Importantly, *dEaat1* overexpression in human tau expressing flies (*alrm>Eaat1;nsyb>tau*) significantly rescued lifespan. These data demonstrate that the functional consequences of neuronal tau depends on glutamate homeostasis by astrocytes.

Neuronal tau expression decreases motor function in *Drosophila* (Ali et al., 2011). We assessed performance in a startle-induced negative geotaxis climbing assay to determine if loss of dEaat1 exacerbates this phenotype. *nsyb>tau* flies showed reduced climbing (Figure 1B), as previously reported (Ali et al., 2011). *alrm>Eaat1.IR* flies exhibited a seizure-like response reaction to the initial mechanical impulse, as documented (Rival et al., 2004), which greatly reduced climbing immediately after the impulse compared to *nsyb>+* animals. The *alrm>Eaat1.IR;nsyb>tau* flies were indistinguishable from *alrm>Eaat1.IR* flies.

Due to the seizure-like reaction that interfered with the immediate climbing response in *alrm>Eaat1.IR* flies, we also measured negative geotaxis following a prolonged recovery (Figure 1C). All experimental genotypes, with the exception of *alrm>Eaat1*, showed a reduction of climbing compared to *nsyb>+*. While *alrm>Eaat1.IR;nsyb>tau* flies exhibited reduced climbing as compared to *alrm>Eaat1.IR* flies, *alrm>Eaat1.IR;nsyb>tau* flies did not reduce climbing compared with *nsyb>tau* flies. Interestingly, increased geotaxis was observed in

alm>Eaat1;nsyb>tau flies as compared to *nsyb>tau* flies. While decreased dEaat1 did not exacerbate the impairment of negative geotaxis, increased dEaat1 partially rescued geotaxis response in human tau expressing flies. Together with the lifespan analysis, this indicates that dEaat1 moderates tau pathology.

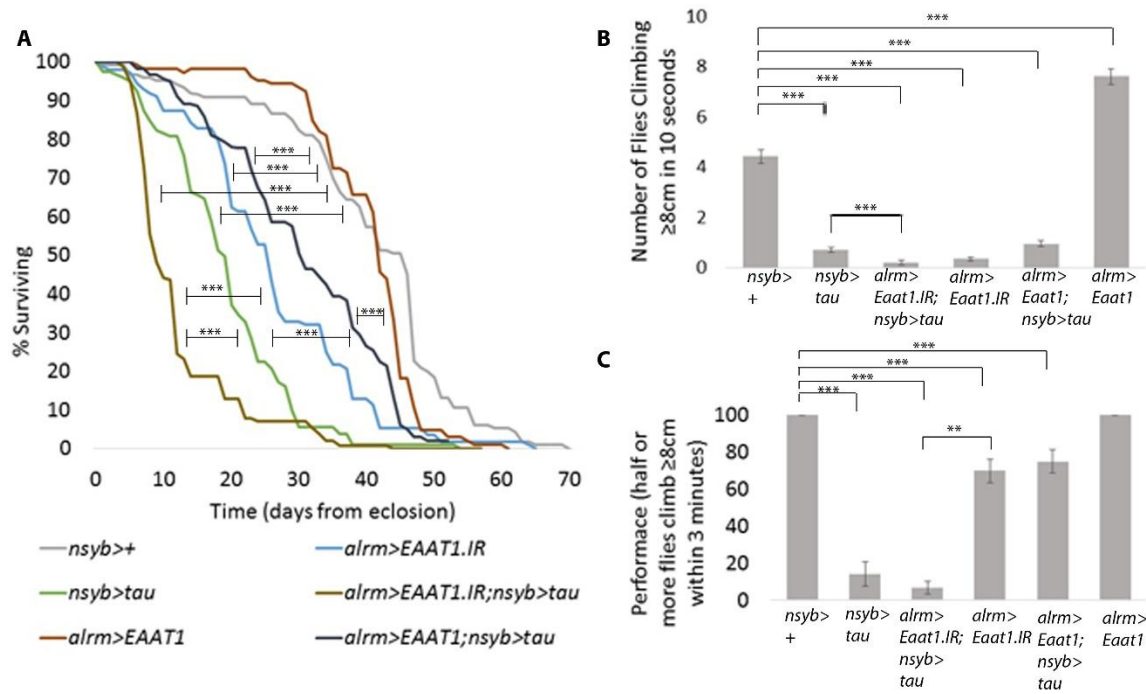


Figure 1: RNAi decreased dEaat1 worsens and overexpressed dEaat1 partially rescues tau phenotypes. (A) Survival curve of *nsyb>+* (*nSyb-LexA/+*), *alm>Eaat1.IR* (*UAS-Eaat1.dsRNA/Y;alm-Gal4/+*), *nSyb>tau* (*nSyb-LexA/+;LexAop-htau/+*), *alm>Eaat1.IR;nsyb>tau* (*UAS-Eaat1.dsRNA/Y;nSyb-LexA/alm-Gal4;LexAop-htau/+*) flies, *alm>Eaat1* (*alm-Gal4/+;UAS-Eaat1/+*), and *alm>Eaat1;nsyb;tau* (*nsyb-LexA/alm-Gal4;LexAop-htau/UAS-Eaat1*) flies. By log rank test *alm>Eaat1.IR* ($p<0.001$), *nSyb>tau* ($p<0.001$), *alm>Eaat1.IR;nsyb>tau* ($p<0.001$), and *alm>Eaat1;nsyb;tau* ($p<0.001$) show reduced lifespan compared to the control. *alm>Eaat1.IR;nsyb>tau* flies have reduced lifespan as compared to both *alm>Eaat1* ($p<0.001$) and *nsyb>tau* ($p<0.001$). *alm>Eaat1;nsyb>tau* flies show increased lifespan compared to *nsyb>tau*, but reduced compared to *alm>Eaat1*. $n \geq 100$ flies per genotype. (B) Climbing response, determined by the number of flies that climb ≥ 8 cm in 10 seconds after mechanical impulse. Flies 3 days after eclosion were used to minimize age dependent performance decreases. *alm>Eaat1.IR* ($p<0.001$), *nSyb>tau* ($p<0.001$), *alm>Eaat1.IR;nsyb>tau* ($p<0.001$), and *alm>Eaat1;nsyb;tau* ($p<0.001$) exhibited reduced response compared to *nsyb>+*, while *alm>Eaat1* showed increased response ($p<0.001$). *alm>Eaat1.IR;nsyb>tau* flies perform worse than *nsyb>tau* flies ($p<0.01$). $n = 5$ independent biological replicates, with 10 flies per replicate. (C) Geotaxis response of control and test flies, expressed as a percentage of trials where 50% or more of the flies climbed ≥ 8 cm by 180 seconds. $n = 5$. Each bar is the mean \pm the standard error of the mean. ** $p \leq 0.01$, *** $p \leq 0.001$.

4.5.2 Expression of hTau or loss of Eaat1 does not significantly alter overall synaptic or neuronal loss in Drosophila brain

Extensive neuronal loss has previously been reported in human tau overexpressing *Drosophila* models (Jackson et al., 2002; Wittmann et al., 2001). We attempted to detect any synaptic and neuronal loss in our *Drosophila* models as a pathological outcome using various techniques. However, quantification of the post-synaptic density marker DLG1 detected no significant differences comparing *nsyb>+* to either *nsyb>tau*, *alrm>Eaat1.IR*, or *alrm>Eaat1.IR;nsyb>tau* fly brains in whole brains imaging (Figure 2A and B) or protein quantification (Figure 2C and 2D). Similarly, TUNEL or active caspase-3 staining did not show significant difference among these groups (data not shown). As small scale neuronal loss may be difficult to detect in whole brain assays, we next attempted to stain a well-defined subpopulation of neurons. Dopaminergic neurons in the dopaminergic PPL1 cluster were significantly reduced in *nsyb>tau* flies compared to *nsyb>+* control group (Figure 2E and F). The loss of dEaat1 in tau flies (*alrm>Eaat1.IR;nsyb>tau*) further reduced the number of dopaminergic neurons in the PPL1 cluster (Figure 2E and F). The overexpression of *dEaat1* in tau flies (*alrm>Eaat1;nsyb>tau*) significantly rescued the number of dopaminergic neurons from (*alrm>Eaat1.IR;nsyb>tau* group but not *nsyb>tau* group (Figure 2E and F).

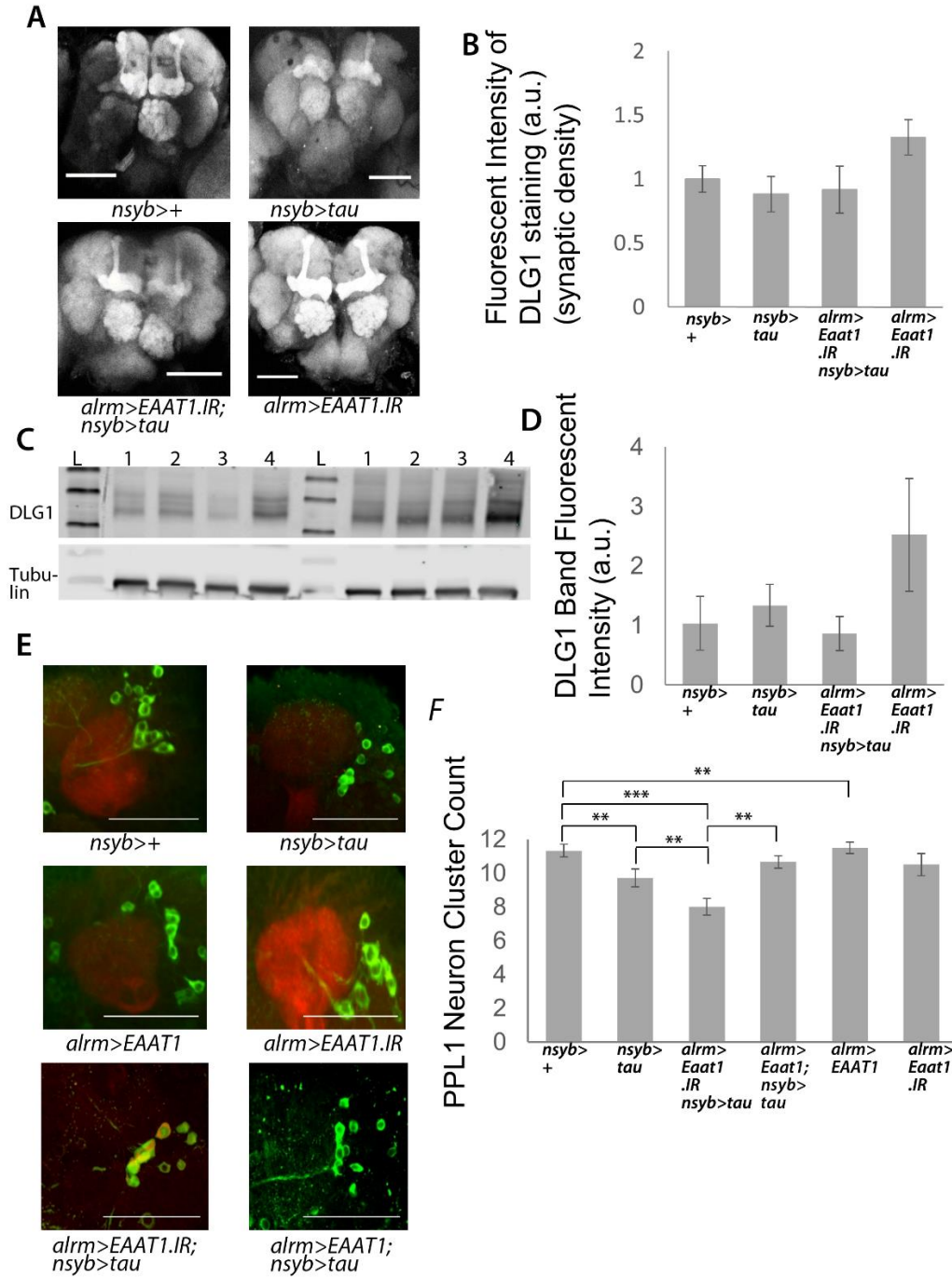


Figure 2: Human Tau expression shows no general neuronal loss but does induce reduction in a limited neuronal subset. (A) Representative images of adult fly brains immunostained for the post-synaptic protein DLG1 for *nsyb>+*, *nsyb>tau*, *alrm>Eaat1.IR;nsyb>tau*, and *alrm>Eaat1.IR* flies. (B) Fluorescent quantification of total synaptic density in the central brain and protocerebrum structures by DLG1 staining of adult flies 12 days after eclosion. No differences were found between experimental genotypes. n = 5. (C) Representative western blot bands for DLG1 from whole brain homogenate with tubulin loading control. L- molecular weight ladder 1- *nsyb>+* 2- *nsyb>tau* 3- *alrm>Eaat1.IR;nsyb>tau* 4- *alrm>Eaat1.IR*. (D) Densitometric quantification of DLG1 western blot band intensity normalized to tubulin loading control. n = 4. (E) PPL1 dopamine neuron cell bodies detected with anti-tyrosine hydroxylase (green) and anti-DLG1 (red). (F) Number of PPL1 cell bodies in adult flies 12 days after eclosion. n=4-9. Each bar is the mean \pm the standard error of the mean. ** $p \leq 0.01$, *** $p \leq 0.001$. Scale bars 100 μ m.

4.5.3 Changes in dEaat1 glutamate transporter expression do not change the accumulation of insoluble tau

Quantification of total and phosphorylated tau levels was performed by western blot using both the soluble fraction and sarkosyl insoluble fraction from adult flies approximately 12 days after eclosion. There was no detectable shift in the amount of total tau present in *nsyb>tau*, *alrm>Eaat1.IR;nsyb>tau*, or *alrm>Eaat1;nsyb>tau* fly heads in either total protein extraction or the sarkosyl insoluble protein fraction (Figure 3A). Similarly, no change in the relative burden of phosphorylated tau species was detected (Figure 3B). This suggests that the observed pathology is not dependent on tau levels.

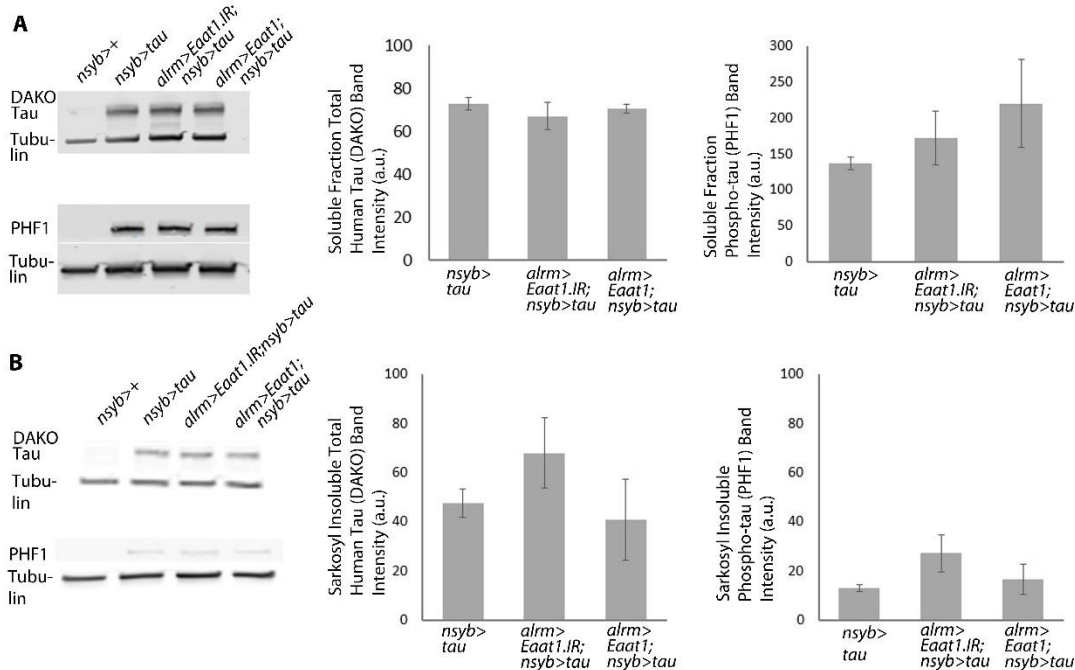


Figure 3: Dysregulation of astrocytic dEaat1 does not affect human tau accumulation. Protein samples taken from flies 10-12 days after eclosion, matching with the 50% survival point for the most severe phenotype (*alrm>Eaat1.IR;nsyb>tau*). (A) Representative western blot bands for soluble fraction human total (DAKO antibody) tau and phospho-tau (PHF1 antibody), with tubulin antibody for load control, of *nsyb>+*, *nsyb>tau*, *alrm>Eaat1.IR;nsyb>tau*, and *alrm>Eaat1;nsyb>tau* whole brain homogenate protein samples. Quantification of band intensity normalized to tubulin loading control. No difference between genotypes was found using two-way ANOVA. (B) Representative western blot bands for sarkosyl insoluble fraction total tau (DAKO antibody) and phospho-tau (PHF1 antibody) and quantification by band intensity. No difference between genotypes was found using two-way ANOVA. n=3-4. Each bar is the mean \pm the standard error of the mean.

4.5.4 Repeated overstimulation of neurons in the *Drosophila* eye increases tau load

To test if increased neuronal activity promotes tau pathology, we co-expressed the temperature-sensitive cation channel, TrpA1, with human wildtype tau in neurons in the fly eye. Human tau expression causes reduced eye size, a rough eye surface, and degeneration of the optic lobes (Jackson et al., 2002; Wittmann et al., 2001). Using GMR-Gal4, we generated flies expressing human tau (*GMR>tau*), TrpA1 (*GMR>TrpA1*), and the combination (*GMR>TrpA1,tau*). These flies were repeatedly exposed to TrpA1 activation conditions. At 3 weeks after eclosion, treated *GMR>tau* and *GMR>TrpA1,tau* showed a reduction in eye size and a rough eye phenotype compared to *GMR>TrpA1* flies; there was no difference between *GMR>tau* and *GMR>TrpA1,tau* (Figure 4A). Repeated neuronal activation lead to a marked increase of tau positive cells in the optic lobe (Figure 4B, 4C). Importantly, there was no difference in tau accumulation between *GMR>tau* and *GMR>TrpA1,tau* control flies without temperature activation of TrpA1 (Figure 4D). Temperature activated *GMR>TrpA1,tau* flies exhibited increased levels of total tau compared to the *GMR>TrpA1* flies, but not *GMR>tau* flies (Figure 4E). The accumulation of phosphorylated tau levels were also significantly increased with temperature activation of TrpA1 in *GMR>TrpA1,tau* flies as compared to *GMR>tau* flies (Figure 4F). Together, these results suggest that tau accumulation is increased by increased neuronal activity.

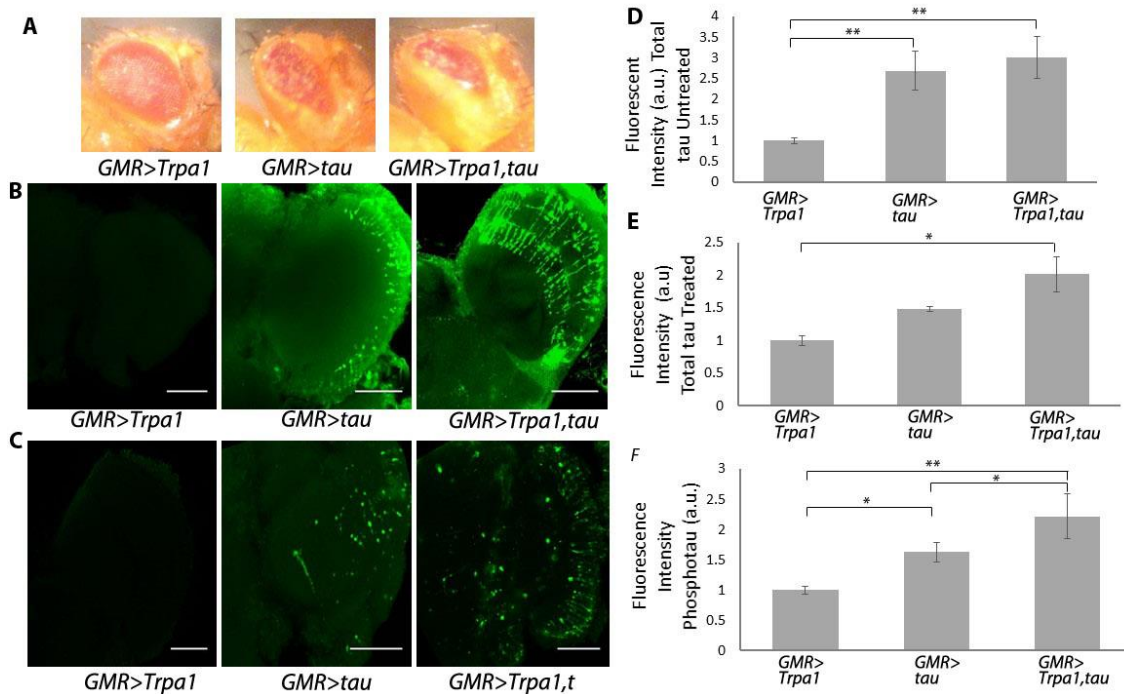


Figure 4: Chronic activation of neurons in the eye increased tau accumulation. (A) Brightfield images of the *Drosophila* eye of *GMR>TrpA1* (*GMR-Gal4/+;UAS-TrpA1/+*), *GMR>tau* (*GMR-Gal4/UAS-Tau^{wt1.13}*), and *GMR>TrpA1,tau* (*GMR-Gal4/UAS-Tau^{wt1.13};UAS-TrpA1/+*) genotypes. *GMR>tau* and *GMR>TrpA1,tau* show roughness and reduced eye size. (B) Representative staining of *Drosophila* optic lobe neurons for human total tau of *GMR>TrpA1*, *GMR>tau*, and *GMR>TrpA1,tau* genotypes. (C) Representative staining of *Drosophila* optic lobe neurons for p-tau. (D) Fluorescence intensity quantification of tau immunofluorescence in non-temperature treated *GMR>TrpA1*, *GMR>tau*, and *GMR>TrpA1,tau* flies. (E) Fluorescence intensity quantification of total human tau based immunofluorescence. (F) Fluorescence intensity quantification with p-tau antibody of optic lobes. N= 4-5. Each bar is the mean \pm the standard error of the mean. * $p \leq 0.05$, ** $p \leq 0.01$. Scale bars 50 μ m.

4.6 Discussion

We report that glutamate transporter dEaat1 levels in a *Drosophila* model of tauopathy moderate reduction in lifespan and geotaxis. However, we failed to detect any significant pathological changes, including overall synaptic or neuronal loss and buildup of tau in the brain. Although our models showed a lack of definitive association between phenotypes and the CNS pathology, the importance of tau and its neurotoxicity has been reported in several *Drosophila* models (Jackson et al., 2002; Wittmann et al., 2001) with shortened lifespan following the introduction of human tau gene, similar to our current finding. In this study, we also report that changes in

neuronal excitation frequency by temperature-sensitive TrpA increase tau load, suggesting a potential avenue for the link between the loss of dEaat1, glutamate-induced excitotoxicity, and the buildup of tau in neurons.

The discrepancy between results in our dEaat1 models and TrpA1 model may be in part due to technical limitations to detect human tau in these flies. We failed to detect tau in our newly generated human wildtype overexpressing fly brains by immunostaining using various tau antibodies in the LexA-LexAop driver system (data not shown). As a result, we were unable to examine the effect of dEaat1 on the localization or intensity of tau. *Drosophila* tau protein dTau, a homolog of human tau, is potentially a complicating factor in interpreting results. However, it has been found that tau protein toxicity is mainly mediated by soluble phosphorylated human tau even when dTau is present in the *Drosophila* model (Feuillette et al., 2010), suggesting that the effects of dTau on pathology in this model are minimal. While increased levels of phosphorylated tau or insoluble tau are widely accepted pathological phenomena, mislocalization of tau in synapses and somatodendritic compartments equally impacts neuropathological and phenotypic alterations (L. M. Ittner et al., 2010). Migration and propagation of tau in neurons when glutamate transporter activity is reduced in astrocytes needs to be further investigated, and adverse effects of tau and dEaat1 dysregulation must be considered regarding exacerbation of pathological phenotypes. The ability to rescue tau phenotypes by overexpression of dEaat1, along with results from our group using ceftriaxone in a mouse model of AD (Zumkehr et al., 2015), strongly implies that glutamate transport deficiency plays a pivotal role in tau pathology. Investigation of vesicular glutamate transport, which has been shown to be increased in conjunction with reduced GLT-1 levels in human tau expressing mice (Hunsberger et al., 2015),

in this model may elucidate the interaction between tau pathology and glutamate transport observed.

Recent findings clearly demonstrate the ability of tau to spread between anatomically connected neurons (De Calignon et al., 2012; L. Liu et al., 2012; Martin et al., 2013; J. W. Wu et al., 2013, 2016). While the underlying mechanisms are currently unknown, the release of tau may depend on neuronal activity (Pooler et al., 2013), exosomes (Asai et al., 2015), or both. These new findings help to better understand the development and progression of tau pathology in AD and tauopathies. Our data support that neuronal over stimulation promotes tau burden, suggesting the possibility that initial tau pathology leads to over-excitation, which in turn leads to propagation of tau pathology to proximal neurons. In all, it is suggested that initial tau pathology triggers glutamate dysregulation, which is then involved in the spread and continuation of further tau pathology by inducing neuronal over stimulation. However, direct excitation by TrpA1 channel induction may provide a stronger stimulus than glutamate based over-excitation, and further study is needed to confirm that reduction of glutamate clearance induces neuronal activity in a manner similar to TrpA1 induction in *Drosophila*. Additionally, the acute treatment regimen used here may poorly reflect chronic over-excitation potentially found with glutamate transporter malfunction. Further study using spatially limited neuronal tau expression may determine if the increase in tau load and tau spread seen by TrpA1 activation can be replicated using the glutamate transporter knockdown model, as tau spread may be masked under a pan neuronal expression pattern as used here. Extensive neuronal and synaptic loss is a well-documented characteristics in AD (Scheff et al., 2006; Terry et al., 1991), and is also observed in mouse models (L Mucke et al., 2000; Oddo et al., 2003). In our model, we were unable to detect wide scale loss of neurons or a major change in the synaptic neuropil concurrent with tau expression

or reduced dEAAT1 expression. As the time point chosen for analysis coincides with the 50% lethality point of *alrm>Eaat1.IR;nsyb>tau* flies, this indicates that general synaptic loss may not be a primary cause of early lethality. We considered the possibility that smaller scale neuronal loss, not detectable by general synaptic density assays, accounts for some phenotypic change. Loss of neurons in the PPL1 cluster does occur in *nsyb>tau* flies, and is exacerbated in *alrm>Eaat1.IR;nsyb>tau* flies, indicating the possibility of low levels of neuronal toxicity. Interestingly, the PPL1 cluster is dopaminergic, and not directly affected by dEaat1 loss. Although *Drosophila* uses cholinergic neurotransmission as excitatory input more than glutamatergic neurotransmission in the CNS, a number of glutamatergic neurons are distributed throughout the *Drosophila* brain (Daniels et al., 2008); dysregulation of glutamatergic input by modulating the glutamate transporter appears to exhibit global effects in the brain. Thus, it is likely that changes in neuronal function and activity in connected neurons account for the toxicity seen in the PPL1 cluster.

We propose that tau pathology is moderated by glutamate transporter activity. Further, this likely occurs by glutamate based neuronal over-excitation, which leads to spread and propagation of tau between neurons. This matches with our findings that dEaat1 expression affects the phenotypic effects of human tau in *Drosophila*, and that excitation of neurons leads to increased tau burden. Further studies are needed to confirm that these effects are due to changes in neuronal activity resulting from glutamate over-excitation, and to determine the effects of glutamate transporter knockdown on tau spread and propagation in the brain. Our study supports our earlier finding that glutamate transporter activity affects tau pathology, and therefore the possibility that Eaat2 may be an effective target for disease-modifying treatment of tauopathies.

Chapter 5: Discussion, future projects, and conclusion

There is increasing recognition of air pollutants, such as particulate matter (PM), nitric oxide species (NO_x), sulfur dioxide, ozone, and toxic hydrocarbons such as poly aromatic hydrocarbons and benzene, as neurotoxic agents leading to intellectual and cognitive impairment in individuals with wide range of ages (J. A. Ailshire & Crimmins, 2014; Gatto et al., 2014; Lertxundi et al., 2015; Perera et al., 2009; Porta et al., 2016; Power et al., 2011; Rocha et al., 2020). Among elderly population, exposure to elevated levels of air pollutants markedly increases the risk for dementia and Alzheimer's disease (AD) (Oudin et al., 2016; Ranft et al., 2009; Tzivian et al., 2016). While there are a number of existing reports examining the neurotoxic effects of these constituents in the central nervous system (CNS), the underlying molecular mechanisms linking to neuronal damage and cognitive decline remain incompletely understood. Particularly, the body of work examining how chronic exposure to PM and other constituents interacts with disease models of AD and other dementias is currently limited. Existing data in non-AD model animals has shown a correlation between PM exposure and an altered immune state including increases in inflammatory cytokines such as the interleukins IL-1 α , IL-1 β , and IL-6, and tumor necrosis factor α , changes in glial activation markers glial fibrillary acid protein (GFAP), Iba1, and CD68, and NF- κ B activation in the CNS (Bhatt et al., 2015; Calderón-Garcidueñas, Solt, et al., 2008; Campbell et al., 2005; Cheng et al., 2016; Guerra et al., 2013; Kleinman et al., 2008; Morgan et al., 2011; Park et al., 2020). Additionally, PM exposures in non-AD models have shown some ability to induce build-up of amyloid precursor protein (APP) and amyloid- β (A β) peptides (Bhatt et al., 2015; S. H. Kim et al., 2012; Levesque et al., 2011). More recently, neurotoxic effects of PM exposure have been tested in mouse models of AD (Cacciottolo et al., 2017; Jew et al., 2019). These studies find compelling gene

and environment interactions of PM exposure with the APOE4 genotype on A β pathology and cognition in 5xFAD mice (Cacciottolo et al., 2017) and cognitive decline following a short, 2-week exposure in 3xTg-AD mice (Jew et al., 2019). However, impediments to comprehensively understand the neurotoxic effects of PM in these animals include lacking of evaluation of AD neuropathology (Jew et al., 2019) and limited effect of PM exposure without the additional APOE risk genes (Cacciottolo et al., 2017). Thus, I hypothesized that exposure to ultra-fine particulate matter (UF PM) would exacerbate AD pathology and cognitive impairment in a mouse model of AD by increasing glial inflammation in the brain and accelerating A β buildup. To test my hypothesis, we exposed mice of the heterozygous *App*^{NL-G-F/+}-KI (Saito et al., 2014) model of AD to concentrated UF PM as adults (Chapter 2) or *in utero* (Chapter 3). In all groups UF PM exposure showed decreased performance in the object location and recognition memory tasks, indicating some ability of PM to impact CNS function. While in certain cases this impairment was only seen when comparing wild-type animals exposed to filtered air only to animals with both the *App*^{NL-G-F/+}-KI genotype and UF PM exposure, implying some additive effect between the two, it was also observed comparing exposure status within the wild-type groups. In the adult exposure no changes were observed in microglia or astrocytes in either the 6 month or 12 month group. A β plaque burden, a hallmark for AD pathology, was increased. However, this increase was only seen in the 12 month old *App*^{NL-G-F/+}-KI mice with established A β pathology (Saito et al., 2014). Together these data showed that, while UF PM exposure may increase behavioral deficits in combination with an AD genotype, our initial hypothesis that glial inflammation and A β were the critical molecular pathways for this link is not supported in the model. While additional assays of synaptic proteins and the integrity of the blood brain barrier tight junctions also showed no changes with exposure, there was a non-genotype specific effect

of UF PM exposure on the astrocytic glutamate transporter GLT-1 at both age points in the adult exposure. While these data alone are not enough to prove a mechanism or that GLT-1 is in the causal pathway for behavior deficits, they do suggest a relation between glutamate dyshomeostasis and UF PM exposure. Linking back to AD risk, glutamate disruption and excitotoxicity are well connected to AD pathology (Dabir et al., 2006; Masliah et al., 1996; Mookherjee et al., 2011). Specifically, tau pathology and propagation is affected by glutamate related excitotoxicity (Dabir et al., 2006; Hunsberger et al., 2015; J. W. Wu et al., 2016), potentially linking UF PM mechanisms to previous work we have done examining excitotoxicity and tau in a *Drosophila* model of tauopathy (Chapter 4). In these experiments we showed that genetic loss or increase of the *Drosophila* GLT-1 homolog dEaat1 modulates lifespan and geotaxic response in a human tau expressing model. We also demonstrated that over excitation by heat mediated depolarization events increased the propagation of tau. These results may inform future studies of the effects of PM in AD models.

Interestingly, in the *in utero* exposure experiment adult *App^{NL-G-F/+}-KI* and wild-type animals exposed to UF PM during development did display changes in glial inflammation and A β plaque burden. Additionally, there is evidence that the synaptic marker PSD95 may be reduced, which was not apparent in the adult exposure model. Lastly, there was not a significant drop in GLT-1 in the hippocampus as seen in the adult animals. As in the adult exposure, in certain comparisons there were only statistical differences when looking at the wild-type air exposed animals versus the *App^{NL-G-F/+}-KI* UF PM exposed group, implying additive effects of genotype and exposure on pathological outcomes. Otherwise, these data establish two main points: that there is a link between developmental exposure to UF PM and A β pathology in later life in the *App^{NL-G-F/+}-KI* model and that the mechanisms by which *in utero* PM exposure affect the CNS

may differ from those of adult PM exposure in this model. While this experiment did establish the link between *in utero* exposure and A β pathology, it was not designed to and does not prove a mechanism for this link. It is tempting to suggest the observed changes in reactive microglia and astrocytes lead to the increased A β accumulation and behavior deficits, but investigation in younger animals may indicate otherwise as in the adult exposure model.

5.1 Future research in the *App*^{NL-G-F}-KI model of AD

As mentioned, the current work is insufficient to prove mechanisms connecting UF PM exposure in the mouse model to observed behavioral deficits. Thus, further work in the model guided by the findings here is required to thoroughly investigate the molecular pathways involved. The immediate primary area of interest will be to determine the extent of glutamate transport disruption, the effects thereof, and whether this is directly due to PM exposure or a derivative effect from some other, yet unobserved, neurobiological or systemic changes. For the last, *in vitro* investigation using primary astrocyte and neuron co-culture, as has been performed by the lab previously (Zumkehr et al., 2018), and direct application of collected UF PM to the media will indicate whether PM has a direct effect on GLT-1 and the tripartite synapse system.

Regarding glutamate transport, changes in proteins levels of α -amino-3-hydroxy-5-methyl-4-isoxazolepropionic acid (AMPA) receptor subunits GluR1 and GluR2 have been associated with PM exposure outcomes previously (Cacciottolo et al., 2017; Morgan et al., 2011), suggesting that the changes may not be limited to GLT-1. The N-methyl-D-aspartate (NMDA) receptor is also well associated with AD and neurodegeneration (Danysz & Parsons, 2012; R. Wang & Reddy, 2017) and *in vitro* work has indicated an increase in NDMA toxicity in neuronal culture when nano-scale PM is also applied (Morgan et al., 2011), providing another avenue to explore connecting the effects of PM in AD progression. To connect the memory behavior deficits in the

UF PM exposed groups, measurement of LTP in *ex vivo* hippocampal slices should indicate whether the changes in glutamate transport are impairing this function, which is critical for memory. As LTP has been shown to be highly dependent on GLT-1 mediated glutamate uptake (Katagiri et al., 2001; Pita-Almenar et al., 2012), impairment is expected with loss of GLT-1. Finally, pharmacological upregulation of GLT-1 has been previously shown to ameliorate AD pathology (Takahashi et al., 2015; Zumkehr et al., 2015), and a similar experiment in the current model may provide further insight into whether the behavior effects observed are dependent on GLT-1 loss.

5.2 Tau models of AD and PM

Multiple reports indicate that exposure to air pollutants increases hyper-phosphorylation of tau in animal models (Calderón-Garcidueñas et al., 2018, 2020; S. H. Kim et al., 2012; Levesque et al., 2011) and in humans (Calderón-Garcidueñas, Kavanaugh, et al., 2012; Calderón-Garcidueñas et al., 2020). As tau and tau phosphorylation are highly involved in the pathology of AD, these results suggest tau interactions as another potential pathway to link PM exposure to AD risk. The phosphorylation and propagation of tau are affected by glutamate transport disruption driven neuronal over-excitation (Hunsberger et al., 2015; J. W. Wu et al., 2016), providing an additional link between the current finding of a loss of GLT-1 with UF PM exposure in mice. Further, it is possible that PM driven tau hyperphosphorylation can feed back into glutamate excitotoxicity. Hyperphosphorylated tau aggregates into neurofibrillary tangles (NFTs), which mislocalize to the cell bodies and dendrites (Holtzman et al., 2016; A. Ittner & Ittner, 2018). At the dendrites, they facilitate Fyn mediated phosphorylation of the NMDA receptor subunit GluN2B, leaving the post synapse vulnerable to over stimulation (L. M. Ittner et al., 2010; Miyamoto et al., 2017). However, to date there is no report examining the effects of PM exposure in a humanized tau

animal model of AD. Recently, a humanized tau (hTau) knock in model also expressing the *App^{NL-G-F}-KI* genotype has been created (Saito et al., 2019), providing a strong option to explore the effects of PM exposure on tau and in turn tau pathology as another potential pathway linking exposure to AD, while still maintaining the characterized effects in the *App^{NL-G-F/+}-KI* model here. Given the suggestive links between UF PM and tau pathology progression we would anticipate that the effects of UF PM exposure would be magnified in the model expressing both *App^{NL-G-F/+}-KI* and hTau.

5.3 Analysis of PM associated metals in the brain

UF PM potentially acts as a carrier for other potentially toxic constituents such as metals and organic compounds to infiltrate the body (Seaton et al., 1995). Due to its small size it can bypass blood brain barrier defenses via the olfactory nerves, demonstrated in animal models and humans (Block & Calderón-Garcidueñas, 2009; González-Maciel et al., 2017). Alternatively, it can enter the bloodstream directly through the lungs after inhalation and exert toxicity in the CNS or systemically (Kreyling et al., 2002; Nemmar et al., 2002), presenting unique risk compared to the exposure through oral ingestion. However, little work has been done to identify the extent to which PM related metals accumulate in the CNS after PM exposure. Such work will provide a foundation to indicate whether metal toxicity may be playing a role in the CNS effects of PM exposure. The extent of build-up of PM associated metals in the brain may help suggest whether direct infiltration of PM is a major exposure pathway as compared to systemic effects in the blood. Similarly, in the *in utero* exposure model, analysis of metal build up may help determine whether PM and PM related components are directly affecting the fetus, or acting primarily on the mother.

5.4 Conclusion

This dissertation shows that exposure to UF PM both *in utero* and in adult mice causes memory deficits in wild-type and *App*^{NL-G-F/+}-KI mouse model of AD, as well as increases in A β plaque load. In the *in utero* model, we demonstrate that glial inflammation and A β pathology at adult age are increased with exposure during development, suggesting potential pathways by which PM exposure influences behavior and A β burden consistent with our hypothesis (Chapter 3). In the adult exposure model, however, no changes are seen in examined inflammation markers and A β increase does not appear to be required for PM induced cognitive deficit, but levels of the astrocytic glutamate transporter GLT-1 are decreased (Chapter 2). This result links to previous work in a *Drosophila* model showing that expression of the *Drosophila* homolog of GLT-1 and direct excitation of neurons can increase tau pathology (Chapter 4), establishing a potential non-A β driven link between PM exposure and AD. In all, our findings suggest that PM exposure does induce cognitive decline and increase AD like pathology in an AD model mouse, but that glial inflammation and A β build up are not the primary pathways by which this occurs. Further studies both in the *App*^{NL-G-F/+}-KI model and in tau models of neuronal disease are required to fully understand the mechanisms linking PM exposure and AD risk outcomes.

References

- Ailshire, J. A., & Clarke, P. (2014). *Fine Particulate Matter Air Pollution and Cognitive Function Among U. S. Older Adults*. *70*(September), 322–328. <https://doi.org/10.1093/geronb/gbu064>.
- Ailshire, J. A., & Crimmins, E. M. (2014). Fine particulate matter air pollution and cognitive function among older US adults. *American Journal of Epidemiology*, *180*(4), 359–366. <https://doi.org/10.1093/aje/kwu155>
- Ailshire, J., Karraker, A., & Clarke, P. (2017). Neighborhood social stressors, fine particulate matter air pollution, and cognitive function among older U.S. adults. *Social Science and Medicine*, *172*, 56–63. <https://doi.org/10.1016/j.socscimed.2016.11.019>
- ALA. (2018). *State of the Air 2018 | American Lung Association*. <https://www.lung.org/local-content/california/our-initiatives/state-of-the-air/2018/state-of-the-air-2018.html>
- Ali, Y. O., Escala, W., Ruan, K., & RG., Z. (2011). Assaying Locomotor, Learning, and Memory Deficits in Drosophila Models of Neurodegeneration. *J Vis Exp*, *49*, 1–6.
- Allen, J. L., Conrad, K., Oberdörster, G., Johnston, C. J., Sleezer, B., & Cory-Slechta, D. A. (2013). Developmental exposure to concentrated ambient particles and preference for immediate reward in mice. *Environmental Health Perspectives*, *121*(1), 32–38. <https://doi.org/10.1289/ehp.1205505>
- Allen, J. L., Liu, X., Pelkowski, S., Palmer, B., Conrad, K., Oberdörster, G., Weston, D., Mayer-Pröschel, M., & Cory-Slechta, D. A. (2014). Early postnatal exposure to ultrafine particulate matter air pollution: Persistent ventriculomegaly, neurochemical disruption, and glial activation preferentially in male mice. *Environmental Health Perspectives*, *122*(9), 939–945. <https://doi.org/10.1289/ehp.1307984>
- Allen, J. L., Liu, X., Weston, D., Prince, L., Oberdörster, G., Finkelstein, J. N., Johnston, C. J., & Cory-Slechta, D. A. (2014). Developmental exposure to concentrated ambient ultrafine particulate matter air pollution in mice results in persistent and sex-dependent behavioral neurotoxicity and glial activation. *Toxicological Sciences*, *140*(1), 160–178. <https://doi.org/10.1093/toxsci/kfu059>
- Alonso, A., Grundke-Iqbal, I., & Iqbal, K. (1996). Alzheimer's disease hyperphosphorylated tau sequesters normal tau into tangles of filaments and disassembles microtubules. *Nature Medicine*, *2*, 783–787.
- Alzheimer's Association. (2018). Alzheimer's Facts and Figures Report | Alzheimer's Association. *Alzheimer's Association*, 1. <https://www.alz.org/alzheimers-dementia/facts-figures>
- Alzheimer's Association. (2020). *2020 Alzheimer's Disease Facts and Figures*. *16*(3). <https://doi.org/10.1016/j.jalz.2019.01.010>
- Asai, H., Ikezu, S., Tsunoda, S., Medalla, M., Luebke, J., Haydar, T., Wolozin, B., Butovsky, O., Kogler, S., & Ikezu, T. (2015). Depletion of microglia and inhibition of exosome synthesis

- halt tau propagation. *Nat Neurosci.*, 18(11), 1584–1593.
- Ballatore, C., M-y, L. V., & JQ., T. (2007). Tau-mediated neurodegeneration in Alzheimer's disease and related disorders. *Nature Reviews Neuroscience*, 8, 663–672.
- Bermudez, E., Mangum, J. B., Wong, B. A., Asgharian, B., Hext, P. M., Warheit, D. B., & Everitt, J. I. (2004). Pulmonary responses of mice, rats, and hamsters to subchronic inhalation of ultrafine titanium dioxide particles. *Toxicological Sciences*, 77(2), 347–357. <https://doi.org/10.1093/toxsci/kfh019>
- Besson, M. T., Sinakevitch, I., Melon, C., Iche-Torres, M., & Birman, S. (2011). Involvement of the drosophila taurine/aspartate transporter dEaat2 in selective olfactory and gustatory perceptions. *J Comparative Neurology*, 519(14), 2734–2757.
- Besson, M. T., Soustelle, L., & Birman, S. (2000). Selective high-affinity transport of aspartate by a Drosophila homologue of the excitatory amino-acid transporters. *Current Biology*, 10, 207–210.
- Bhatt, D. P., Puig, K. L., Gorr, M. W., Wold, L. E., & Combs, C. K. (2015). A pilot study to assess effects of long-term inhalation of airborne particulate matter on early Alzheimer-like changes in the mouse brain. *PLoS ONE*, 10(5), 1–20. <https://doi.org/10.1371/journal.pone.0127102>
- Block, M. L., & Calderón-Garcidueñas, L. (2009). Air pollution: mechanisms of neuroinflammation and CNS disease. In *Trends in Neurosciences* (Vol. 32, Issue 9, pp. 506–516). <https://doi.org/10.1016/j.tins.2009.05.009>
- Bookheimer, S. Y., Strojwas, M. H., Mas, C., Saunders, A. M., Pericak-Vance, M. A., Mazziotta, J. C., & GW., S. (2000). Patterns of Brain activation in people at risk from Alzheimer's disease. 2000. *New England Journal of Medicine*, 343(7), 450–456.
- Brauer, M., Avila-Casado, C., Fortoul, T. I., Vedal, S., Stevens, B., & Churg, A. (2001). Air pollution and retained particles in the lung. *Environmental Health Perspectives*, 109(10), 1039–1043. <https://doi.org/10.1289/ehp.011091039>
- Brothers, H. M., Gosztyla, M. L., & Robinson, S. R. (2018). The physiological roles of amyloid- β peptide hint at new ways to treat Alzheimer's disease. In *Frontiers in Aging Neuroscience* (Vol. 10, Issue APR, p. 118). Frontiers Media S.A. <https://doi.org/10.3389/fnagi.2018.00118>
- Brusco, L. I., Marquez, M., & Cardinali, D. P. (1998). Monozygotic twins with Alzheimer's disease treated with melatonin: Case report. *J.Pineal Res.*, 25(4), 260–263.
- Cacciottolo, M., Wang, X., Driscoll, I., Woodward, N., Saffari, A., Reyes, J., Serre, M. L., Vizuete, W., Sioutas, C., Morgan, T. E., Gatz, M., Chui, H. C., Shumaker, S. A., Resnick, S. M., Espeland, M. A., Finch, C. E., & Chen, J. C. (2017). Particulate air pollutants, APOE alleles and their contributions to cognitive impairment in older women and to amyloidogenesis in experimental models. *Translational Psychiatry*, 7(1), e1022. <https://doi.org/10.1038/tp.2016.280>
- Calderón-Garcidueas, L., Kavanaugh, M., Block, M., D'Angiulli, A., Delgado-Chávez, R., Torres-Jardón, R., González-Maciél, A., Reynoso-Robles, R., Osnaya, N., Villarreal-

- Calderon, R., Guo, R., Hua, Z., Zhu, H., Perry, G., & Diaz, P. (2012). Neuroinflammation, hyperphosphorylated tau, diffuse amyloid plaques, and down-regulation of the cellular prion protein in air pollution exposed children and young adults. *Journal of Alzheimer's Disease*, 28(1), 93–107. <https://doi.org/10.3233/JAD-2011-110722>
- Calderón-Garcidueas, L., Mora-Tiscareño, A., Styner, M., Gómez-Garza, G., Zhu, H., Torres-Jardón, R., Carlos, E., Solorio-López, E., Medina-Cortina, H., Kavanaugh, M., & D'Angiulli, A. (2012). White matter hyperintensities, systemic inflammation, brain growth, and cognitive functions in children exposed to air pollution. *Journal of Alzheimer's Disease*, 31(1), 183–191. <https://doi.org/10.3233/JAD-2012-120610>
- Calderón-Garcidueñas, L., Engle, R., Antonieta Mora-Tiscareño, A. M., Styner, M., Gómez-Garza, G., Zhu, H., Jewells, V., Torres-Jardón, R., Romero, L., Monroy-Acosta, M. E., Bryant, C., González-González, L. O., Medina-Cortina, H., & D'Angiulli, A. (2011). Exposure to severe urban air pollution influences cognitive outcomes, brain volume and systemic inflammation in clinically healthy children. *Brain and Cognition*, 77(3), 345–355. <https://doi.org/10.1016/j.bandc.2011.09.006>
- Calderón-Garcidueñas, L., González-Maciél, A., Reynoso-Robles, R., Kulesza, R. J., Mukherjee, P. S., Torres-Jardón, R., Rönkkö, T., & Doty, R. L. (2018). Alzheimer's disease and alpha-synuclein pathology in the olfactory bulbs of infants, children, teens and adults ≤ 40 years in Metropolitan Mexico City. APOE4 carriers at higher risk of suicide accelerate their olfactory bulb pathology. *Environmental Research*, 166, 348–362. <https://doi.org/10.1016/j.envres.2018.06.027>
- Calderón-Garcidueñas, L., Herrera-Soto, A., Jury, N., Maher, B. A., González-Maciél, A., Reynoso-Robles, R., Ruiz-Rudolph, P., van Zundert, B., & Varela-Nallar, L. (2020). Reduced repressive epigenetic marks, increased DNA damage and Alzheimer's disease hallmarks in the brain of humans and mice exposed to particulate urban air pollution. *Environmental Research*, 183, 109226. <https://doi.org/10.1016/j.envres.2020.109226>
- Calderón-Garcidueñas, L., Jewells, V., Galaz-Montoya, C., van Zundert, B., Pérez-Calatayud, A., Ascencio-Ferrel, E., Valencia-Salazar, G., Sandoval-Cano, M., Carlos, E., Solorio, E., Acuña-Ayala, H., Torres-Jardón, R., & D'Angiulli, A. (2016). Interactive and additive influences of Gender, BMI and Apolipoprotein 4 on cognition in children chronically exposed to high concentrations of PM2.5 and ozone. APOE 4 females are at highest risk in Mexico City. *Environmental Research*, 150, 411–422. <https://doi.org/10.1016/j.envres.2016.06.026>
- Calderon-Garciduenas, L., Maronpot, R. R., Torres-Jardon, R., Henriquez-Roldan, C., Schoonhoven, R., Acuna-Ayala, H., Villarreal-Calderon, A., Nakamura, J., Fernando, R., Reed, W., Azzarelli, B., & Swenberg, J. A. (2003). DNA Damage in Nasal and Brain Tissues of Canines Exposed to Air Pollutants Is Associated with Evidence of Chronic Brain Inflammation and Neurodegeneration. *Toxicologic Pathology*, 31(5), 524–538. <https://doi.org/10.1080/01926230390226645>
- Calderón-Garcidueñas, L., Mora-Tiscareño, A., Ontiveros, E., Gómez-Garza, G., Barragán-Mejía, G., Broadway, J., Chapman, S., Valencia-Salazar, G., Jewells, V., Maronpot, R. R., Henríquez-Roldán, C., Pérez-Guillé, B., Torres-Jardón, R., Herrit, L., Brooks, D., Osnaya-

- Brizuela, N., Monroy, M. E., González-Maciél, A., Reynoso-Robles, R., ... Engle, R. W. (2008). Air pollution, cognitive deficits and brain abnormalities: A pilot study with children and dogs. *Brain and Cognition*, *68*(2), 117–127. <https://doi.org/10.1016/j.bandc.2008.04.008>
- Calderón-Garcidueñas, L., Reed, W., Maronpot, R. R., Henriquez-Roldán, C., Delgado-Chavez, R., Calderón-Garcidueñas, A., Dragustinovis, I., Franco-Lira, M., Aragón-Flores, M., Solt, A. C., Altenburg, M., Torres-Jardón, R., & Swenberg, J. A. (2004). Brain Inflammation and Alzheimer's-Like Pathology in Individuals Exposed to Severe Air Pollution. *Toxicologic Pathology*, *32*(6), 650–658. <https://doi.org/10.1080/01926230490520232>
- Calderón-Garcidueñas, L., Solt, A. C., Henríquez-Roldán, C., Torres-Jardón, R., Nuse, B., Herritt, L., Villarreal-Calderón, R., Osnaya, N., Stone, I., García, R., Brooks, D. M., González-Maciél, A., Reynoso-Robles, R., Delgado-Chávez, R., & Reed, W. (2008). Long-term Air Pollution Exposure Is Associated with Neuroinflammation, an Altered Innate Immune Response, Disruption of the Blood-Brain Barrier, Ultrafine Particulate Deposition, and Accumulation of Amyloid β -42 and α -Synuclein in Children and Young Adult. *Toxicologic Pathology*, *36*(2), 289–310. <https://doi.org/10.1177/0192623307313011>
- Campbell, A., Oldham, M., Becaria, A., Bondy, S. C., Meacher, D., Sioutas, C., Misra, C., Mendez, L. B., & Kleinman, M. (2005). Particulate matter in polluted air may increase biomarkers of inflammation in mouse brain. *NeuroToxicology*, *26*(1), 133–140. <https://doi.org/10.1016/j.neuro.2004.08.003>
- Campdelacreu, J. (2014). Parkinson's disease and Alzheimer disease: environmental risk factors. *Neurología*, *29*(9), 541–549. <https://doi.org/10.1016/j.nrleng.2012.04.022>
- Chameau, P., Inta, D., Vitalis, T., Monyer, H., Wadman, W. J., & Van Hooft, J. A. (2009). The N-terminal region of reelin regulates postnatal dendritic maturation of cortical pyramidal neurons. *Proceedings of the National Academy of Sciences of the United States of America*, *106*(17), 7227–7232. <https://doi.org/10.1073/pnas.0810764106>
- Chang, K., & Suh, Y.-H. (2010). Possible roles of amyloid intracellular domain of amyloid precursor protein. *BMB Reports*, *43*(10), 656–663. <https://doi.org/10.5483/BMBRep.2010.43.10.656>
- Chang, M., Sioutas, C., Cassee, F. R., & Fokkens, P. H. B. (2001). Field evaluation of a mobile high-capacity particle size classifier (HCPSC) for separate collection of coarse, fine and ultrafine particles. *Journal of Aerosol Science*, *32*(1), 139–156. [https://doi.org/10.1016/S0021-8502\(00\)00061-6](https://doi.org/10.1016/S0021-8502(00)00061-6)
- Chapuis, J., Hansmannel, F., Gistelinck, M., Mounier, A., Van Cauwenberghe, C., Kolen, K. V., Geller, F., Sottejeau, Y., Harold, D., Dourlen, P., Grenier-Boley, B., Kamatani, Y., Delepine, B., Demiautte, F., Zelenika, D., Zommer, N., Hamdane, M., Bellenguez, C., Dartigues, J. F., ... Dermaut, B. (2013). Increased expression of BIN1 mediates Alzheimer genetic risk by modulating tau pathology. *Mol Psychiatry*, *18*(11), 1225–1234.
- Chasseigneaux, S., Dinc, L., Rose, C., Chabret, C., Couplier, F., Topilko, P., Mauger, G., & Allinquant, B. (2011). Secreted Amyloid Precursor Protein β and Secreted Amyloid Precursor Protein α Induce Axon Outgrowth In Vitro through Egr1 Signaling Pathway.

PLoS ONE, 6(1), e16301. <https://doi.org/10.1371/journal.pone.0016301>

- Chatterjee, S., Sang, T. K., Lawless, G. M., & GR., J. (2009). Dissociation of tau toxicity and phosphorylation: role of GSK-3 β , MARK and Cdk5 in a *Drosophila* model. *Human Molecular Genetics*, 18(1), 164–177.
- Chen, H., Kwong, J. C., Copes, R., Hystad, P., van Donkelaar, A., Tu, K., Brook, J. R., Goldberg, M. S., Martin, R. V., Murray, B. J., Wilton, A. S., Kopp, A., & Burnett, R. T. (2017). Exposure to ambient air pollution and the incidence of dementia: A population-based cohort study. *Environment International*, 108, 271–277. <https://doi.org/10.1016/j.envint.2017.08.020>
- Chen, H., Kwong, J. C., Copes, R., Tu, K., Villeneuve, P. J., van Donkelaar, A., Hystad, P., Martin, R. V., Murray, B. J., Jessiman, B., Wilton, A. S., Kopp, A., & Burnett, R. T. (2017). Living near major roads and the incidence of dementia, Parkinson's disease, and multiple sclerosis: a population-based cohort study. *The Lancet*, 389(10070), 718–726. [https://doi.org/10.1016/S0140-6736\(16\)32399-6](https://doi.org/10.1016/S0140-6736(16)32399-6)
- Chen, J.-C., & Schwartz, J. (2009). Neurobehavioral effects of ambient air pollution on cognitive performance in US adults. *NeuroToxicology*, 30(2), 231–239. <https://doi.org/10.1016/j.neuro.2008.12.011>
- Cheng, H., Saffari, A., Sioutas, C., Forman, H. J., Morgan, T. E., & Finch, C. E. (2016). Nanoscale particulate matter from urban traffic rapidly induces oxidative stress and inflammation in olfactory epithelium with concomitant effects on brain. *Environmental Health Perspectives*, 124(10), 1537–1546. <https://doi.org/10.1289/EHP134>
- Chiu, Y. H. M., Bellinger, D. C., Coull, B. A., Anderson, S., Barber, R., Wright, R. O., & Wright, R. J. (2013). Associations between traffic-related black carbon exposure and attention in a prospective birth cohort of urban children. *Environmental Health Perspectives*, 121(7), 859–864. <https://doi.org/10.1289/ehp.1205940>
- Cho, M. H., Cho, K., Kang, H. J., Jeon, E. Y., Kim, H. S., Kwon, H. J., Kim, H. M., Kim, D. H., & Yoon, S. Y. (2014). Autophagy in microglia degrades extracellular β -amyloid fibrils and regulates the NLRP3 inflammasome. *Autophagy*, 10(10), 1761–1775. <https://doi.org/10.4161/auto.29647>
- Chow, V. W., Mattson, M. P., Wong, P. C., & Gleichmann, M. (2010). An overview of APP processing enzymes and products. In *Neuromolecular medicine* (Vol. 12, Issue 1, pp. 1–12). NIH Public Access. <https://doi.org/10.1007/s12017-009-8104-z>
- Churg, a, & Brauer, M. (2000). Ambient atmospheric particles in the airways of human lungs. *Ultrastructural Pathology*, 24(6), 353–361. <https://doi.org/10.1080/019131200750060014>
- Cifuentes, D., Poittevin, M., Dere, E., Broquères-You, D., Bonnin, P., Benessiano, J., Pocard, M., Mariani, J., Kubis, N., Merkulova-Rainon, T., & Lévy, B. I. (2015). Hypertension accelerates the progression of Alzheimer-like pathology in a mouse model of the disease. *Hypertension (Dallas, Tex. : 1979)*, 65(1), 218–224. <https://doi.org/10.1161/HYPERTENSIONAHA.114.04139>
- Cleary, J. P., Walsh, D. M., Hofmeister, J. J., Shankar, G. M., Kuskowski, M. A., Selkoe, D. J.,

- & Ashe, K. H. (2005). Natural oligomers of the amyloid- β protein specifically disrupt cognitive function. *Nature Neuroscience*, 8(1), 79–84. <https://doi.org/10.1038/nn1372>
- Cohen, A. J., Brauer, M., Burnett, R., Anderson, H. R., Frostad, J., Estep, K., Balakrishnan, K., Brunekreef, B., Dandona, L., Dandona, R., Feigin, V., Freedman, G., Hubbell, B., Jobling, A., Kan, H., Knibbs, L., Liu, Y., Martin, R., Morawska, L., ... Forouzanfar, M. H. (2017). Estimates and 25-year trends of the global burden of disease attributable to ambient air pollution: an analysis of data from the Global Burden of Diseases Study 2015. *The Lancet*, 389(10082), 1907–1918. [https://doi.org/10.1016/S0140-6736\(17\)30505-6](https://doi.org/10.1016/S0140-6736(17)30505-6)
- Colangelo, A. M., Alberghina, L., & Papa, M. (2014). Astroglialosis as a therapeutic target for neurodegenerative diseases. In *Neuroscience Letters* (Vol. 565, pp. 59–64). Elsevier Ireland Ltd. <https://doi.org/10.1016/j.neulet.2014.01.014>
- Colodner, K. J., & MB., F. (2010). Glial fibrillary tangles and JAK/STAT-mediated glial and neuronal cell death in a *Drosophila* model of glial tauopathy. *J. Neuroscience.*, 30(48), 16102–16113.
- Coraci, I. (2002). CD36, a class B scavenger receptor, is expressed on microglia in Alzheimer's disease brains and can mediate production of reactive oxygen species in response to beta-amyloid fibrils. *Am. J. Pathol.*, 160, 101–112.
- Cowan, C. M., Bossing, T., Page, A., Shepherd, D., & Mudher, A. (2010). Soluble hyperphosphorylated tau causes microtubule breakdown and functionally compromises normal tau in vivo. *Acta Neuropathologica.*, 120(5), 593–604.
- Craig, L., Brook, J. R., Chiotti, Q., Croes, B., Gower, S., Hedley, A., Krewski, D., Krupnick, A., Krzyzanowski, M., Moran, M. D., Pennell, W., Samet, J. M., Schneider, J., Shortreed, J., & Williams, M. (2008). Air Pollution and Public Health: A Guidance Document for Risk Managers. *Journal of Toxicology and Environmental Health, Part A*, 71(9–10), 588–698. <https://doi.org/10.1080/15287390801997732>
- Dabir, D. V, Robinson, M. B., Swanson, E., Zhang, B., Trojanowski, J. Q., Lee, V. M., & MS., F. (2006). Impaired glutamate transport in a mouse model of tau pathology in astrocytes. *J Neurosci*, 26, 644–654.
- Dagher, N. N., Najafi, A. R., Kayala, K. M. N., Elmore, M. R. P., White, T. E., Medeiros, R., West, B. L., & Green, K. N. (2015). Colony-stimulating factor 1 receptor inhibition prevents microglial plaque association and improves cognition in 3xTg-AD mice. *Journal of Neuroinflammation*, 12(1). <https://doi.org/10.1186/s12974-015-0366-9>
- Danbolt, N. C., Storm-Mathisen, J., & BI., K. (1992). An [Na⁺ + K⁺]coupled L-glutamate transporter purified from rat brain is located in glial cell processes. *Neuroscience*, 51, 295–310.
- Daniels, R. W., Gelfand, M., Collins, C., & DiAntonio, A. (2008). Visualizing Glutamatergic Cell Bodies and Synapses in *Drosophila* Larval and Adult CNS. *J. Comparative Neurology*, 508, 131–152.
- Danzysz, W., & Parsons, C. G. (2012). Alzheimer's disease, β -amyloid, glutamate, NMDA receptors and memantine - Searching for the connections. In *British Journal of*

Pharmacology (Vol. 167, Issue 2, pp. 324–352). John Wiley and Sons Inc.
<https://doi.org/10.1111/j.1476-5381.2012.02057.x>

- De Calignon, A., Polydoro, M., Suarez-Calvet, M., William, C., Adamowicz, D. H., Kopeikina, K. J., Pittstick, R., Sahara, N., Ashe, K. H., Carlson, G. A., Spires-Jones, T. L., & BT., H. (2012). Propagation of tau pathology in a model of early Alzheimer's disease. *Neuron*, *73*(4), 685–697.
- De Strooper, B., Saftig, P., Vanderstichele, H., Guhde, G., Annaert, W., Von Figura, K., & Van Leuven, F. (1998). Deficiency of presenilin-1 inhibits the normal cleavage of amyloid precursor protein. *Nature*, *391*, 387–390.
- Dickson, D. W., Crystal, H. A., Mattiace, L. A., Masur, D. M., Blau, A. D., Davies, P., Yen, S. H., & Aronson, M. K. (1992). Identification of normal and pathological aging in prospectively studied nondemented elderly humans. *Neurobiology of Aging*, *13*(1), 179–189. [https://doi.org/10.1016/0197-4580\(92\)90027-U](https://doi.org/10.1016/0197-4580(92)90027-U)
- Doherty, J., Logan, M. A., Tasdemir, O. E., & MR., F. (2009). Ensheathing Glia Function as Phagocytes in the Adult *Drosophila* Brain. *J Neurosci.*, *29*(15), 4768–4781.
- Durga, M., Devasena, T., & Rajasekar, A. (2015). Determination of LC<inf>50</inf> and sub-chronic neurotoxicity of diesel exhaust nanoparticles. *Environmental Toxicology and Pharmacology*, *40*(2), 615–625. <https://doi.org/10.1016/j.etap.2015.06.024>
- Edwards, S. C., Jedrychowski, W., Butscher, M., Camann, D., Kieltyka, A., Mroz, E., Flak, E., Li, Z., Wang, S., Rauh, V., & Perera, F. (2010). Prenatal exposure to airborne polycyclic aromatic hydrocarbons and children's intelligence at 5 years of age in a prospective cohort study in Poland. *Environmental Health Perspectives*, *118*(9), 1326–1331. <https://doi.org/10.1289/ehp.0901070>
- Elmore, M. R. P., Najafi, A. R., Koike, M. A., Dagher, N. N., Spangenberg, E. E., Rice, R. A., Kitazawa, M., Matusow, B., Nguyen, H., West, B. L., & Green, K. N. (2014). Colony-stimulating factor 1 receptor signaling is necessary for microglia viability, unmasking a microglia progenitor cell in the adult brain. *Neuron*, *82*(2), 380–397. <https://doi.org/10.1016/j.neuron.2014.02.040>
- Erikson, K. M., Suber, R. L., & Aschner, M. (2002). Glutamate/Aspartate Transporter (GLAST), Taurine Transporter and Metallothionein mRNA Levels are Differentially Altered in Astrocytes Exposed to Manganese Chloride, Manganese Phosphate or Manganese Sulfate. *NeuroToxicology*, *23*(3), 281–288. [https://doi.org/10.1016/S0161-813X\(02\)00041-4](https://doi.org/10.1016/S0161-813X(02)00041-4)
- Feuillette, S., Miguel, L., Frebourg, T., Champion, D., & Lecourtois, M. (2010). *Drosophila* models of human tauopathies indicate that Tau protein toxicity in vivo is mediated by soluble cytosolic phosphorylated forms of the protein. *Journal of Neurochemistry*, *113*, 895–903. <https://doi.org/10.1111/j.1471-4159.2010.06663.x>
- Finckh, U., Kuschel, C., Anagnostouli, M., Patsouris, E., Pantos, G. V., Gatzonis, S., Kapaki, E., Davaki, P., Lamszus, K., Stavrou, D., & Gal, A. (2005). Novel mutations and repeated findings of mutations in familial Alzheimer disease. *Neurogenetics*, *6*(2), 85–89. <https://doi.org/10.1007/s10048-005-0211-x>

- Folstein, M. F., Folstein, S. E., & McHugh, P. R. (1975). “Mini-mental state”. A practical method for grading the cognitive state of patients for the clinician. *Journal of Psychiatric Research*, *12*(3), 189–198. [https://doi.org/10.1016/0022-3956\(75\)90026-6](https://doi.org/10.1016/0022-3956(75)90026-6)
- Fonken, L. K., Xu, X., Weil, Z. M., Chen, G., Sun, Q., Rajagopalan, S., & Nelson, R. J. (2011). Air pollution impairs cognition, provokes depressive-like behaviors and alters hippocampal cytokine expression and morphology. *Molecular Psychiatry*, *16*(10), 987–995. <https://doi.org/10.1038/mp.2011.76>
- Freire, C., Ramos, R., Puertas, R., Lopez-Espinosa, M.-J., Julvez, J., Aguilera, I., Cruz, F., Fernandez, M.-F., Sunyer, J., & Olea, N. (2010). Association of traffic-related air pollution with cognitive development in children. *Journal of Epidemiology & Community Health*, *64*(3), 223–228. <https://doi.org/10.1136/jech.2008.084574>
- García-González, L., Pilat, D., Baranger, K., & Rivera, S. (2019). Emerging alternative proteinases in APP metabolism and alzheimer’s disease pathogenesis: A focus on MT1-MMP and MT5-MMP. In *Frontiers in Aging Neuroscience* (Vol. 11, Issue SEP, p. 244). Frontiers Media S.A. <https://doi.org/10.3389/fnagi.2019.00244>
- Gatto, N. M., Henderson, V. W., Hodis, H. N., St. John, J. A., Lurmann, F., Chen, J. C., & Mack, W. J. (2014). Components of air pollution and cognitive function in middle-aged and older adults in Los Angeles. *NeuroToxicology*, *40*, 1–7. <https://doi.org/10.1016/j.neuro.2013.09.004>
- Gatz, M., Reynolds, C. A., Fratiglioni, L., Johansson, B., Mortimer, J. A., Berg, S., Fiske, A., & Pedersen, N. L. (2006). Role of Genes and Environments for Explaining Alzheimer Disease. *Archives of General Psychiatry*, *63*(2), 168. <https://doi.org/10.1001/archpsyc.63.2.168>
- Geller, M. D., Chang, M., Sioutas, C., Ostro, B. D., & Lipsett, M. J. (2002). Indoor/outdoor relationship and chemical composition of fine and coarse particles in the southern California deserts. *Atmospheric Environment*, *36*(6), 1099–1110. [https://doi.org/10.1016/S1352-2310\(01\)00340-5](https://doi.org/10.1016/S1352-2310(01)00340-5)
- Glenner, G. G., & Wong, C. W. (1984). Alzheimer’s disease: Initial report of the purification and characterization of a novel cerebrovascular amyloid protein. *Biochemical and Biophysical Research Communications*, *120*(3), 885–890. [https://doi.org/10.1016/S0006-291X\(84\)80190-4](https://doi.org/10.1016/S0006-291X(84)80190-4)
- Goedert, M., Spillantini, M. G., Cairns, N. J., & RA., C. (1992). Tau proteins of Alzheimer paired helical filaments: Abnormal phosphorylation of all six brain isoforms. *Neuron*, *8*(1), 159–168.
- González-Maciél, A., Reynoso-Robles, R., Torres-Jardón, R., Mukherjee, P. S., & Calderón-Garcidueñas, L. (2017). Combustion-Derived Nanoparticles in Key Brain Target Cells and Organelles in Young Urbanites: Culprit Hidden in Plain Sight in Alzheimer’s Disease Development. *Journal of Alzheimer’s Disease*, *59*(1), 189–208. <https://doi.org/10.3233/JAD-170012>
- Götz, J., Bodea, L. G., & Goedert, M. (2018). Rodent models for Alzheimer disease. In *Nature Reviews Neuroscience* (Vol. 19, Issue 10, pp. 583–598). Nature Publishing Group.

<https://doi.org/10.1038/s41583-018-0054-8>

- Götz, J., Chen, F., Barmettler, R., & RM., N. (2000). Tau Filament Formation in Transgenic Mice Expressing P301L Tau. *Journal of Biological Chemistry*, 276, 529–534.
- Guerra, R., Vera-Aguilar, E., Uribe-Ramirez, M., Gookin, G., Camacho, J., Osornio-Vargas, A. R., Mugica-Alvarez, V., Angulo-Olais, R., Campbell, A., Froines, J., Kleinman, T. M., & De Vizcaya-Ruiz, A. (2013). Exposure to inhaled particulate matter activates early markers of oxidative stress, inflammation and unfolded protein response in rat striatum. *Toxicology Letters*, 222(2), 146–154. <https://doi.org/10.1016/j.toxlet.2013.07.012>
- Guxens, M., Garcia-Esteban, R., Giorgis-Allemand, L., Forns, J., Badaloni, C., Ballester, F., Beelen, R., Cesaroni, G., Chatzi, L., de Agostini, M., de Nazelle, A., Eeftens, M., Fernandez, M. F., Fernández-Somoano, A., Forastiere, F., Gehring, U., Ghassabian, A., Heude, B., Jaddoe, V. W. V., ... Sunyer, J. (2014). Air Pollution During Pregnancy and Childhood Cognitive and Psychomotor Development. *Epidemiology*, 25(5), 636–647. <https://doi.org/10.1097/EDE.000000000000133>
- Haass, C., & Selkoe, D. J. (2007). Soluble protein oligomers in neurodegeneration: Lessons from the Alzheimer's amyloid β -peptide. In *Nature Reviews Molecular Cell Biology* (Vol. 8, Issue 2, pp. 101–112). Nature Publishing Group. <https://doi.org/10.1038/nrm2101>
- Hämäläinen, A., Pihlajamäki, M., Tanila, H., Hännien, T., Niskanen, E., Tervo, S., Karjalainen, P. A., Vanninen, R. L., & Soininen, H. (2007). Increased fMRI responses during encoding in mild cognitive impairment. 2007. *Neurobiology of Aging*, 28(12), 1889–1903.
- Hand, J. L., Schichtel, B. A., Pitchford, M., Malm, W. C., & Frank, N. H. (2012). Seasonal composition of remote and urban fine particulate matter in the United States. *Journal of Geophysical Research Atmospheres*, 117(5). <https://doi.org/10.1029/2011JD017122>
- Hansen, D. V., Hanson, J. E., & Sheng, M. (2018). Microglia in Alzheimer's disease. In *Journal of Cell Biology* (Vol. 217, Issue 2, pp. 459–472). Rockefeller University Press. <https://doi.org/10.1083/jcb.201709069>
- Harris, M. H., Gold, D. R., Rifas-Shiman, S. L., Melly, S. J., Zanobetti, A., Coull, B. A., Schwartz, J. D., Gryparis, A., Kloog, I., Koutrakis, P., Bellinger, D. C., White, R. F., Sagiv, S. K., & Oken, E. (2015). Prenatal and childhood traffic-related pollution exposure and childhood cognition in the project viva cohort (Massachusetts, USA). *Environmental Health Perspectives*, 123(10), 1072–1078. <https://doi.org/10.1289/ehp.1408803>
- Harrison, R. M., & Yin, J. (2000). Particulate matter in the atmosphere: Which particle properties are important for its effects on health? *Science of the Total Environment*, 249(1–3), 85–101. [https://doi.org/10.1016/S0048-9697\(99\)00513-6](https://doi.org/10.1016/S0048-9697(99)00513-6)
- Hazell, A. S., & Norenberg, M. D. (1997). Manganese decreases glutamate uptake in cultured astrocytes. *Neurochemical Research*, 22(12), 1443–1447. <https://doi.org/10.1023/A:1021994126329>
- He, Y., Wei, M., Wu, Y., Qin, H., Li, W., Ma, X., Cheng, J., Ren, J., Shen, Y., Chen, Z., Sun, B., Huang, F. De, Shen, Y., & Zhou, Y. D. (2019). Amyloid β oligomers suppress excitatory transmitter release via presynaptic depletion of phosphatidylinositol-4,5-bisphosphate.

- Nature Communications*, 10(1), 1–18. <https://doi.org/10.1038/s41467-019-09114-z>
- Hemonnot, A. L., Hua, J., Ulmann, L., & Hirbec, H. (2019). Microglia in Alzheimer disease: Well-known targets and new opportunities. In *Frontiers in Cellular and Infection Microbiology* (Vol. 9, Issue JUL, p. 233). Frontiers Media S.A. <https://doi.org/10.3389/fnagi.2019.00233>
- Heppner, F. L., Ransohoff, R. M., & Becher, B. (2015). Immune attack: The role of inflammation in Alzheimer disease. In *Nature Reviews Neuroscience* (Vol. 16, Issue 6, pp. 358–372). Nature Publishing Group. <https://doi.org/10.1038/nrn3880>
- Holtzman, D. M., Carrillo, M. C., Hendrix, J. A., Bain, L. J., Catafau, A. M., Gault, L. M., Goedert, M., Mandelkow, E., Mandelkow, E. M., Miller, D. S., Ostrowitzki, S., Polydoro, M., Smith, S., Wittmann, M., & Hutton, M. (2016). Tau: From research to clinical development. In *Alzheimer's and Dementia* (Vol. 12, Issue 10, pp. 1033–1039). Elsevier Inc. <https://doi.org/10.1016/j.jalz.2016.03.018>
- Hong, S. (2016). Complement and microglia mediate early synapse loss in Alzheimer mouse models. *Science*, 352, 712–716.
- Hunsberger, H., Rudy, C., Batten, S., Gerhardt, G., & Reed, M. (2015). P301L tau expression affects glutamate release and clearance in the hippocampal trisynaptic pathway. *Journal of Neurochemistry*, 132, 169–182.
- Ittner, A., & Ittner, L. M. (2018). Dendritic Tau in Alzheimer's Disease. In *Neuron* (Vol. 99, Issue 1, pp. 13–27). Cell Press. <https://doi.org/10.1016/j.neuron.2018.06.003>
- Ittner, L. M., Ke, Y. D., Delerue, F., Bi, M., Gladbach, A., van Eersel, J., Wolfing, H., Chieng, B. C., Christie, M. J., Napier, I. A., Eckert, A., Staufienbiel, M., Hardeman, E., & Gtz, J. (2010). Dendritic function of tau mediates amyloid-beta toxicity in Alzheimer's disease mouse models. *Cell*, 142(3), 387–397.
- Jackson, G. R., Wiedau-Pazos, M., Sang, T. K., Wagle, N., Brown, C. A., Massachi, S., & DH., G. (2002). Human Wild-Type Tau Interacts with wingless Pathway Components and Produces Neurofibrillary Pathology in Drosophila. *Neuron*, 34, 509–519.
- Jacob, C. P., Koutsilieri, E., Bartl, J., Neuen-Jacob, E., Arzberger, T., Zander, N., Ravid, R., Roggendorf, W., Riederer, P., & Grünblatt, E. (2007). Alterations in expression of glutamatergic transporters and receptors in sporadic Alzheimer's disease. *Journal of Alzheimer's Disease*, 11(1), 97–116. <https://doi.org/10.3233/JAD-2007-11113>
- Jang, S., Kim, E. W., Zhang, Y., Lee, J., Cho, S. Y., Ha, J., Kim, H., & Kim, E. (2018). Particulate matter increases beta-amyloid and activated glial cells in hippocampal tissues of transgenic Alzheimer's mouse: Involvement of PARP-1. *Biochemical and Biophysical Research Communications*, 500(2), 333–338. <https://doi.org/10.1016/j.bbrc.2018.04.068>
- Jay, T. R., Miller, C. M., Cheng, P. J., Graham, L. C., Bemiller, S., Broihier, M. L., Xu, G., Margevicius, D., Karlo, J. C., Sousa, G. L., Cotleur, A. C., Butovsky, O., Bekris, L., Staugaitis, S. M., Leverenz, J. B., Pimplikar, S. W., Landreth, G. E., Howell, G. R., Ransohoff, R. M., & BT., L. (2015). TREM2 deficiency eliminates TREM2+ inflammatory macrophages and ameliorates pathology in Alzheimer's disease mouse models. *J Exp Med*,

212(3), 287–295.

- Jedrychowski, W. A., Perera, F. P., Camann, D., Spengler, J., Butscher, M., Mroz, E., Majewska, R., Flak, E., Jacek, R., & Sowa, A. (2015). Prenatal exposure to polycyclic aromatic hydrocarbons and cognitive dysfunction in children. *Environmental Science and Pollution Research*, 22(5), 3631–3639. <https://doi.org/10.1007/s11356-014-3627-8>
- Jew, K., Herr, D., Wong, C., Kennell, A., Morris-Schaffer, K., Oberdörster, G., O'Banion, M. K., Cory-Slechta, D. A., & Elder, A. (2019). Selective memory and behavioral alterations after ambient ultrafine particulate matter exposure in aged 3xTgAD Alzheimer's disease mice. *Particle and Fibre Toxicology*, 16(1), 45. <https://doi.org/10.1186/s12989-019-0323-3>
- Jin, M., Shepardson, N., Yang, T., Chen, G., Walsh, D., & Selkoe, D. J. (2011). Soluble amyloid β -protein dimers isolated from Alzheimer cortex directly induce Tau hyperphosphorylation and neuritic degeneration. *Proceedings of the National Academy of Sciences of the United States of America*, 108(14), 5819–5824. <https://doi.org/10.1073/pnas.1017033108>
- Johnston, J. A., Cowburn, R. F., Norgren, S., Wiehager, B., Venizelos, N., Winblad, B., Vigo-Pelfrey, C., Schenk, D., Lannfelt, L., & O'Neill, C. (1994). Increased β -amyloid release and levels of amyloid precursor protein (APP) in fibroblast cell lines from family members with the Swedish Alzheimer's disease APP670/671 mutation. *FEBS Letters*, 354(3), 274–278. [https://doi.org/10.1016/0014-5793\(94\)01137-0](https://doi.org/10.1016/0014-5793(94)01137-0)
- Jongbloed, W., Bruggink, K. A., Kester, M. I., Visser, P. J., Scheltens, P., Blankenstein, M. A., Verbeek, M. M., Teunissen, C. E., & Veerhuis, R. (2015). Amyloid- β oligomers relate to cognitive decline in Alzheimer's disease. *Journal of Alzheimer's Disease*, 45(1), 35–43. <https://doi.org/10.3233/JAD-142136>
- Jung, C.-R., Lin, Y.-T., & Hwang, B.-F. (2015). Ozone, particulate matter, and newly diagnosed Alzheimer's disease: a population-based cohort study in Taiwan. *Journal of Alzheimer's Disease : JAD*, 44(2), 573–584. <https://doi.org/10.3233/JAD-140855>
- Karagulian, F., Belis, C. A., Dora, C. F. C., Pr??ss-Ust??n, A. M., Bonjour, S., Adair-Rohani, H., & Amann, M. (2015). Contributions to cities' ambient particulate matter (PM): A systematic review of local source contributions at global level. *Atmospheric Environment*, 120, 475–483. <https://doi.org/10.1016/j.atmosenv.2015.08.087>
- Katagiri, H., Tanaka, K., & Manabe, T. (2001). Requirement of appropriate glutamate concentrations in the synaptic cleft for hippocampal LTP induction. *European Journal of Neuroscience*, 14(3), 547–553. <https://doi.org/10.1046/j.0953-816X.2001.01664.x>
- Kelly, K. E., Kotchenruther, R., Kuprov, R., & Silcox, G. D. (2013). Receptor model source attributions for Utah's Salt Lake City airshed and the impacts of wintertime secondary ammonium nitrate and ammonium chloride aerosol. *Journal of the Air and Waste Management Association*, 63(5), 575–590. <https://doi.org/10.1080/10962247.2013.774819>
- Khafaie, M. A., Yajnik, C. S., Salvi, S. S., & Ojha, A. (2016). Critical Review of Air Pollution Health Effects With Special Concern on Respiratory Health. *Journal of Air Pollution and Health*, 1(12), 123–136. <http://japh.tums.ac.ir>
- Kilian, J. G., Hsu, H. W., Mata, K., Wolf, F. W., & Kitazawa, M. (2017). Astrocyte transport of

- glutamate and neuronal activity reciprocally modulate tau pathology in *Drosophila*. *Neuroscience*, 348, 191–200. <https://doi.org/10.1016/j.neuroscience.2017.02.011>
- Kim, S. H., Knight, E. M., Saunders, E. L., Cuevas, A. K., Popovech, M., Chen, L.-C., & Gandy, S. (2012). Rapid doubling of Alzheimer's amyloid- β 40 and 42 levels in brains of mice exposed to a nickel nanoparticle model of air pollution. *F1000Research*, 1(0), 70. <https://doi.org/10.12688/f1000research.1-70.v1>
- Kim, S., PA, J., M, C., T, B., C, X., SK, F., & C., S. (2001). VERSATILE AEROSOL CONCENTRATION ENRICHMENT SYSTEM (VACES) FOR SIMULTANEOUS IN VIVO AND IN VITRO EVALUATION OF TOXIC EFFECTS OF ULTRAFINE, FINE AND COARSE AMBIENT PARTICLES. PART II: FIELD EVALUATION. (R827352C001). *Journal of Aerosol Science*.
- Kimura, T., Whitcomb, D. J., Jo, J., Regan, P., Piers, T., Heo, S., Brown, C., Hashikawa, T., Murayama, M., Seok, H., Sotiropoulos, I., Kim, E., Collingridge, G. L., Takashima, A., & Cho, K. (2013). Microtubule-associated protein tau is essential for long-term depression in the hippocampus. *Philos Trans R Soc Lond B Biol Sci*, 369(1633), 1–8.
- Kioumourtoglou, M. A., Schwartz, J. D., Weisskopf, M. G., Melly, S. J., Wang, Y., Dominici, F., & Zanobetti, A. (2016). Long-term PM_{2.5} exposure and neurological hospital admissions in the northeastern United States. *Environmental Health Perspectives*, 124(1), 23–29. <https://doi.org/10.1289/ehp.1408973>
- Kleeman, M. J., Schauer, J. J., & Cass, G. R. (2000). Size and composition distribution of fine particulate matter emitted from motor vehicles. *Environmental Science and Technology*, 34(7), 1132–1142. <https://doi.org/10.1021/es981276y>
- Klein, W. L. (2013). Synaptotoxic amyloid- β oligomers: A molecular basis for the cause, diagnosis, and treatment of Alzheimer's disease? In *Journal of Alzheimer's Disease* (Vol. 33, Issue SUPPL. 1). IOS Press. <https://doi.org/10.3233/JAD-2012-129039>
- Kleinman, M. T., Araujo, J. A., Nel, A., Sioutas, C., Campbell, A., Cong, P. Q., Li, H., & Bondy, S. C. (2008). Inhaled ultrafine particulate matter affects CNS inflammatory processes and may act via MAP kinase signaling pathways. *Toxicology Letters*, 178(2), 127–130. <https://doi.org/10.1016/j.toxlet.2008.03.001>
- Kobayashi, E., Nakano, M., Kubota, K., Himuro, N., Mizoguchi, S., Chikenji, T., Otani, M., Mizue, Y., Nagaishi, K., & Fujimiya, M. (2018). Activated forms of astrocytes with higher GLT-1 expression are associated with cognitive normal subjects with Alzheimer pathology in human brain. *Scientific Reports*, 8(1), 1–12. <https://doi.org/10.1038/s41598-018-19442-7>
- Kobro-Flatmoen, A., Nagelhus, A., & Witter, M. P. (2016). Reelin-immunoreactive neurons in entorhinal cortex layer II selectively express intracellular amyloid in early Alzheimer's disease. *Neurobiology of Disease*, 93, 172–183. <https://doi.org/10.1016/j.nbd.2016.05.012>
- Komura, Y., Xu, G., Bhaskar, K., & BT., L. (2015). Human tau expression reduces adult neurogenesis in a mouse model of tauopathy. *Neurobiology of Aging*, 36(6), 2034–2042.
- Kreyling, W. G., Semmler, M., Erbe, F., Mayer, P., Takenaka, S., Schulz, H., Oberdörster, G., & Ziesenis, A. (2002). Translocation of ultrafine insoluble iridium particles from lung

- epithelium to extrapulmonary organs is size dependent but very low. *Journal of Toxicology and Environmental Health - Part A*, 65(20), 1513–1530.
<https://doi.org/10.1080/00984100290071649>
- Kulas, J. A., Hettwer, J. V., Sohrabi, M., Melvin, J. E., Manocha, G. D., Puig, K. L., Gorr, M. W., Tanwar, V., McDonald, M. P., Wold, L. E., & Combs, C. K. (2018). In utero exposure to fine particulate matter results in an altered neuroimmune phenotype in adult mice. *Environmental Pollution*, 241, 279–288. <https://doi.org/10.1016/j.envpol.2018.05.047>
- Lautarescu, B. A., Holland, A. J., & Zaman, S. H. (2017). The Early Presentation of Dementia in People with Down Syndrome: a Systematic Review of Longitudinal Studies. In *Neuropsychology Review* (Vol. 27, Issue 1, pp. 31–45). Springer New York LLC.
<https://doi.org/10.1007/s11065-017-9341-9>
- Lee, D. (2010). LPS- induced inflammation exacerbates phospho-tau pathology in rTg4510 mice. *J. Neuroinflammation*, 7.
- Leissring, M. A., Murphy, M. P., Mead, T. R., Akbari, Y., Sugarman, M. C., Jannatipour, M., Anliker, B., Müller, U., Saftig, P., De Strooper, B., Wolfe, M. S., Golde, T. E., & LaFerla, F. M. (2002). A physiologic signaling role for the γ -secretase-derived intracellular fragment of APP. *Proceedings of the National Academy of Sciences of the United States of America*, 99(7), 4697–4702. <https://doi.org/10.1073/pnas.072033799>
- Lertxundi, A., Baccini, M., Lertxundi, N., Fano, E., Aranbarri, A., Martínez, M. D., Ayerdi, M., Álvarez, J., Santa-Marina, L., Dorronsoro, M., & Ibarluzea, J. (2015). Exposure to fine particle matter, nitrogen dioxide and benzene during pregnancy and cognitive and psychomotor developments in children at 15months of age. *Environment International*, 80, 33–40. <https://doi.org/10.1016/j.envint.2015.03.007>
- Levesque, S., Surace, M. J., McDonald, J., & Block, M. L. (2011). Air pollution & the brain: Subchronic diesel exhaust exposure causes neuroinflammation and elevates early markers of neurodegenerative disease. *Journal of Neuroinflammation*, 8(1), 105.
<https://doi.org/10.1186/1742-2094-8-105>
- Lewerenz, J., & Maher, P. (2015). Chronic glutamate toxicity in neurodegenerative diseases- What is the evidence? In *Frontiers in Neuroscience* (Vol. 9, Issue DEC, p. 469). Frontiers Media S.A. <https://doi.org/10.3389/fnins.2015.00469>
- Li, C., & Götz, J. (2017). Tau-based therapies in neurodegeneration: Opportunities and challenges. In *Nature Reviews Drug Discovery* (Vol. 16, Issue 12, pp. 863–883). Nature Publishing Group. <https://doi.org/10.1038/nrd.2017.155>
- Li, N., Sioutas, C., Cho, A., Schmitz, D., Misra, C., Sempf, J., Wang, M., Oberley, T., Froines, J., & Nel, A. (2003). Ultrafine particulate pollutants induce oxidative stress and mitochondrial damage. *Environmental Health Perspectives*, 111(4), 455–460.
<https://doi.org/10.1289/ehp.6000>
- Li, Q., Liu, H., Alattar, M., Jiang, S., Han, J., Ma, Y., & Jiang, C. (2015). The preferential accumulation of heavy metals in different tissues following frequent respiratory exposure to PM2.5 in rats. *Scientific Reports*, 5(1), 1–8. <https://doi.org/10.1038/srep16936>

- Li, S., Mallory, M., Alford, M., Tanaka, S., & Masliah, E. (1997). Glutamate transporter alterations in Alzheimer disease are possibly associated with abnormal APP expression. *J Neuropathol Exp Neurol.*, *56*(8), 901–911.
- Lin, C.-C., Yang, S.-K., Lin, K.-C., Ho, W.-C., Hsieh, W.-S., Shu, B.-C., & Chen, P.-C. (2014). Multilevel Analysis of Air Pollution and Early Childhood Neurobehavioral Development. *International Journal of Environmental Research and Public Health*, *11*(7), 6827–6841. <https://doi.org/10.3390/ijerph110706827>
- Lin, H., Guo, Y., Zheng, Y., Zhao, X., Cao, Z., Rigdon, S. E., Xian, H., Li, X., Liu, T., Xiao, J., Zeng, W., Weaver, N. L., Qian, Z. M., Ma, W., & Wu, F. (2017). Exposure to ambient PM_{2.5} associated with overall and domain-specific disability among adults in six low- and middle-income countries. *Environment International*, *104*, 69–75. <https://doi.org/10.1016/j.envint.2017.04.004>
- Liu, L., Drouet, V., Wu, J. W., Witter, M. P., Small, S. A., Clelland, C., & Duff, K. (2012). Trans-synaptic spread of tau pathology in vivo. *PLoS One*, *7*, 1–9.
- Liu, Y., Walter, S., Stagi, M., Cherny, D., Letiembre, M., Schulz-Schaeffer, W., Heine, H., Penke, B., Neumann, H., & Fassbender, K. (2005). LPS receptor (CD14): A receptor for phagocytosis of Alzheimer's amyloid peptide. *Brain*, *128*(8), 1778–1789. <https://doi.org/10.1093/brain/awh531>
- Lu, B., & Vogel, H. (2009). Drosophila models of neurodegenerative disease. *Annual Review Pathology* (, *4*, 315–342.
- Lundborg, M., Johard, U., Låstbom, L., Gerde, P., & Camner, P. (2001). Human Alveolar Macrophage Phagocytic Function is Impaired by Aggregates of Ultrafine Carbon Particles. *Environmental Research*, *86*(3), 244–253. <https://doi.org/10.1006/enrs.2001.4269>
- Mann, D. M. A., Iwatsubo, T., Ihara, Y., Cairns, N. J., Lantos, P. L., Bogdanovic, N., Lannfelt, L., Winblad, B., Maat-Schieman, M. L. C., & Rossor, M. N. (1996). Predominant deposition of amyloid- β ₄₂(43) in plaques in cases of Alzheimer's disease and hereditary cerebral hemorrhage associated with mutations in the amyloid precursor protein gene. *American Journal of Pathology*, *148*(4), 1257–1266.
- Marina, G. B., Kirkitadze, D., Lomakin, A., Vollers, S. S., Benedek, G. B., & Teplow, D. B. (2003). Amyloid β -protein (A β) assembly: A β ₄₀ and A β ₄₂ oligomerize through distinct pathways. *Proceedings of the National Academy of Sciences of the United States of America*, *100*(1), 330–335. <https://doi.org/10.1073/pnas.222681699>
- Martin, L., Latypova, X., Wilson, C. M., Magnaudeix, A., Perrin, M. L., Yardin, C., & Terro, F. (2013). Tau protein kinases: involvement in Alzheimer's disease. *Ageing Research Reviews*, *12*(1), 289–309.
- Masliah, E., Hansen, L., Alford, M., Deteresa, R., & Mallory, M. (1996). Deficient glutamate transport is associated with neurodegeneration in Alzheimer's disease. *Annals of Neurology*, *40*, 759–766.
- Mazzei, F., D'Alessandro, A., Lucarelli, F., Nava, S., Prati, P., Valli, G., & Vecchi, R. (2008). Characterization of particulate matter sources in an urban environment. *Science of the Total*

- Environment*, 401(1–3), 81–89. <https://doi.org/10.1016/j.scitotenv.2008.03.008>
- McGeer, P. L., Schulzer, M., & McGeer, E. G. (1996). Arthritis and anti-inflammatory agents as possible protective factors for Alzheimer's disease: a review of 17 epidemiologic studies. *Neurology*, 47(2), 425–432. <https://doi.org/10.1212/wnl.47.2.425>
- McGurk, L., Berson, A., & Bonini, N. (2015). Drosophila as an In Vivo Model for Human Neurodegenerative Disease. *Genetics*, 201(2), 377–402.
- Meeker, K. D., Meabon, J. S., & DG., C. (2015). Partial Loss of the Glutamate Transporter GLT-1 Alters Brain Akt and Insulin Signaling in a Mouse Model of Alzheimer's Disease. *J Alzheimers Dis*, 45(2), 509–520.
- Miyamoto, T., Stein, L., Thomas, R., Djukic, B., Taneja, P., Knox, J., Vossel, K., & Mucke, L. (2017). Phosphorylation of tau at Y18, but not tau-fyn binding, is required for tau to modulate NMDA receptor-dependent excitotoxicity in primary neuronal culture. *Molecular Neurodegeneration*, 12(1), 1–19. <https://doi.org/10.1186/s13024-017-0176-x>
- MohanKumar, S. M. J., Campbell, A., Block, M., & Veronesi, B. (2008). Particulate matter, oxidative stress and neurotoxicity. *NeuroToxicology*, 29(3), 479–488. <https://doi.org/10.1016/j.neuro.2007.12.004>
- Mookherjee, P., Green, P. S., Watson, G. S., Marques, M. A., Tanaka, K., Meeker, K. D., Meabon, J. S., Li, N., Zhu, P., Olson, V. G., & DG., C. (2011). GLT-1 loss accelerates cognitive deficit onset in an Alzheimer's disease animal model. *Journal of Alzheimer's Disease*, 26, 447–455.
- Morales-Rubio, R. A., Alvarado-Cruz, I., Manzano-León, N., Andrade-Oliva, M. D. L. A., Uribe-Ramirez, M., Quintanilla-Vega, B., Osornio-Vargas, Á., & De Vizcaya-Ruiz, A. (2019). In utero exposure to ultrafine particles promotes placental stress-induced programming of renin-angiotensin system-related elements in the offspring results in altered blood pressure in adult mice. *Particle and Fibre Toxicology*, 16(1), 1–16. <https://doi.org/10.1186/s12989-019-0289-1>
- Moreno, T., Querol, X., Pey, J., Minguillón, M. C., Pérez, N., Alastuey, A., Bernabé, R. M., Blanco, S., Cárdenas, B., Eichinger, W., Salcido, A., & Gibbons, W. (2008). Spatial and temporal variations in inhalable CuZnPb aerosols within the Mexico City pollution plume. *Journal of Environmental Monitoring*, 10(3), 370–378. <https://doi.org/10.1039/b716507b>
- Morgan, T. E., Davis, D. A., Iwata, N., Tanner, J. A., Snyder, D., Ning, Z., Kam, W., Hsu, Y. T., Winkler, J. W., Chen, J. C., Petasis, N. A., Baudry, M., Sioutas, C., & Finch, C. E. (2011). Glutamatergic neurons in rodent models respond to nanoscale particulate urban air pollutants in vivo and in vitro. *Environmental Health Perspectives*, 119(7), 1003–1009. <https://doi.org/10.1289/ehp.1002973>
- Morley, J. E., Farr, S. A., Banks, W. A., Johnson, S. N., Yamada, K. A., & Xu, L. (2010). A physiological role for amyloid- β protein: Enhancement of learning and memory. *Journal of Alzheimer's Disease*, 19(2), 441–449. <https://doi.org/10.3233/JAD-2010-1230>
- Mucke, L., Masliah, E., Yu, G., Mallory, M., Rockenstein, E. M., Tatsuno, G., Hu, K., Kholodenko, D., Johnson-Wood, K., & McConlogue, L. (2000). High-level neuronal

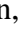
- expression of Ab 1-42 in wild- type human amyloid protein precursor transgenic mice: synaptotoxicity without plaque formation. *J. Neurosci*, 20, 4050–4058.
- Mucke, Lennart, & Selkoe, D. J. (2012). Neurotoxicity of amyloid β -protein: Synaptic and network dysfunction. *Cold Spring Harbor Perspectives in Medicine*, 2(7), a006338. <https://doi.org/10.1101/cshperspect.a006338>
- Muhleisen, H., Gehrman, J., & Meyermann, R. (1995). Reactive microglia in Creutzfeldt-Jakob disease. *Neuropathology and Applied Neurobiology*, 21(6), 505–517. <https://doi.org/10.1111/j.1365-2990.1995.tb01097.x>
- Mullan, M., Crawford, F., Axelman, K., Houlden, H., Lilius, L., Winblad, B., & Lannfelt, L. (1992). A pathogenic mutation for probable Alzheimer's disease in the APP gene at the N-terminus of β -amyloid. *Nature Genetics*, 1(5), 345–347. <https://doi.org/10.1038/ng0892-345>
- Müller, A. K., Farombi, E. O., Møller, P., Autrup, H. N., Vogel, U., Wallin, H., Dragsted, L. O., Loft, S., & Binderup, M. L. (2004). DNA damage in lung after oral exposure to diesel exhaust particles in Big Blue® rats. *Mutation Research - Fundamental and Molecular Mechanisms of Mutagenesis*, 550(1–2), 123–132. <https://doi.org/10.1016/j.mrfmmm.2004.02.010>
- Müller, T., Meyer, H. E., Egensperger, R., & Marcus, K. (2008). The amyloid precursor protein intracellular domain (AICD) as modulator of gene expression, apoptosis, and cytoskeletal dynamics-Relevance for Alzheimer's disease. In *Progress in Neurobiology* (Vol. 85, Issue 4, pp. 393–406). <https://doi.org/10.1016/j.pneurobio.2008.05.002>
- Müller, U. C., & Deller, T. (2017). Editorial: The physiological functions of the APP gene family. In *Frontiers in Molecular Neuroscience* (Vol. 10). Frontiers Media S.A. <https://doi.org/10.3389/fnmol.2017.00334>
- Murphy, M. P., & Levine, H. (2010). Alzheimer's disease and the amyloid- β peptide. In *Journal of Alzheimer's Disease* (Vol. 19, Issue 1, pp. 311–323). IOS Press. <https://doi.org/10.3233/JAD-2010-1221>
- Murrell, J., Farlow, M., Ghetti, B., & Benson, M. D. (1991). A mutation in the amyloid precursor protein associated with hereditary Alzheimer's disease. *Science*, 254(5028), 97–99. <https://doi.org/10.1126/science.1925564>
- Mutkus, L., Aschner, J. L., Fitsanakis, V., & Aschner, M. (2005). The in vitro uptake of glutamate in GLAST and GLT-1 transfected mutant CHO-K1 cells is inhibited by manganese. *Biological Trace Element Research*, 107(3), 221–230. <https://doi.org/10.1385/BTER:107:3:221>
- Nalivaeva, N. N., & Turner, A. J. (2013). The amyloid precursor protein: A biochemical enigma in brain development, function and disease. In *FEBS Letters* (Vol. 587, Issue 13, pp. 2046–2054). <https://doi.org/10.1016/j.febslet.2013.05.010>
- Nemmar, A., Hoet, P., Vanquickenborne, B., Dinsdale, D., Thomeer, M., Hoylaerts, M., Vanbillioen, H., Mortelmans, L., & Nemery, B. (2002). Passage of inhaled particles into the blood circulation in humans. *Circulation*, 105(4), 411–414.

<https://doi.org/10.1161/hc0402.104118>

- NIA. (2016). *Alzheimer's Disease Genetics Fact Sheet*. National Institute on Aging. <https://www.nia.nih.gov/health/alzheimers-disease-genetics-fact-sheet>
- Oddo, S., Caccamo, A., Shepherd, J. D., Murphy, M., Golde, T. E., Kaye, R., Metherate, R., Mattson, M. P., Akbari, Y., & FM., L. (2003). Triple-Transgenic Model of Alzheimer's Disease with Plaques and Tangles: Intracellular A β and Synaptic Dysfunction. *Neuron*, 39(3), 409–421.
- Oddo, S., Caccamo, A., Tran, L., Lambert, M. P., Glabe, C. G., Klein, W. L., & FM., L. (2006). Temporal profile of amyloid-beta (A β) oligomerization in an in vivo model of Alzheimer disease. A link between A β and tau pathology. *J Biol Chem*, 281(3), 1599–1604.
- Oudin, A., Forsberg, B., Adolfsson, A. N., Lind, N., Modig, L., Nordin, M., Nordin, S., Adolfsson, R., & Nilsson, L. G. (2016). Traffic-related air pollution and dementia incidence in Northern Sweden: A longitudinal study. *Environmental Health Perspectives*, 124(3), 306–312. <https://doi.org/10.1289/ehp.1408322>
- Pajarillo, E., Johnson, J., Kim, J., Karki, P., Son, D. S., Aschner, M., & Lee, E. (2018). 17 β -estradiol and tamoxifen protect mice from manganese-induced dopaminergic neurotoxicity. *NeuroToxicology*, 65, 280–288. <https://doi.org/10.1016/j.neuro.2017.11.008>
- Pajarillo, E., Rizer, A., Lee, J., Aschner, M., & Lee, E. (2019). The role of astrocytic glutamate transporters GLT-1 and GLAST in neurological disorders: Potential targets for neurotherapeutics. In *Neuropharmacology* (Vol. 161, p. 107559). Elsevier Ltd. <https://doi.org/10.1016/j.neuropharm.2019.03.002>
- Paresce, D. M., Ghosh, R. N., & Maxfield, F. R. (1996). Microglial cells internalize aggregates of the Alzheimer's disease amyloid β -protein via a scavenger receptor. *Neuron*, 17(3), 553–565. [https://doi.org/10.1016/S0896-6273\(00\)80187-7](https://doi.org/10.1016/S0896-6273(00)80187-7)
- Park, S. J., Lee, J., Lee, S., Lim, S., Noh, J., Cho, S. Y., Ha, J., Kim, H., Kim, C., Park, S., Lee, D. Y., & Kim, E. (2020). Exposure of ultrafine particulate matter causes glutathione redox imbalance in the hippocampus: A neurometabolic susceptibility to Alzheimer's pathology. *Science of The Total Environment*, 137267. <https://doi.org/10.1016/j.scitotenv.2020.137267>
- Parsons, M. P., & Raymond, L. A. (2014). Extrasynaptic NMDA receptor involvement in central nervous system disorders. *Neuron*, 82(2), 279–293.
- Pearson, H. A., & Peers, C. (2006). Physiological roles for amyloid β peptides. *The Journal of Physiology*, 575(1), 5–10. <https://doi.org/10.1113/jphysiol.2006.111203>
- Perera, F. P., Li, Z., Whyatt, R., Hoepner, L., Wang, S., Camann, D., & Rauh, V. (2009). Prenatal Airborne Polycyclic Aromatic Hydrocarbon Exposure and Child IQ at Age 5 Years. *Pediatrics*, 124(2), e195–e202. <https://doi.org/10.1542/peds.2008-3506>
- Perera, F. P., Rauh, V., Whyatt, R. M., Tsai, W. Y., Tang, D., Diaz, D., Hoepner, L., Barr, D., Tu, Y. H., Camann, D., & Kinney, P. (2006). Effect of prenatal exposure to airborne polycyclic aromatic hydrocarbons on neurodevelopment in the first 3 years of life among inner-city children. *Environmental Health Perspectives*, 114(8), 1287–1292. <https://doi.org/10.1289/ehp.9084>

- Perrone, M. G., Gualtieri, M., Consonni, V., Ferrero, L., Sangiorgi, G., Longhin, E., Ballabio, D., Bolzacchini, E., & Camatini, M. (2013). Particle size, chemical composition, seasons of the year and urban, rural or remote site origins as determinants of biological effects of particulate matter on pulmonary cells. *Environmental Pollution*, *176*, 215–227. <https://doi.org/10.1016/j.envpol.2013.01.012>
- Pfeiffer, B. D., Ngo, T. T., Hibbard, K. L., Murphy, C., Jenett, A., Truman, J. W., & GM., R. (2010). Refinement of Tools for Targeted Gene Expression in *Drosophila*. *Genetics*, *186*(2), 735–755.
- Pita-Almenar, J. D., Zou, S., Colbert, C. M., & Eskin, A. (2012). Relationship between increase in astrocytic GLT-1 glutamate transport and late-LTP. *Learning and Memory*, *19*(12), 615–626. <https://doi.org/10.1101/lm.023259.111>
- Pooler, A. M., Phillips, E. C., Lau, D. H. W., Noble, W., & Hanger, D. P. (2013). Physiological release of endogenous tau is stimulated by neuronal activity. *EMBO Reports*, *14*(4), 389–394. <https://doi.org/10.1038/embor.2013.15>
- Pope, C. A., & Dockery, D. W. (2006). Health Effects of Fine Particulate Air Pollution: Lines that Connect. *Journal of the Air & Waste Management Association*, *56*(6), 709–742. <https://doi.org/10.1080/10473289.2006.10464485>
- Porta, D., Narduzzi, S., Badaloni, C., Bucci, S., Cesaroni, G., Colelli, V., Davoli, M., Sunyer, J., Zirro, E., Schwartz, J., & Forastiere, F. (2016). Air pollution and cognitive development at age 7 in a prospective Italian birth cohort. *Epidemiology*, *27*(2), 228–236. <https://doi.org/10.1097/EDE.0000000000000405>
- Power, M. C., Weisskopf, M. G., Alexeeff, S. E., Coull, B. A., Avron, S., & Schwartz, J. (2011). Traffic-related air pollution and cognitive function in a cohort of older men. *Environmental Health Perspectives*, *119*(5), 682–687. <https://doi.org/10.1289/ehp.1002767>
- Prüssing, K., Voigt, A., & Schulz, J. (2013). *Drosophila melanogaster* as a model organism for Alzheimer's disease. *Molecular Neurodegeneration*, *8*(35), 1–11.
- Pujol, J., Martínez-Vilavella, G., Macià, D., Fenoll, R., Alvarez-Pedrerol, M., Rivas, I., Forns, J., Blanco-Hinojo, L., Capellades, J., Querol, X., Deus, J., & Sunyer, J. (2016). Traffic pollution exposure is associated with altered brain connectivity in school children. *NeuroImage*, *129*, 175–184. <https://doi.org/10.1016/j.neuroimage.2016.01.036>
- Puzzo, D., Privitera, L., Fa', M., Staniszewski, A., Hashimoto, G., Aziz, F., Sakurai, M., Ribe, E. M., Troy, C. M., Mercken, M., Jung, S. S., Palmeri, A., & Arancio, O. (2011). Endogenous amyloid- β is necessary for hippocampal synaptic plasticity and memory. *Annals of Neurology*, *69*(5), 819–830. <https://doi.org/10.1002/ana.22313>
- Ranft, U., Schikowski, T., Sugiri, D., Krutmann, J., & Krämer, U. (2009). Long-term exposure to traffic-related particulate matter impairs cognitive function in the elderly. *Environmental Research*, *109*(8), 1004–1011. <https://doi.org/10.1016/j.envres.2009.08.003>
- Rees, D., & Hattis, D. (2004). Developing quantitative strategies for animal to human extrapolation. In Hayes AW ed. *Principles And Methods Of Toxicology* (pp. 275–315).
- Reitz, C., Brayne, C., & Mayeux, R. (2011). Epidemiology of Alzheimer's Disease. *Nature*

Reviews Neurobiology, 7, 137–152.

- Rival, T., Soustelle, L., Strambi, C., Besson, M. T., Ich , M., & Birman, S. (2004). Decreasing Glutamate Buffering Capacity Trigger Oxidative Stress and Neuropil Degeneration in the *Drosophila* Brain. *Current Biology*, 14, 599–605.
- Roberson, E. D., Scarce-Levie, K., Palop, J. J., Yan, F., Cheng, I. H., Wu, T., Gerstein, H., Yu, G. Q., & Mucke, L. (2007). Reducing endogenous tau ameliorates amyloid beta-induced deficits in an Alzheimer's disease mouse model. *Science*, 316, 750–754.
- Rocha, I. I., Narasimhalu, K., & De Silva, D. A. (2020). Impact of Air Pollution and Seasonal Haze on Neurological Conditions. In *Annals of the Academy of Medicine, Singapore* (Vol. 49, Issue 1, pp. 26–36). NLM (Medline).
- Rychlik, K. A., Secrest, J. R., Lau, C., Pulczynski, J., Zamora, M. L., Leal, J., Langley, R., Myatt, L. G., Raju, M., Chang, R. C. A., Li, Y., Golding, M. C., Rodrigues-Hoffmann, A., Molina, M. J., Zhang, R., & Johnson, N. M. (2019). In utero ultrafine particulate matter exposure causes offspring pulmonary immunosuppression. *Proceedings of the National Academy of Sciences of the United States of America*, 116(9), 3443–3448.
<https://doi.org/10.1073/pnas.1816103116>
- Saito, T., Matsuba, Y., Mihira, N., Takano, J., Nilsson, P., Itohara, S., Iwata, N., & Saido, T. C. (2014). Single App knock-in mouse models of Alzheimer's disease. *Nature Neuroscience*, 17(5), 661–663. <https://doi.org/10.1038/nn.3697>
- Saito, T., Mihira, N., Matsuba, Y., Sasaguri, H., Hashimoto, S., Narasimhan, S., Zhang, B., Murayama, S., Higuchi, M., Lee, V. M. Y., Trojanowski, J. Q., & Saido, T. C. (2019). Humanization of the entire murine Mapt gene provides a murine model of pathological human tau propagation. *Journal of Biological Chemistry*, 294(34), 12754–12765.
<https://doi.org/10.1074/jbc.RA119.009487>
- Sánchez-Rodríguez, M. A., Santiago, E., Arronte-Rosales, A., Vargas-Guadarrama, L. A., & Mendoza-Núñez, V. M. (2006). Relationship between oxidative stress and cognitive impairment in the elderly of rural vs. urban communities. *Life Sciences*, 78(15), 1682–1687.
<https://doi.org/10.1016/j.lfs.2005.08.007>
- Sardar, S. B., Fine, P. M., & Sioutas, C. (2005). Seasonal and spatial variability of the size-resolved chemical composition of particulate matter (PM10) in the Los Angeles Basin. *Journal of Geophysical Research: Atmospheres*, 110(D7).
[https://doi.org/10.1029/2004JD004627@10.1002/\(ISSN\)2169-8996.PMSUPERST1](https://doi.org/10.1029/2004JD004627@10.1002/(ISSN)2169-8996.PMSUPERST1)
- SCAQMD. (2016). Final 2016 Air Quality Management Plan. *AQMD*.
- Schauer, J. J., Rogge, W. F., Hildemann, L. M., Mazurek, M. A., Cass, G. R., & Simoneit, B. R. T. (1996). Source apportionment of airborne particulate matter using organic compounds as tracers. *Atmospheric Environment*, 30(22), 3837–3855. [https://doi.org/10.1016/1352-2310\(96\)00085-4](https://doi.org/10.1016/1352-2310(96)00085-4)
- Scheff, S. W., Price, D. A., Schmitt, F. A., & EJ., M. (2006). Hippocampal synaptic loss in early Alzheimer's disease and mild cognitive impairment. *Neurobiology of Aging*, 27, 1372–1384.

- Scheuner, D., Eckamn, C., Jensen, M., Song, X., Citron, M., Suzuki, N., Bird, T. D., Hardy, J., Hutton, M., Kukull, W., Larson, E., Levy-Lahad, L., Viitanen, M., Peskind, E., Poorkaj, P., Schellenberg, G., Tanzi, R., Wasco, W., Lannfelt, L., ... Younkin, S. (1996). Secreted amyloid β -protein similar to that in the senile plaques of Alzheimer's disease is increased in vivo by the presenilin 1 and 2 and APP mutations linked to familial Alzheimer's disease. *Nat Med*, 2, 864–870.
- Schikowski, T., Vossoughi, M., Vierkötter, A., Schulte, T., Teichert, T., Sugiri, D., Fehsel, K., Tzivian, L., Bae, I. S., Ranft, U., Hoffmann, B., Probst-Hensch, N., Herder, C., Krämer, U., & Luckhaus, C. (2015). Association of air pollution with cognitive functions and its modification by APOE gene variants in elderly women. *Environmental Research*, 142, 10–16. <https://doi.org/10.1016/j.envres.2015.06.009>
- Seaton, A., MacNee, W., Donaldson, K., & Godden, D. (1995). Particulate air pollution and acute health effects. *Lancet*, 345(8943), 176–178. [https://doi.org/10.1016/S0140-6736\(95\)90173-6](https://doi.org/10.1016/S0140-6736(95)90173-6)
- Shankar, G. M., Li, S., Mehta, T. H., Garcia-Munoz, A., Shepardson, N. E., Smith, I., Brett, F. M., Farrell, M. A., Rowan, M. J., Lemere, C. A., Regan, C. M., Walsh, D. M., Sabatini, B. L., & Selkoe, D. J. (2008). Amyloid- β protein dimers isolated directly from Alzheimer's brains impair synaptic plasticity and memory. *Nature Medicine*, 14(8), 837–842. <https://doi.org/10.1038/nm1782>
- Shipton, O. A., Leitz, J. R., Dworzak, J., Acton, C. E., Tunbridge, E. M., Denk, F., Dawson, H. N., Vitek, M. P., Wade-Martins, R., Paulsen, O., & Vargas-Caballero, M. (2011). Tau protein is required for amyloid β -induced impairment of hippocampal long-term potentiation. *J Neurosci*, 31(5), 1688–1692.
- Simoneit, B. R. T., Kobayashi, M., Mochida, M., Kawamura, K., Lee, M., Lim, H. J., Turpin, B. J., & Komazaki, Y. (2004). Composition and major sources of organic compounds of aerosol particulate matter sampled during the ACE-Asia campaign. *Journal of Geophysical Research D: Atmospheres*, 109(19), 1–22. <https://doi.org/10.1029/2004JD004598>
- Slegers, K., Brouwers, N., Gijssels, I., Theuns, J., Goossens, D., Wauters, J., Del-Favero, J., Cruts, M., Van Duijn, C. M., & Van Broeckhoven, C. (2006). APP duplication is sufficient to cause early onset Alzheimer's dementia with cerebral amyloid angiopathy. *Brain*, 129(11), 2977–2983. <https://doi.org/10.1093/brain/awl203>
- Soucek, T., Cumming, R., Dargusch, R., Maher, P., & Schubert, D. (2003). The regulation of glucose metabolism by HIF-1 mediates a neuroprotective response to amyloid beta peptide. *Neuron*, 39(1), 43–56. [https://doi.org/10.1016/S0896-6273\(03\)00367-2](https://doi.org/10.1016/S0896-6273(03)00367-2)
- Spangenberg, E. E., Lee, R. J., Najafi, A. R., Rice, R. A., Elmore, M. R. P., Blurton-Jones, M., West, B. L., & Green, K. N. (2016). Eliminating microglia in Alzheimer's mice prevents neuronal loss without modulating amyloid- β pathology. *Brain*, 139(4), 1265–1281. <https://doi.org/10.1093/brain/aww016>
- Stearns, R. C., Paulauskis, J. D., & Godleski, J. J. (2001). Endocytosis of ultrafine particles by A549 cells. *American Journal of Respiratory Cell and Molecular Biology*, 24(2), 108–115. <https://doi.org/10.1165/ajrcmb.24.2.4081>

- Stephenson, J., Nutma, E., van der Valk, P., & Amor, S. (2018). Inflammation in CNS neurodegenerative diseases. *Immunology*, *154*(2), 204–219. <https://doi.org/10.1111/imm.12922>
- Stranahan, A. M., Haberman, R. P., & Gallagher, M. (2011). Cognitive decline is associated with reduced reelin expression in the entorhinal cortex of aged rats. *Cerebral Cortex (New York, N.Y. : 1991)*, *21*(2), 392–400. <https://doi.org/10.1093/cercor/bhq106>
- Suglia, S. F., Gryparis, A., Wright, R. O., Schwartz, J., & Wright, R. J. (2008). Association of black carbon with cognition among children in a prospective birth cohort study. *American Journal of Epidemiology*, *167*(3), 280–286. <https://doi.org/10.1093/aje/kwm308>
- Sullivan, P. F., Daly, M. J., & O'Donovan, M. (2012). Genetic architectures of psychiatric disorders: The emerging picture and its implications. In *Nature Reviews Genetics* (Vol. 13, Issue 8, pp. 537–551). <https://doi.org/10.1038/nrg3240>
- Sweeney, M. D., Sagare, A. P., & Zlokovic, B. V. (2018). Blood-brain barrier breakdown in Alzheimer disease and other neurodegenerative disorders. In *Nature Reviews Neurology* (Vol. 14, Issue 3, pp. 133–150). Nature Publishing Group. <https://doi.org/10.1038/nrneurol.2017.188>
- Takahashi, K., Kong, Q., Lin, Y., Stouffer, N., Schulte, D. A., Lai, L., Chang, L. C., Dominguez, S., Xing, X., Cuny, G. D., Hodgetts, K. J., Glicksman, M. A., & CLG., L. (2015). Restored glial glutamate transporter Ea2 function as a potential therapeutic approach for Alzheimer's disease. *J Exp Med*, *212*(3), 319–332.
- Tanaka, K., Watase, K., Manabe, T., Yamada, K., Watanabe, M., Takahashi, K., Iwama, H., Nishikawa, T., Ichihara, N., Kikuchi, T., Okuyama, S., Kawashima, N., Hori, S., Takimoto, M., & Wada, K. (1997). Epilepsy and exacerbation of brain injury in mice lacking the glutamate transporter GLT- 1. *Science*, *276*, 1699–1702.
- Tang, B. L. (2019). Amyloid Precursor Protein (APP) and GABAergic Neurotransmission. *Cells*, *8*(6), 550. <https://doi.org/10.3390/cells8060550>
- Tanwar, V., Adelstein, J. M., Grimmer, J. A., Youtz, D. J., Katapadi, A., Sugar, B. P., Falvo, M. J., Baer, L. A., Stanford, K. I., & Wold, L. E. (2018). Preconception Exposure to Fine Particulate Matter Leads to Cardiac Dysfunction in Adult Male Offspring. *Journal of the American Heart Association*, *7*(24), e010797. <https://doi.org/10.1161/JAHA.118.010797>
- Terry, R. D., Masliah, E., Salmon, D. P., Butters, N., DeTeresa, R., Hill, R., Hansen, L. A., & Katzman, R. (1991). Physical basis of cognitive alterations in Alzheimer's disease: synapse loss is the major correlate of cognitive impairment. *Ann. Neurol.*, *30*, 572–580.
- Tomic, J. L., Pensalfini, A., Head, E., & Glabe, C. G. (2009). Soluble fibrillar oligomer levels are elevated in Alzheimer's disease brain and correlate with cognitive dysfunction. *Neurobiology of Disease*, *35*(3), 352–358. <https://doi.org/10.1016/j.nbd.2009.05.024>
- Tonne, C., Elbaz, A., Beevers, S., & Singh-Manoux, A. (2014). Traffic-related Air Pollution in Relation to Cognitive Function in Older Adults. *Epidemiology*, *25*(5), 674–681. <https://doi.org/10.1097/EDE.000000000000144>
- Tseng, C. Y., Yu, J. Y., Chuang, Y. C., Lin, C. Y., Wu, C. H., Liao, C. W., Yang, F. H., & Chao,

- M. W. (2019). The Effect of Ganoderma Microsporium immunomodulatory proteins on alleviating PM2.5-induced inflammatory responses in pregnant rats and fine particulate matter-induced neurological damage in the offsprings. *Scientific Reports*, 9(1), 1–10. <https://doi.org/10.1038/s41598-019-38810-5>
- Tucsek, Z., Noa Valcarcel-Ares, M., Tarantini, S., Yabluchanskiy, A., Fülöp, G., Gautam, T., Orock, A., Csiszar, A., Deak, F., & Ungvari, Z. (2017). Hypertension-induced synapse loss and impairment in synaptic plasticity in the mouse hippocampus mimics the aging phenotype: implications for the pathogenesis of vascular cognitive impairment. *GeroScience*, 39(4), 385–406. <https://doi.org/10.1007/s11357-017-9981-y>
- Tzivian, L., Dlugaj, M., Winkler, A., Weinmayr, G., Hennig, F., Fuks, K. B., Vossoughi, M., Schikowski, T., Weimar, C., Erbel, R., Jöckel, K. H., Moebus, S., & Hoffmann, B. (2016). Long-term air pollution and traffic noise exposures and mild cognitive impairment in older adults: A cross-sectional analysis of the Heinz Nixdorf recall study. *Environmental Health Perspectives*, 124(9), 1361–1368. <https://doi.org/10.1289/ehp.1509824>
- Tzivian, L., Winkler, A., Dlugaj, M., Schikowski, T., Vossoughi, M., Fuks, K., Weinmayr, G., & Hoffmann, B. (2015). Effect of long-term outdoor air pollution and noise on cognitive and psychological functions in adults. *International Journal of Hygiene and Environmental Health*, 218(1), 1–11. <https://doi.org/10.1016/j.ijheh.2014.08.002>
- US EPA. (2004). *Air Quality Criteria for Particulate Matter (Final Report, 2004)*.
- Valavandis, A., FIOTAKIS, K., & VLACHOGIANNI, T. (2008). Airborne Particulate Matter and Human Health: Toxicological Assessment and Importance of Size and Composition of Particles for Oxidative Damage and Carcinogenic Mechanisms. *Journal of Environmental Science and Health, Part C*, 26(4), 339–362. <https://doi.org/10.1080/10590500802494538>
- Van De Haar, H. J., Burgmans, S., Jansen, J. F. A., Van Osch, M. J. P., Van Buchem, M. A., Muller, M., Hofman, P. A. M., Verhey, F. R. J., & Backes, W. H. (2016). Blood-brain barrier leakage in patients with early Alzheimer disease. *Radiology*, 281(2), 527–535. <https://doi.org/10.1148/radiol.2016152244>
- van Donkelaar, A., Martin, R. V., Brauer, M., & Boys, B. L. (2014). Use of satellite observations for long-term exposure assessment of global concentrations of fine particulate matter. *Environmental Health Perspectives*, 110(October), 135–143. <https://doi.org/10.1289/ehp.1408646>
- van Kempen, E., Fischer, P., Janssen, N., Houthuijs, D., van Kamp, I., Stansfeld, S., & Cassee, F. (2012). Neurobehavioral effects of exposure to traffic-related air pollution and transportation noise in primary schoolchildren. *Environmental Research*, 115, 18–25. <https://doi.org/10.1016/j.envres.2012.03.002>
- Venegas, C. (2017). Microglia-derived ASC specks cross-seed amyloid- β in Alzheimer's disease. *Nature*, 552, 355–361.
- Viana, M., Kuhlbusch, T. A. J., Querol, X., Alastuey, A., Harrison, R. M., Hopke, P. K., Winiwarter, W., Vallius, M., Szidat, S., Prévôt, A. S. H., Hueglin, C., Bloemen, H., Wählin, P., Vecchi, R., Miranda, A. I., Kasper-Giebl, A., Maenhaut, W., & Hitzenberger, R. (2008). Source apportionment of particulate matter in Europe: A review of methods and results.

- Journal of Aerosol Science*, 39(10), 827–849. <https://doi.org/10.1016/j.jaerosci.2008.05.007>
- Vogel-Ciernia, A., & Wood, M. A. (2014). Examining object location and object recognition memory in mice. *Current Protocols in Neuroscience*, 2014, 8.31.1-8.31.17. <https://doi.org/10.1002/0471142301.ns0831s69>
- Vom Berg, J., Prokop, S., Miller, K. R., Obst, J., K♦lin, R. E., Lopategui-Cabezas, I., Wegner, A., Mair, F., Schipke, C. G., Peters, O., Winter, Y., Becher, B., & FL., H. (2012). Inhibition of IL-12/IL-23 signaling reduces Alzheimer’s disease-like pathology and cognitive decline. *Nat Med*, 18(12), 1812–1819.
- Walsh, D. M., Minogue, A. M., Sala Frigerio, C., Fadeeva, J. V., Wasco, W., & Selkoe, D. J. (2007). The APP family of proteins: Similarities and differences. *Biochemical Society Transactions*, 35(2), 416–420. <https://doi.org/10.1042/BST0350416>
- Wang, R., & Reddy, P. H. (2017). Role of Glutamate and NMDA Receptors in Alzheimer’s Disease. In *Journal of Alzheimer’s Disease* (Vol. 57, Issue 4, pp. 1041–1048). IOS Press. <https://doi.org/10.3233/JAD-160763>
- Wang, S., Zhang, J., Zeng, X., Zeng, Y., Wang, S., & Chen, S. (2009). Association of traffic-related air pollution with children’s neurobehavioral functions in Quanzhou, China. *Environmental Health Perspectives*, 117(10), 1612–1618. <https://doi.org/10.1289/ehp.0800023>
- Wang, W. Y., Tan, M. S., Yu, J. T., & Tan, L. (2015). Role of pro-inflammatory cytokines released from microglia in Alzheimer’s disease. In *Annals of Translational Medicine* (Vol. 3, Issue 10). AME Publishing Company. <https://doi.org/10.3978/j.issn.2305-5839.2015.03.49>
- Wang, Y., & Mandelkow, E. (2016). Tau in physiology and pathology. In *Nature Reviews Neuroscience* (Vol. 17, Issue 1, pp. 5–21). Nature Publishing Group. <https://doi.org/10.1038/nrn.2015.1>
- Wellenius, G. A., Boyle, L. D., Coull, B. A., Milberg, W. P., Gryparis, A., Schwartz, J., Mittleman, M. A., & Lipsitz, L. A. (2012). Residential proximity to nearest major roadway and cognitive function in community-dwelling seniors: Results from the mobilize Boston study. *Journal of the American Geriatrics Society*, 60(11), 2075–2080. <https://doi.org/10.1111/j.1532-5415.2012.04195.x>
- Westerdahl, D., Wang, X., Pan, X., & Zhang, K. M. (2009). Characterization of on-road vehicle emission factors and microenvironmental air quality in Beijing, China. *Atmospheric Environment*, 43(3), 697–705. <https://doi.org/10.1016/j.atmosenv.2008.09.042>
- Weuve, J., Puett, R. C., Schwartz, J., Yanosky, J. D., Laden, F., & Grodstein, F. (2012). Exposure to particulate air pollution and cognitive decline in older women. *Archives of Internal Medicine*, 172(3), 219–227. <https://doi.org/10.1001/archinternmed.2011.683>
- WHO. (2016). *Ambient (outdoor) air pollution*. WHO Fact Sheet. [https://www.who.int/en/news-room/fact-sheets/detail/ambient-\(outdoor\)-air-quality-and-health](https://www.who.int/en/news-room/fact-sheets/detail/ambient-(outdoor)-air-quality-and-health)
- WHO. (2017). *The top 10 causes of death*. <http://www.who.int/mediacentre/factsheets/fs310/en/>

- Wisniewski, K. E., Wisniewski, H. M., & Wen, G. Y. (1985). Occurrence of neuropathological changes and dementia of Alzheimer's disease in Down's syndrome. *Annals of Neurology*, *17*(3), 278–282. <https://doi.org/10.1002/ana.410170310>
- Wittmann, C. W., Wszolek, M. F., Shulman, J. M., Salvaterra, P. M., Lewis, J., Hutton, M., & MB., F. (2001). Tauopathy in Drosophila: Neurodegeneration without Neurofibrillary Tangles. *Science*, *293*, 711–714.
- Wolfe, M. (2012). The Role of Tau in Neurodegenerative Diseases and Its Potential as a Therapeutic Target. *Scientifica.*, 1–20.
- Wu, J. S., & Luo, L. (2006). A protocol for dissecting Drosophila melanogaster brains for live imaging or immunostaining. *Nat Protocols*, *1*, 2110–2115.
- Wu, J. W., Herman, M., Liu, L., Simoes, S., Acker, C. M., Figueroa, H., Steinberg, J. I., Margittai, M., Kaye, R., Zurzolo, C., Di Paolo, G., & KE., D. (2013). Small misfolded Tau species are internalized via bulk endocytosis and anterogradely and retrogradely transported in neurons. *J Biol Chem*, *288*(3), 1856–1870.
- Wu, J. W., Hussaini, S. A., Bastille, I. M., Rodriguez, G. A., Mrejeru, A., Rilett, K., Sanders, D. W., Cook, C., Fu, H., Boonen, R. A., Herman, M., Nahmani, E., Emrani, S., Figueroa, Y. H., Diamond, M. I., Clelland, C. L., Wray, S., & KE., D. (2016). Neuronal activity enhances tau propagation and tau pathology in vivo. *Nat Neurosci*, *19*(8), 1085–1092. <https://doi.org/10.1038/nn.4328>
- Wu, Y.-C., Lin, Y.-C., Yu, H.-L., Chen, J.-H., Chen, T.-F., Sun, Y., Wen, L.-L., Yip, P.-K., Chu, Y.-M., & Chen, Y.-C. (2015). Association between air pollutants and dementia risk in the elderly. *Alzheimer's & Dementia: Diagnosis, Assessment & Disease Monitoring*, *1*(2), 220–228. <https://doi.org/10.1016/j.dadm.2014.11.015>
- Xiong, M., Jones, O. D., Peppercorn, K., Ohline, S. M., Tate, W. P., & Abraham, W. C. (2017). Secreted amyloid precursor protein-alpha can restore novel object location memory and hippocampal LTP in aged rats. *Neurobiology of Learning and Memory*, *138*, 291–299. <https://doi.org/10.1016/j.nlm.2016.08.002>
- Xu, L., He, D., & Bai, Y. (2016). Microglia-Mediated Inflammation and Neurodegenerative Disease. In *Molecular Neurobiology* (Vol. 53, Issue 10, pp. 6709–6715). Humana Press Inc. <https://doi.org/10.1007/s12035-015-9593-4>
- Ye, Z., Lu, X., Deng, Y., Wang, X., Zheng, S., Ren, H., Zhang, M., Chen, T., Jose, P. A., Yang, J., & Zeng, C. (2018). In Utero Exposure to Fine Particulate Matter Causes Hypertension Due to Impaired Renal Dopamine D₁ Receptor in Offspring. *Cellular Physiology and Biochemistry*, *46*(1), 148–159. <https://doi.org/10.1159/000488418>
- Yegambaram, M., Manivannan, B., Beach, T. G., & Halden, R. U. (2015). Role of Environmental Contaminants in the Etiology of Alzheimer's Disease: A Review. *Current Alzheimer Research*, *12*, 116–146. <https://doi.org/10.2174/1567205012666150204121719>
- Younan, D., Petkus, A. J., Widaman, K. F., Wang, X., Casanova, R., Espeland, M. A., Gatz, M., Henderson, V. W., Manson, J. E., Rapp, S. R., Sachs, B. C., Serre, M. L., Gaussoin, S. A., Barnard, R., Saldana, S., Vizuete, W., Beavers, D. P., Salinas, J. A., Chui, H. C., ... Chen,

- J.-C. (2020). Particulate matter and episodic memory decline mediated by early neuroanatomic biomarkers of Alzheimer's disease. *Brain*, *143*(1), 289–302. <https://doi.org/10.1093/brain/awz348>
- Yu, H., Li, Z., Zhang, H., & Wang, X. (2006). Role of potassium channels in A β 1–40-activated apoptotic pathway in cultured cortical neurons. *Journal of Neuroscience Research*, *84*(7), 1475–1484. <https://doi.org/10.1002/jnr.21054>
- Zanchi, A. C. T., Fagundes, L. S., Barbosa, F., Bernardi, R., Rhoden, C. R., Saldiva, P. H. N., & do Valle, A. C. (2010). Pre and post-natal exposure to ambient level of air pollution impairs memory of rats: the role of oxidative stress. *Inhalation Toxicology*, *22*(11), 910–918. <https://doi.org/10.3109/08958378.2010.494313>
- Zavala, M., Barrera, H., Morante, J., & Molina, L. T. (2013). Analysis of model-based PM_{2.5} emission factors for on-road mobile sources in Mexico. *Atmosfera*, *26*(1), 109–124. [https://doi.org/10.1016/S0187-6236\(13\)71065-8](https://doi.org/10.1016/S0187-6236(13)71065-8)
- Zeng, Y., Gu, D., Purser, J., Hoenig, H., & Christakis, N. (2010). Associations of environmental factors with elderly health and mortality in china. *American Journal of Public Health*, *100*(2), 298–305. <https://doi.org/10.2105/AJPH.2008.154971>
- Zhang, K. M., Wexler, A. S., Niemeier, D. A., Yi, F. Z., Hinds, W. C., & Sioutas, C. (2005). Evolution of particle number distribution near roadways. Part III: Traffic analysis and on-road size resolved particulate emission factors. *Atmospheric Environment*, *39*(22), 4155–4166. <https://doi.org/10.1016/j.atmosenv.2005.04.003>
- Zhang, X., Chen, X., & Zhang, X. (2018). The impact of exposure to air pollution on cognitive performance. *Proceedings of the National Academy of Sciences of the United States of America*, *115*(37), 9193–9197. <https://doi.org/10.1073/pnas.1809474115>
- Zhu, Y., Hinds, W. C., Kim, S., & Sioutas, C. (2002). Concentration and Size Distribution of Ultrafine Particles Near a Major Highway. *Journal of the Air & Waste Management Association*, *52*(9), 1032–1042. <https://doi.org/10.1080/10473289.2002.10470842>
- Zumkehr, J., Rodriguez-Ortiz, C. J., Cheng, D., Kieu, Z., Wai, T., Hawkins, C., Kilian, J., Lim, S. L., Medeiros, R., & Kitazawa, M. (2015). Ceftriaxone ameliorates tau pathology and cognitive decline via restoration of glial glutamate transporter in a mouse model of Alzheimer's disease. *Neurobiology of Aging*, *36*(7), 2260–2271.
- Zumkehr, J., Rodriguez-Ortiz, C. J., Medeiros, R., & Kitazawa, M. (2018). Inflammatory Cytokine, IL-1 β , Regulates Glial Glutamate Transporter via microRNA-181a in vitro. *Journal of Alzheimer's Disease*, *63*(3), 965–975. <https://doi.org/10.3233/JAD-170828>

Appendix A- Abbreviations

A β - Amyloid β

AD- Alzheimer's Disease

AICD- Amyloid precursor protein intracellular/cytoplasmic C-terminal domain

Alrm- astrocytic leucine-rich repeat molecule

AMPA- α -amino-3-hydroxy-5-methyl-4-isoxazolepropionic acid

ANOVA- Analysis of variance

APOE- Apolipoprotein E

APP- Amyloid precursor protein. Alternative: shorthand in figures for *App*^{NL-G-F/+}-KI genotype

BBB- Blood brain barrier

BSA- Bovine serum albumin

CD31, CD68- Cluster of differentiation 31, cluster of differentiation 68

CNS- Central nervous system

Cor- Cortex

COX2- Cyclooxygenase 2

Dlg1- discs large 1

Eaat- excitatory amino acid transporter

F- *APP* Iberian mutation I716F

FA- Filtered air

G- *APP* Arctic mutation E693G

GAPDH- Glyceraldehyde 3-phosphate dehydrogenase

GFAP- Glial fibrillary acid protein

GLT- glutamate transporter

GluR1, GlurR2- Glutamate receptor 1, Glutamate receptor 2

GMR- Glass multiple reporter

GS3K β - Glycogen synthase kinase 3 beta

HC- Hippocampus

Htau- Human tau

Iba1- Ionized calcium binding adaptor molecule 1

Il6, Il1 β - interleukin 6, interleukin 1 β
IR- Interfering RNA
KI- Knock in
LTP- Long term potentiation
MAPT- Microtubule associated protein tau
MRI- Magnetic resonance imaging
NF- κ B- Nuclear factor kappa-light-chain-enhancer of activated B cells
NFT- Neurofibrillary tangle
NIA- National Institute on Aging
NIEHS- National Institute of Environmental Health Sciences
NIH- National Institute of Health
NL- *APP* Swedish mutation KM670/671NL
NMDA- N-methyl-D-aspartate
NO_x⁻ Nitrogen oxides
nSyB- Neuronal synaptobrevin
OLM- Object location memory
ORM- Object recognition memory
PAH- Poly aromatic hydrocarbon
PBS- Phosphate buffered saline
PBT- Phosphate buffered saline + 0.5% tween
PCR- Polymerase chain reaction
PET- positron emission tomography
PHF- Paired helical filament
PM-Particulate matter
PSD95- Post synaptic density protein 95
SYP- Synaptophysin
TBS- Tris buffered saline
TNF- Tumor necrosis factor
Trpa1- Transient receptor potential cation channel, subfamily A, member 1
Tub- Tubulin

TUNEL- terminal deoxynucleotidyl transferase dUTP nick end labeling

UF- UF PM (see below)

UF PM- Ultrafine particulate matter

VACES- Versatile aerosol concentration and enrichment system

ZO- Zonula occludens